INSIGHTS INTO ORGANOSULFUR ASSIMILATION IN STAPHYLOCOCCUS AUREUS

Ву

Joshua Michael Lensmire

A DISSERTATION

Submitted to
Michigan State University
in partial fulfillment of the requirements
for the degree of

Microbiology and Molecular Genetics—Doctor of Philosophy

2021

ABSTRACT

INSIGHTS INTO ORGANOSULFUR ASSIMILATION IN STAPHYLOCOCCUS AUREUS

By

Joshua Michael Lensmire

Bacterial pathogens deploy sophisticated strategies to acquire vital nutrients from the host during infection. *Staphylococcus aureus* is a considerable human pathogen due to its capacity to cause numerous life-threatening diseases. As such *S. aureus* has an intricate metabolism that promotes proliferation in distinct host environments. However, little is known regarding the sulfur sources the pathogen scavenges from host tissues. Sulfur is an essential nutrient due to its extensive redox capacity and consequently, it is a critical component of many cofactors. Prior studies started to define sulfur sources *S. aureus* can use including the inorganic sulfur sources, sulfide and thiosulfate, and organosulfur sources, cysteine, cystine, and glutathione. While we understand some of the sulfur sources *S. aureus* can use, we do not know the genetic determinants facilitating assimilation. The present studies sought to explain how *S. aureus* imports and catabolizes organic sources of sulfur.

First, we wanted to uncover the proteins allowing *S. aureus* to utilize cystine and cysteine as sulfur sources. The *S. aureus* homologues of characterized cystine transporters, TcyP and TcyABC, were experimentally validated as cystine and cysteine transporters. We expanded the sulfur sources *S. aureus* can utilize to include homocystine and *N*-acetyl cysteine and show that both TcyABC and TcyP support growth on *N*-acetyl cysteine while only TcyABC supports growth on homocystine. Finally, a *tcyP* mutant is impaired in murine heart and liver when competing with WT *S. aureus* suggesting import of TcyP substrates is important for heart and liver colonization.

While a *tcyP* mutant is reduced in competition with WT in murine heart and liver colonization is not fully ablated signifying more sulfur sources must be catabolized. We next examined how *S. aureus* imports and catabolizes GSSG. To identify *S. aureus* GSSG utilization strategies, we used a chemically defined medium containing GSSG as the sulfur source and

isolated mutants harboring transposon insertions within a putative ABC-transporter and Y-glutamyl transpeptidase that fail to proliferate. The mutants also do not grow in medium supplemented with GSH. Consistent with these findings, we named the locus the **g**lutathione import **s**ystem (*gisABCD-ggt*). Biochemical analysis of recombinant Ggt confirms *in silico* functional predictions by demonstrating that Ggt cleaves both GSH and GSSG. Though Gis mutants display wildtype virulence, we find that Gis-Ggt promotes competition with *Staphylococcus epidermidis* when GSH or GSSG is supplied as the sole sulfur source *in vitro*.

S. aureus resides as a nasal commensal in 30% of the population and once inside the body can infect nearly every organ. Throughout the changing host environments, S. aureus must sense and acclimate to nutrient availability. We sought to define how sulfur starvation and growth on different sulfur sources changes the transcriptional profile of S. aureus. We described the transcriptional changes when WT S. aureus or a CymR, the sulfur transcriptional regulator, mutant were grown in sulfur replete and deplete conditions. We show sulfur starvation leads to significant expression changes including upregulation of iron acquisition encoding genes and oxidative stress encoding genes. Furthermore, we provide evidence showing upregulation of CymR dependent sulfur transporters when S. aureus is grown on GSH and thiosulfate both of which are conditions in which CymR repression should be occurring.

Finally, this dissertation ends with areas of future exploration of sulfur source utilization in *S. aureus*. These avenues include examining nutrient sulfur available in distinct infection sites and expansion of the sulfur sources *S. aureus* can use. Overall, the work presented here substantially contributes to our understanding of what sulfur sources *S. aureus* imports and catabolizes and how different sulfur sources change the transcriptional states of the cell.

This dissertation is dedicated to my family.

ACKNOWLEDGEMENTS

I would like to thank my advisor, Dr. Neal Hammer, for taking me into the lab and introducing me to the research and people of the Staph field. The projects allowed me to gain experience in many aspects of microbiology and these skills have set me up for success in the future. I am quite excited to see the future work that comes out of the lab. I would also like to thank past Hammer lab members, Dr. Phillip Delekta and John Shook, who would always allow time for me to discuss my research ideas while lending a useful ear. Throughout my PhD journey, members of the DiRita, Waters, and Crosson labs have been very generous with their time allowing me to drop in and brainstorm ideas with them, and these conversations led me to devise much improved experiments. The MMG department office staff is owed a lot of gratitude due to their endless help during my PhD career. The generosity of their time and advice in navigating the department has helped me immensely.

My committee members which include Drs. Abramovitch, DiRita, Martinez-Gomez, Parent, and TerAvest have served as invaluable resources with whom I have had conversations improving my science, finding my career trajectory, and helping me make substantial career related decisions. Each committee member pushed me in unique ways to become a much better scientist and each was very generous with their time whether I wanted to discuss research or career related topics. Each member provided a unique perspective on my projects and taught me invaluable new skills.

An interesting opportunity during my graduate career was the ability to work with the department to explore how science is taught to graduate students. I would like to thank Dr. DiRita for his willingness to go forward with this idea and allow me to explore important parts of graduate training. I remember promoting an exciting idea that I had read about, and Dr. DiRita allowed for this idea to be explored. Courses stemming from this idea will hopefully be implemented in the

future and I am excited to hear about how they progress. This experience has made me into a better scientist.

Finally, I would like to acknowledge my friends and family. I have great groups of friends that allow me to escape the science world and the stresses of the PhD process. I would like to thank my family. They have always been supportive of my science adventures even when they lead me to move to different states. They are always a reminder that there is more to life than science and spending so much time being at the bench. Furthermore, trips back to Wisconsin to visit family have been invaluable breaks from science during my time at MSU. Getting to spend time with my niece and nephew and seeing them question the world around them reconnects me with my driving curiosity that propelled me to start down this path in the first place.

TABLE OF CONTENTS

LIST OF TABLES	x
LIST OF FIGURES	x
Chapter 1 Nutrient sulfur acquisition strategies employed by bacterial pathogens	
Abstract	
Introduction	
Inorganic sulfur assimilation	
Sulfate	
Thiosulfate	
Organosulfur acquisition	7
Cysteine (Cys) and Cystine (CSSC)	
Methionine (Met)	
Glutathione (GSH)	
Taurine	
Frontiers in pathogen nutrient sulfur acquisition	11
Concluding remarks	
Acknowledgments	12
Chapter 2 The Staphylococcus aureus cystine transporters TcyABC and TcyP fac	ilitate
nutrient sulfur acquisition during infection	13
Abstract	14
Introduction	14
Results	17
Genetic inactivation of tcyA increases resistance to the toxic CSSC analogue	
selenocystine	17
Disruption of both tcyA and tcyP leads to complete selenocystine resistance and re	
growth in a defined medium supplemented with CSSC as the sole sulfur source	
S. aureus TcyABC and TcyP support proliferation in medium containing Cys or N-a	
cysteine as the sole source of sulfur	
TcyABC supports growth on homocystine (hCSSC) but not glutathione	22
tcyP and tcyA are induced in sulfur starvation conditions.	24
TcyP is required for maximal fitness in the murine liver while TcyABC and TcyP are	Э
required for maximal fitness in the murine heart.	25
TcyP is conserved across many bacterial phyla	26
Discussion	
Materials and methods	34
Bacterial strains	34
Generation of complementation vectors.	34
Growth Analysis.	35
Selenocystine disk diffusion assays and isolation of resistant mutants	35
Genomic DNA isolation and gene sequencing	
qRT-PCR analysis	
Competition in murine model of systemic infection.	
Phylogenetic analyses of TcyP	
Acknowledgements	

acquisition and promotes interspecies competition	Chapter 3 The glutathione import system expands Staphylococcus aureus nutrient s	
Author summary		
Introduction		
Results	· · · · · · · · · · · · · · · · · · ·	
S. aureus proliferates in medium supplemented with GSSG as a sole source of nutrient sulfur		
sulfur		
supports proliferation on both GSH and GSSG	sulfur	
Recombinant GisA displays ATPase activity		
rGgt liberates glutamate from both GSH and GSSG		
Ggt is cell associated in <i>S. aureus</i>	Recombinant GisA displays ATPase activity.	49
Ggt is cell associated in <i>S. aureus</i>	rGgt liberates glutamate from both GSH and GSSG	50
GisABCD-Ggt independent utilization of physiological concentrations of GSH		
Ggt homologues are present across Firmicutes. 55 GisABCD-Ggt promotes interspecies competition in a GSH-specific manner 56 Discussion. 57 Materials and Methods 63 Bacterial strains used in this study. 63 Growth analysis. 64 Isolation and growth of clinical isolates. 64 Isolation and growth of clinical isolates. 64 Anaerobic growth. 65 Domain prediction of GisABCD-Ggt. 65 Construction of pET28b::ggt and pET28b::gisA and purification of tagged protein. 66 ATPase activity of GisA. 67 Quantitation of Ggt enzyme kinetics. 67 Quantitation of Ggt enzyme kinetics. 67 Western blotting analysis of S. aureus Ggt. 68 Murine systemic infections. 69 Resolving of GisABCD-Ggt homologs across bacteria. 69 In vitro S. aureus and S. epidermidis competitions. 70 Acknowledgements. 70 Chapter 4 Defining Staphylococcus aureus transcriptional adaptation to sulfur starvation and distinct sources of nutrient sulfur. 72 Abstract. 73 Importance. 74 Introduction 74 Results and discussion. 77 Sulfur starvation and the CymR response 77 S. aureus transcriptional response to sulfur starvation 81 Sulfur starvation induces changes in numerous transcriptional regulators. 85 Genes associated with iron transport and acquisition and the oxidative stress response are upregulated in response to sulfur starvation 85 Comparison of S. aureus transcriptional adaptation to specific sources of nutrient sulfur. 88 Materials and methods. 94		
GisABCD-Ggt promotes interspecies competition in a GSH-specific manner		
Discussion		
Materials and Methods Bacterial strains used in this study. Growth analysis. 64 Isolation and growth of clinical isolates. Anaerobic growth. 55 Domain prediction of GisABCD-Ggt. 65 Construction of pET28b::ggt and pET28b::gisA and purification of tagged protein. 66 ATPase activity of GisA. 67 Quantitation of Ggt enzyme kinetics. 67 Western blotting analysis of S. aureus Ggt. 68 Murine systemic infections. 69 Resolving of GisABCD-Ggt homologs across bacteria. 69 In vitro S. aureus and S. epidermidis competitions. 70 Acknowledgements 70 Chapter 4 Defining Staphylococcus aureus transcriptional adaptation to sulfur starvation and distinct sources of nutrient sulfur. 72 Abstract. 73 Importance. 74 Introduction 75 Results and discussion. 77 Sulfur starvation and the CymR response 77 S. aureus transcriptional response to sulfur starvation. 81 Sulfur starvation induces changes in numerous transcriptional regulators. 85 Genes associated with iron transport and acquisition and the oxidative stress response are upregulated in response to sulfur starvation. 85 Comparison of S. aureus transcriptional adaptation to specific sources of nutrient sulfur. 88 Materials and methods		
Bacterial strains used in this study. 63 Growth analysis. 64 Isolation and growth of clinical isolates 64 Anaerobic growth. 65 Domain prediction of GisABCD-Ggt. 65 Construction of pET28b::ggt and pET28b::gisA and purification of tagged protein. 66 ATPase activity of GisA. 67 Quantitation of Ggt enzyme kinetics. 67 Western blotting analysis of S. aureus Ggt. 68 Murine systemic infections. 69 Resolving of GisABCD-Ggt homologs across bacteria. 69 Resolving of GisABCD-Ggt homologs across bacteria. 69 In vitro S. aureus and S. epidermidis competitions. 70 Acknowledgements. 70 Chapter 4 Defining Staphylococcus aureus transcriptional adaptation to sulfur starvation and distinct sources of nutrient sulfur. 72 Abstract. 73 Importance. 74 Introduction 74 Results and discussion. 77 Sulfur starvation and the CymR response. 77 S. aureus transcriptional response to sulfur starvation. 81 Sulfur starvation induces changes in numerous transcriptional regulators. 85 Genes associated with iron transport and acquisition and the oxidative stress response are upregulated in response to sulfur starvation. 85 Comparison of S. aureus transcriptional adaptation to specific sources of nutrient sulfur. 88 Materials and methods. 94		
Growth analysis		
Isolation and growth of clinical isolates		
Anaerobic growth		
Domain prediction of GisABCD-Ggt		
Construction of pET28b::ggt and pET28b::gisA and purification of tagged protein	Anaerobic growth.	05
ATPase activity of GisA		
Quantitation of Ggt enzyme kinetics		
Western blotting analysis of S. aureus Ggt		
Murine systemic infections		
Resolving of GisABCD-Ggt homologs across bacteria		
In vitro S. aureus and S. epidermidis competitions		
Acknowledgements		
Chapter 4 Defining Staphylococcus aureus transcriptional adaptation to sulfur starvation and distinct sources of nutrient sulfur	In vitro S. aureus and S. epidermidis competitions	70
Abstract	Acknowledgements	70
Abstract		
Importance		
Introduction		
Results and discussion	· ·	
Sulfur starvation and the CymR response		
S. aureus transcriptional response to sulfur starvation		
S. aureus transcriptional response to sulfur starvation	Sulfur starvation and the CymR response.	77
Genes associated with iron transport and acquisition and the oxidative stress response are upregulated in response to sulfur starvation	S. aureus transcriptional response to sulfur starvation.	81
Genes associated with iron transport and acquisition and the oxidative stress response are upregulated in response to sulfur starvation	Sulfur starvation induces changes in numerous transcriptional regulators	85
upregulated in response to sulfur starvation		
Comparison of <i>S. aureus</i> transcriptional adaptation to specific sources of nutrient sulfur88 Materials and methods94		
Materials and methods94		
Racterial strains used in this study	Bacterial strains used in this study.	
Sulfur starvation sample collection	,	
Sulfur source growth conditions95		
RNA isolation and sequencing95		
RNA-seg data processing and visualization95		

96
96
97
98
02
02
03
04
06
is
06
80
09
30
(

LIST OF TABLES

Table 1-1. Evidence for pathogen acquisition and utilization of host-derived sulfur sources 6
Table 2-1. Mutations identified in the <i>tcyP</i> opening reading frame of <i>tcyA</i> ::Tn selenocystine resistant mutants
Table 4-1. Culture conditions comparing sulfur starvation and the CymR regulon78
Table 4-2. Sulfur status independent CymR regulon
Table 4-3. Genes encoding transcriptional regulators that are differentially regulated in response to sulfur starvation
Table 4-4. Sulfur starvation induces expression of iron import and oxidative stress genes86
Table A-1. Bacterial strains used in chapter 2110
Table A-2. Primers used in chapter 2111
Table B-1. Bacterial strains used in chapter 3116
Table B-2. Primers used in chapter 3117
Table C-1. Genes that are shared between our data and the published <i>cymR</i> mutant data129

LIST OF FIGURES

Figure 1-1. Overview of the enzymatic processes that support sulfur assimilation and integration of exogenous sulfur-containing metabolites
Figure 2-1. A <i>S. aureus tcyA</i> mutant demonstrates enhanced resistance to the toxic cystine analogue selenocystine
Figure 2-2. Selenocystine resistant colonies in <i>tcyA</i> ::Tn background maintain resistance to selenocystine
Figure 2-3. TcyABC and TcyP are required for sensitivity to selenocystine and utilization of cystine as a nutrient sulfur source
Figure 2-4. TcyABC and TcyP support proliferation in medium supplemented with cysteine (Cys) or N-acetyl-cysteine (NAC) as the sole sulfur sources
Figure 2-5. TcyABC supports growth of S. aureus in medium containing homocystine but not GSH as a sulfur source
Figure 2-6. tcyP and tcyA are induced in sulfur starvation conditions24
Figure 2-7. TcyP is required for maximal fitness in the murine heart and liver25
Figure 2-8. TcyP is broadly conserved in bacteria
Figure 3-1. Supplementation of GSSG as sole sulfur source supports growth of <i>Staphylococcus</i> aureus
Figure 3-2. SAUSA300_0200-ggt supports growth on GSH and GSSG as sulfur sources48
Figure 3-3. GisA harbors ATPase domain signatures and has demonstrates ATPase activity50
Figure 3-4. S. aureus Ggt liberates glutamate from GSH and GSSG51
Figure 3-5. S. aureus Ggt is cell associated
Figure 3-6. <i>S. aureus</i> encodes another transporter that supports growth on physiologically relevant concentrations of GSH
Figure 3-7. GisABCD promotes competition in GSH- or GSSG-supplemented media57
Figure 4-1. Experimental design employed to define the CymR-dependent and –independent response to sulfur starvation in <i>S. aureus</i> 77
Figure 4-2. <i>cymR</i> -replete dataset is enriched for genes involved in amino acid and sulfur compound transport

Figure 4-3. Comparison of the <i>S. aureus</i> sulfur starvation transcriptional response to the CymR regulon
Figure 4-4. Supplementation with the inorganic, oxidized sulfur source, thiosulfate induces considerable transcriptional changes90
Figure 4-5. CymR repressed nutrient sulfur transporters are upregulated in response to both GSH and thiosulfate92
Figure A-1. Strain Newman tcyA mutants demonstrate enhanced selenocystine resistance112
Figure A-2. Newman TcyABC and TcyP are required for selenocystine sensitivity113
Figure A-3. Ectopic expression of tcyP and tcyABC restores selenocystine sensitivity and growth in cystine-supplemented medium of the tcyAP double mutant114
Figure A-4. TcyP is conserved across many bacterial phyla
Figure B-1. Supplementation with GSSG as the sole source of nutrient sulfur stimulates growth of clinical isolates
Figure B-2. Domain architectures and secondary structure predictions for the S. aureus GisABCD-Ggt system119
Figure B-3. GisABCD-Ggt promotes anaerobic growth in media supplemented with GSSG or GSH120
Figure B-4. Coomassie blue stained SDS-PAGE gel demonstrating purification of histidine tagged GisA expressed in <i>E. coli</i>
Figure B-5. His-tagged Ggt complements growth of <i>ggt</i> mutant
Figure B-6. Heterologous expression and purification of <i>S. aureus</i> Ggt from <i>E. coli</i> 123
Figure B-7. Inactivation of <i>gisB</i> or <i>gisB</i> and <i>tcyP</i> does not affect virulence in a murine systemic model of infection
Figure B-8. Gis mutant can grow in physiologically relevant concentrations of GSH125
Figure B-9. Conservation of Ggt and GisABCD across Firmicutes
Figure B-10. <i>S. epidermidis</i> shows delayed growth and is outcompete by <i>S. aureus</i> in GSH containing media
Figure B-11. A proposed model of GisABCD-Ggt acquisition of GSH and GSSG128

KEY TO ABBREVIATIONS

ABC — ATP binding cassette ACME — arginine catabolism mobile element ANOVA — analysis of variance ATP — adenosine triphosphate BCA — bicinchoninic acid BLAST — basic local alignment search tool BP — base pair BSA — bovine serum albumin CA-MRSA — community acquired methicillin resistant Staphylococcus aureus CBZ — carboxybenzyl CFU --- colony forming units CI — competitive index CoA — coenzyme A COG — Cluster of orthologous groups CSSC — cystine Cys — cysteine DELTA-BLAST — domain enhanced lookup time accelerated BLAST DNA — deoxyribonucleic acid Erm — erythromycin FDR — false discovery rate GO — Gene ontology GSH — reduced glutathione

GSSG — oxidized glutathione

hCSSC — homocystine

His — histidine tag

HRP — horseradish peroxidase

IPTG — isopropyl-D-1-thiogalactopyranoside

kB — kilobase

kDa — kilodalton

LB — lysogeny broth

LC — liquid chromatography

MS — mass spectrometry

MSA — mannitol salt agar

Met — methionine

MRSA — methicillin resistant Staphylococcus aureus

MSSA — methicillin sensitive *Staphylococcus aureus*

NAC — N-acetyl cysteine

NARSA — Network on antimicrobial resistance in *Staphylococcus aureus*

NCBI — National Center for Biotechnology Information

NTML — Nebraska transposon mutant library

NTN — n-terminal nucleophile

NTA — nitrilotriacetic acid

OAS — o-acetyl serine

OD₆₀₀ — optical density at 600 nm

ORF — open reading frame

PBS — phosphate buffered saline

PBST — phosphate buffered saline tween-20

PCR — polymerase chain reaction

P_i — inorganic phosphate

PSI-BLAST— position-specific iterative BLAST

Pvdf — polyvinylidene difluoride

qRT PCR— PCR-quantitative real time polymerase chain reaction

RNA — ribonucleic acid

RNA-seq — RNA sequencing

Rpm — rotations per minute

SDS — sodium dodecyl sulfate

TCA — trichloracetic acid

Tet — tetracycline

Tmp — trimethoprim

Tn — transposon

Tn-seq — transposons sequencing

TSA — trypic soy agar

TSB — trypic soy broth

WT — wild type

WCL — whole cell lysate

Chapter 1 Nutrient sulfur acquisition strategies employed by bacterial pathogens
Work presented in this chapter has been published as Lensmire JM , Hammer ND . 2018. Nutrient sulfur acquisition strategies employed by bacterial pathogens. Curr. Opin. Microbiol. 47 :52–58.

Abstract

Pathogens have evolved elegant mechanisms to acquire essential nutrients from host environments. Sulfur is a requirement for bacterial growth and inorganic and organic sulfur-containing metabolites are abundant within the host-pathogen interface. A growing body of evidence suggests that pathogens are capable of scavenging both types of sulfur sources to fulfill the nutritional requirement. While therapeutic strategies focusing on inhibiting inorganic sulfate assimilation and Cys synthesis show promise *in vitro*, *in vivo* efficacy maybe limited due to the diversity of host-derived sulfur sources and the fact that most pathogens are capable of acquiring multiple sources of sulfur.

Introduction

Pathogenic bacteria are adept at procuring essential nutrients from the host environment. Decades of research have revealed mechanisms by which bacterial pathogens acquire transition metals and carbon sources during infection. This review focuses on another nutritional requirement for bacterial growth, sulfur. Compared to our understanding of nutrient metal acquisition, how pathogens fulfill their sulfur requirement is less well understood.

Sulfur is a multivalent atom that conforms to a dynamic range of oxidation states (+6 to -2). This redox activity supports many aspects of eukaryotic and prokaryotic life (1). For example, sulfur is incorporated in the amino acids Cys and methionine (Met), as well as, several essential cofactors including but not limited to coenzyme A, coenzyme M, thiamine, lipoic acid, iron-sulfur [Fe-S] clusters, glutathione (GSH), and biotin (1). The unique chemistry of these sulfur-containing compounds is essential for electron transfer and redox homeostasis. Humans and bacteria use sulfur-containing metabolites for many of the same functions; consequently, the molecules are readily available for pathogens during infection. For example, the host accumulates organosulfur compounds that contain sulfhydryl groups, or thiols, at high concentrations that function as antioxidants (2). Numerous *in vitro* studies describe how bacteria acquire these organosulfur

molecules for use as sulfur sources, and researchers are beginning to understand how these systems function during infection. This review will highlight these studies, define the sulfur sources available within the host, and present examples of pathogen sulfur acquisition strategies.

Inorganic sulfur assimilation

Inorganic sulfur compounds such as sulfate (SO₄²⁻) play crucial roles in host physiology. Plasma levels of sulfate, the most highly oxidized form of sulfur (oxidation state of -6), can reach as high as 215.5 µM (Table 1-1) (3). To use sulfate, bacteria first transport it into the cytoplasm, and subsequently reduce the molecule to an oxidation state of +2 via an energy intensive process involving a series of four enzymatic reactions and the input of eight electrons (Fig. 1-1) (4). Sulfate assimilation leads to production of sulfide which can be readily converted to Cys, a precursor to numerous sulfur-containing cofactors (2, 5). The first of four reactions leading to Cys begins with the enzyme ATP sulfurylase and the substrates sulfate and ATP (4). The reaction produces adenosine phosphosulfate (APS) (Fig. 1-1 #1) which is subsequently phosphorylated by APS kinase creating phosphoadenosine phosphosulfate (PAPS) (Fig. 1-1 #2) (4). PAPS is reduced by PAPS reductase yielding adenosine diphosphate (PAP) and sulfite (SO₃²-) (Fig. 1-1 #3) (4). Sulfite is reduced to sulfide (S²-) (Fig. 1-1 #4) (4). Ultimately, sulfide reacts with O-acetyl serine (OAS) via OAS sulfhydrylase (this enzyme is also called Cys synthase or OAS (thiol)-lyase) that produces Cys (Fig. 1-1 #5) (4). OAS is generated by serine O-acetyltransferase and the substrates serine and acetyl-coenzyme A (acetyl-coA) (Fig. 1.1 # 10) (4). Reactions involved in the production of Cys from an inorganic sulfur molecule will be referred to as assimilation (Fig. 1-1 #1-4).

Sulfate

Sulfate is an established *in vivo* sulfur source for some pathogens (Table 1-1). A transposon-sequencing study examining *Acinetobacter baumannii* infection in the *Galleria*

mellonella larvae infection model revealed that sulfate assimilatory enzymes sulfite reductase, PAPS reductase, serine *O*-acetyltransferase, and ATP sulfurylase are essential for infection (6). Sulfate assimilation is also key for *Mycobacterium tuberculosis* proliferation (7, 8). Researchers established that ATP sulfurylase (Fig. 1-1 #1) and PAPS reductase (Fig. 1-1 #3) are essential for *in vitro* growth using transposon site hybridization (8), and *M. tuberculosis* ATP sulfurylase mutants are impaired for macrophage infection (7). These reports establish *M. tuberculosis* and *A. baumanii* as model pathogens for the study of sulfate assimilation during infection.

Thiosulfate

Thiosulfate (S₂O₃²⁻) can be a substrate of OAS sulfhydrylase in certain species of bacteria (Table 1-1) leading directly to Cys production (Fig. 1-1 #11, 12). Bacteria with thiosulfate assimilatory potential encode a specific OAS sulfhydrylase to generate *S*-sulfocysteine, which is subsequently reduced to Cys by an unknown mechanism (Fig. 1-1 #12) (9). Numerous pathogens including, *Salmonella enterica, Clostridium difficile,* and *Staphylococcus aureus* possess thiosulfate catabolic activity (Table 1-1) (10–12). Despite *in vitro* characterization of pathogen thiosulfate assimilation, *in vivo* acquisition of thiosulfate as a sulfur source during infection has not been demonstrated.

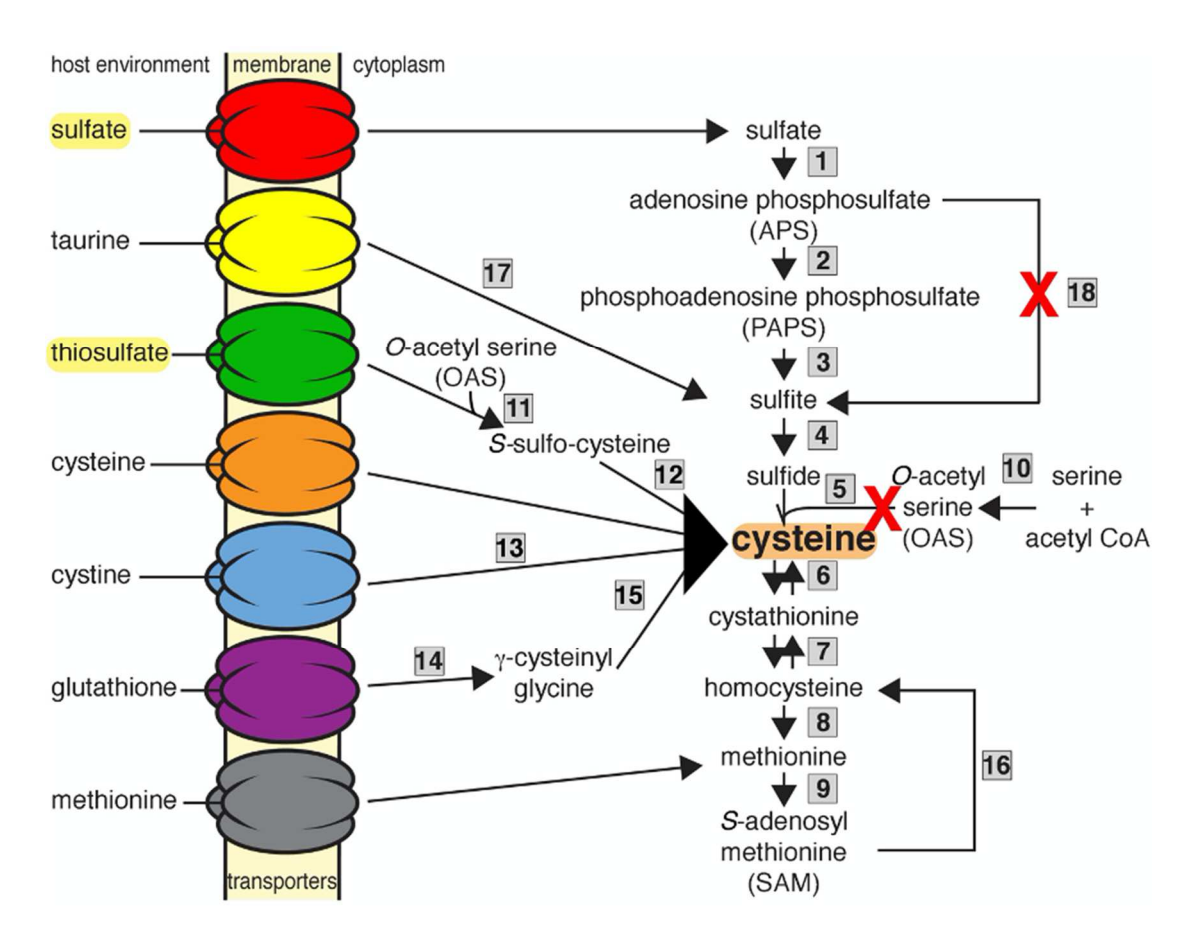


Figure 1-1. Overview of the enzymatic processes that support sulfur assimilation and integration of exogenous sulfur-containing metabolites.

1: ATP sulfurylase, 2: APS Kinase, 3: PAPS Reductase, 4: Sulfite Reductase, 5: Cysteine synthase or OAS sulfhydrylase (also referred to as O-acetylserine (thiol)-lyase), 6: cystathionine-gamma-synthase, 7: cystathionine beta synthase, 8: homocysteine S-methyltransferase, 9: S-adenosylmethionine synthetase, 10: serine O-acetyltransferase,11: Cysteine synthase (OAS sulfhydrylase O-acetylserine (thiol)-lyase) – in some species #5 and #11 are isozymes that catalyze a similar reaction but use different substrates, 12: unknown enzyme that converts S-sulfo-cysteine to cysteine, 13: Unknown reductase that reduces the disulfide bond in cystine,14: γ-glutamyl-transpeptidase, 15: peptidase, 16: SAM undergoes a methyl transfer reaction and becomes S-adenosyl homocysteine. SAH is subsequently converted to homocysteine by SAH hydrolase 17: α-ketoglutarate-dependent dioxygenase 18: APS reductase. The red 'X' indicates enzymes targeted for therapeutic intervention. Sulfur sources highlighted in yellow are inorganic sources of sulfur; The rest are organosulfur metabolites.

Table 1-1. Evidence for pathogen acquisition and utilization of host-derived sulfur sources.

Sulfur Source Concentration in host environments* Example Pathogens Evidence* References Sulfate Plasma: 215.5 μM Mycobacterium in vitro in vitro (4) Pseudomonas aeruginosa in vitro (4) Pseudomonas aeruginosa in vitro (4) Acinetobacter baumannii in vitro (4) Klebsiella aerogenes in vitro (4) Klebsiella aerogenes in vitro (4) Salmonella enterica in vitro (4) Staphylococcus aureus in vitro (11) Clostridium difficile in vitro (15) Giutathione Francisella tularensis in vitro (16) Staphylococcus aureus in vitro (17) Bordetella pertussis in vitr	sources.				
Sulfate Plasma: 215.5 μM tuberculosis Escherichia coli in vitro (4) Pseudomonas aeruginosa in vitro (6) Salmonella enterica in vitro (4) Mebsiella aerogenes in vivo (14) Thiosulfate Serum: 100.8 Escherichia coli in vitro (4) Klebsiella aerogenes in vivo (14) Thiosulfate Serum: 100.8 Escherichia coli in vitro (4) Mebsiella aerogenes in vivo (14) Thiosulfate Serum: 100.8 Escherichia coli in vitro (4) Staphylococcus aureus in vitro (11) Clostridium difficile in vitro (12) Campylobacter jejuni in vitro (15) Giutathione Francisella tularensis in vivo (16) Staphylococcus aureus in vitro (17) Plasma: 37.03 μM Escherichia coli in vitro (19) Intracellular: 0.5- 10 mM Haemophilus influenzae in vitro (20) Streptococcus mutans in vitro (22) Streptococcus mutans in vitro (23) Cysteine Cysteine Cysteine Serum: Listeria monocytogenes in vitro (15) Escherichia coli in vitro (25) Salmonella enterica in vitro (25) Streptococcus mutans in vitro (25) Salmonella enterica in vitro (25) Streptococcus mutans in vitro (25) Streptococcus mutans in vitro (25) Salmonella enterica in vitro (25) Streptococcus mutans in vitro (25)			Example Pathogens	Evidence	References
Sulfate Plasma: 215.5 μM Mycobacterium tuberculosis in vitro (7, 8) Escherichia coli in vitro (4) Pseudomonas aeruginosa in vitro (13) Acinetobacter baumannii in vitro (4) Salmonella enterica in vitro (4) Klebsielia aerogenes in vitro (4) Klebsielia aerogenes in vitro (4) Staphylococcus aureus in vitro (4) Staphylococcus aureus in vitro (11) Clostridium difficile in vitro (15) Glutathione Francisella tularensis in vitro (16) Staphylococcus aureus in vitro (11) Clostridium difficile in vitro (12) Bordetella pertussis in vitro (17) Plasma: 37.03 Neisseria meningitidis in vitro (18) Intracellular: 0.5- Salmonella enterica in vitro (20) Plasma: 37.03 Neisseria meningitidis in vitro (19) Intracellular: 0.5- S	Source				
μΜ tuberculosis Escherichia coli in vitro (4) Pseudomonas aeruginosa in vitro (13) Acinetobacter baumannii in vivo (6) Salmonella enterica in vitro (4) Klebsiella aerogenes in vivo (14) Thiosulfate Serum: 100.8 Escherichia coli in vitro (4) Staphylococcus aureus in vitro (11) Clostridium difficile in vitro (15) Glutathione Francisella tularensis in vivo (16) Staphylococcus aureus in vitro (11) Clostridium difficile in vitro (12) Bordetella pertussis in vitro (17) Plasma: 37.03 Neisseria meningitidis in vitro (18) Intracellular: 0.5- 10 mM Haemophilus influenzae in vitro (20) Streptococcus mutans in vitro (21) Streptococcus mutans in vitro (23) Cysteine/ Cysteine Serum: Listeria monocytogenes in vivo (24) Cysteine 33.5 μΜ ystine Serum: Staphylococcus aureus in vitro (15) Escherichia coli in vitro (15) Escherichia coli in vitro (25) Salmonella enterica in vitro (25) Salmonella enterica in vitro (25) Methionine Serum: 39.8 μΜ Klebsiella aerogenes in vitro (25) Mycobacterium in vitro (25)					
Escherichia coli in vitro (4) Pseudomonas aeruginosa in vitro (13) Acinetobacter baumannii in vivo (6) Salmonella enterica in vitro (4) Klebsiella aerogenes in vivo (14) Thiosulfate Serum: 100.8 Escherichia coli in vitro (4) Implication pub Salmonella enterica in vitro (4) Staphylococcus aureus in vitro (11) Clostridium difficile in vitro (12) Campylobacter jejuni in vitro (15) Glutathione Francisella tularensis in vivo (16) Staphylococcus aureus in vitro (11) Clostridium difficile in vitro (15) Glutathione Francisella tularensis in vivo (16) Staphylococcus aureus in vitro (11) Clostridium difficile in vitro (15) Glutathione Francisella tularensis in vivo (16) Staphylococcus aureus in vitro (17) Plasma: 37.03 Neisseria meningitidis in vitro (18) μΜ Escherichia coli in vitro (19) Intracellular: 0.5- Salmonella enterica in vitro (20) 10 mM Haemophilus influenzae in vitro (21) Streptococcus mutans in vitro (22) Streptococcus pneumoniae in vivo (23) Cysteine/ Cysteine Serum: Listeria monocytogenes in vivo (24) Cystine 33.5 μΜ ystine Serum: Staphylococcus aureus in vitro (15) Escherichia coli in vitro (25) Salmonella enterica in vitro (25) Streptococcus mutans in vitro (25) Salmonella enterica in vitro (25) Streptococcus mutans in vitro (25) Salmonella enterica in vitro (26) Methionine Serum: 39.8 μΜ Klebsiella aerogenes in vitro in vitro (25)	<u>Sulfate</u>		<u>-</u>	in vitro	(7, 8)
Pseudomonas aeruginosa in vitro (13) Acinetobacter baumannii in vivo (6) Salmonella enterica in vitro (4) Klebsiella aerogenes in vivo (14) Thiosulfate Serum: 100.8 Escherichia coli in vitro (4) µM Salmonella enterica in vitro (4) Staphylococcus aureus in vitro (11) Clostridium difficile in vitro (12) Campylobacter jejuni in vitro (15) Glutathione Francisella tularensis in vivo (16) Staphylococcus aureus in vitro (11) Clostridium difficile in vitro (11) Clostridium difficile in vitro (12) Bordetella pertussis in vitro (11) Plasma: 37.03 Neisseria meningitidis in vitro (18) µM Escherichia coli in vitro (19) Intracellular: 0.5- Salmonella enterica in vitro (20) Thiosulfate Serum: Staphylococcus mutans in vitro (21) Streptococcus mutans in vitro (22) Cysteine/ Cysteine Serum: Listeria monocytogenes in vivo (23) Cysteine/ OH Campylobacter jejuni in vitro (15) Escherichia coli in vitro (25) Salmonella enterica in vitro (25) Salmonella enterica in vitro (25) Salmonella enterica in vitro (25) Streptococcus mutans in vitro (25) Salmonella enterica in vitro (25) Streptococcus mutans in vitro (25) Methionine Serum: 39.8 μM Klebsiella aerogenes in vitro in vitro (25) Methionine Serum: 39.8 μM Klebsiella aerogenes in vitro in vitro (25) Nycobacterium in vitro (25)		μM			
Acinetobacter baumannii in vivo (6) Salmonella enterica in vitro (4) Klebsiella aerogenes in vivo (14) Thiosulfate Serum: 100.8 Escherichia coli in vitro (4) µM Salmonella enterica in vitro (4) Staphylococcus aureus in vitro (11) Clostridium difficile in vitro (12) Campylobacter jejuni in vitro (15) Glutathione Francisella tularensis in vivo (16) Staphylococcus aureus in vitro (11) Clostridium difficile in vitro (12) Bordetella pertussis in vitro (12) Bordetella pertussis in vitro (13) µM Escherichia coli in vitro (19) Intracellular: 0.5- 10 mM Haemophilus influenzae in vitro (20) Streptococcus mutans in vitro (21) Streptococcus mutans in vitro (23) Cysteine/ Cysteine Serum: Listeria monocytogenes in vivo (24) Cystine 33.5 µM ystine Serum: Staphylococcus aureus in vitro (15) Escherichia coli in vitro (25) Salmonella enterica in vitro (26) Mycobacterium in vitro (25)	0				· ·
Salmonella enterica in vitro (4) Klebsiella aerogenes in vivo (14) Thiosulfate Serum: 100.8 Escherichia coli in vitro (4) Salmonella enterica in vitro (4) Salmonella enterica in vitro (4) Staphylococcus aureus in vitro (11) Clostridium difficile in vitro (12) Campylobacter jejuni in vitro (15) Glutathione Francisella tularensis in vivo (16) Staphylococcus aureus in vitro (11) Clostridium difficile in vitro (12) Bordetella pertussis in vitro (12) Bordetella pertussis in vitro (17) Plasma: 37.03 Neisseria meningitidis in vitro (18) µM Escherichia coli in vitro (19) Intracellular: 0.5- Salmonella enterica in vitro (20) 10 mM Haemophilus influenzae in vitro (21) Streptococcus mutans in vitro (22) Streptococcus pneumoniae in vivo (23) Cysteine/ Cysteine Serum: Listeria monocytogenes in vivo (24) Cystine 33.5 µM ystine Serum: Staphylococcus aureus in vitro (15) Escherichia coli in vitro (25) Salmonella enterica in vitro (25) Salmonella enterica in vitro (25) Salmonella enterica in vitro (25) Streptococcus mutans in vitro (25) Mycobacterium in vitro (25)	Ĭ				• •
Klebsiella aerogenes in vivo (14) Thiosulfate Serum: 100.8 Escherichia coli in vitro (4) O	-o—s—o- 				* *
Thiosulfate Serum: 100.8 Escherichia coli in vitro (4) pM Salmonella enterica in vitro (4) Staphylococcus aureus in vitro (11) Clostridium difficile in vitro (12) Campylobacter jejuni in vitro (15) Glutathione Francisella tularensis in vitro (11) Clostridium difficile in vitro (15) Glutathione Staphylococcus aureus in vitro (11) Clostridium difficile in vitro (12) Bordetella pertussis in vitro (17) Plasma: 37.03 Neisseria meningitidis in vitro (18) μΜ Escherichia coli in vitro (19) Intracellular: 0.5- Salmonella enterica in vitro (20) 10 mM Haemophilus influenzae in vitro (21) Streptococcus mutans in vitro (23) Cysteine/ Cysteine Serum: Listeria monocytogenes in vitro (24) Cystine 33.5 μΜ ystine Serum: Staphylococcus aureus in vitro (25) Salmonella enterica in vitro (25) Streptococcus mutans in vitro (25) Methionine Serum: 39.8 μΜ Klebsiella aerogenes in vitro in vitro (25) Mycobacterium in vitro (25) Tuberculosis Pseudomonas aeruginosa in vitro	Ö		Salmonella enterica	in vitro	· ·
μΜ Salmonella enterica in vitro (4) Staphylococcus aureus in vitro (11) Clostridium difficile in vitro (12) Campylobacter jejuni in vitro (15) Glutathione Francisella tularensis in vivro (16) Staphylococcus aureus in vitro (11) Clostridium difficile in vitro (11) Clostridium difficile in vitro (12) Bordetella pertussis in vitro (17) Plasma: 37.03 Neisseria meningitidis in vitro (18) μΜ Escherichia coli in vitro (19) Intracellular: 0.5- Salmonella enterica in vitro (20) 10 mM Haemophilus influenzae in vitro (21) Streptococcus mutans in vitro (22) Streptococcus pneumoniae in vivo (23) Cysteine/ Cysteine Serum: Listeria monocytogenes in vitro (24) Cystine 33.5 μΜ ystine Serum: Staphylococcus aureus in vitro (15) Escherichia coli in vitro (25) Salmonella enterica in vitro (25) Streptococcus mutans in vitro (26) Methionine Serum: 39.8 μΜ Klebsiella aerogenes in vitro (25) Mycobacterium in vitro (25) tuberculosis Pseudomonas aeruginosa in vitro			Klebsiella aerogenes	in vivo	(14)
Staphylococcus aureus in vitro (11) Clostridium difficile in vitro (12) Campylobacter jejuni in vitro (15) Glutathione Francisella tularensis in vivo (16) Staphylococcus aureus in vitro (11) Clostridium difficile in vitro (12) Bordetella pertussis in vitro (17) Plasma: 37.03 Neisseria meningitidis in vitro (18) µM Escherichia coli in vitro (19) Intracellular: 0.5- Salmonella enterica in vitro (20) 10 mM Haemophilus influenzae in vitro (21) Streptococcus mutans in vitro (22) Streptococcus pneumoniae in vivo (23) Cysteine/ Cysteine Serum: Listeria monocytogenes in vivo (24) Cystine 33.5 µM ystine Serum: Staphylococcus aureus in vitro (11) Escherichia coli in vitro (25) Salmonella enterica in vitro (25) Salmonella enterica in vitro (25) Streptococcus mutans in vitro (26) Methionine Serum: 39.8 µM Klebsiella aerogenes in vitro (25) tuberculosis Pseudomonas aeruginosa in vitro	<u>Thiosulfate</u>	Serum: 100.8	Escherichia coli	in vitro	(4)
Clostridium difficile in vitro (12) Campylobacter jejuni in vitro (15) Glutathione Francisella tularensis in vivo (16) Staphylococcus aureus in vitro (11) Clostridium difficile in vitro (12) Bordetella pertussis in vitro (17) Plasma: 37.03 Neisseria meningitidis in vitro (18) µM Escherichia coli in vitro (19) Intracellular: 0.5- Salmonella enterica in vitro (20) 10 mM Haemophilus influenzae in vitro (21) Streptococcus mutans in vitro (22) Streptococcus pneumoniae in vivo (23) Cysteine/ Cysteine Serum: Listeria monocytogenes in vivo (24) Cystine 33.5 µM ystine Serum: Staphylococcus aureus in vitro (15) Escherichia coli in vitro (15) Escherichia coli in vitro (25) Salmonella enterica in vitro (25) Streptococcus mutans in vitro (26) Methionine Serum: 39.8 µM Klebsiella aerogenes in vitro (25) tuberculosis Pseudomonas aeruginosa in vitro	O II	μM	Salmonella enterica	in vitro	(4)
Glutathione Francisella tularensis in vitro (15) Glutathione Francisella tularensis in vivo (16) Staphylococcus aureus in vitro (11) Clostridium difficile in vitro (12) Bordetella pertussis in vitro (17) Plasma: 37.03 Neisseria meningitidis in vitro (18) μΜ Escherichia coli in vitro (19) Intracellular: 0.5- 10 mM Haemophilus influenzae in vitro (20) Streptococcus mutans in vitro (21) Streptococcus pneumoniae in vivo (23) Cysteine Cysteine Cysteine Serum: Listeria monocytogenes in vivo (24) Cystine 33.5 μΜ ystine Serum: Staphylococcus aureus in vitro (11) Escherichia coli in vitro (25) Salmonella enterica in vitro (25) Streptococcus mutans in vitro (25) Streptococcus mutans in vitro (25) Streptococcus mutans in vitro (26) Methionine Serum: 39.8 μΜ Klebsiella aerogenes in vitro (25) Mycobacterium in vitro (25) tuberculosis Pseudomonas aeruginosa in vitro	-o—s—o-		Staphylococcus aureus	in vitro	(11)
Glutathione Francisella tularensis in vivo (16) Staphylococcus aureus in vitro (11) Clostridium difficile in vitro (12) Bordetella pertussis in vitro (17) Plasma: 37.03 Neisseria meningitidis in vitro (18) μΜ Escherichia coli in vitro (19) Intracellular: 0.5- 10 mM Haemophilus influenzae in vitro (20) Streptococcus mutans in vitro (21) Streptococcus mutans in vitro (23) Cysteine Cysteine Serum: Listeria monocytogenes in vivo (24) Cystine 33.5 μΜ ystine Serum: Staphylococcus aureus in vitro (15) Escherichia coli in vitro (25) Salmonella enterica in vitro (25) Salmonella enterica in vitro (25) Streptococcus mutans in vitro (26) Methionine Serum: 39.8 μΜ Klebsiella aerogenes in vitro (25) tuberculosis Pseudomonas aeruginosa in vitro	Ĭ		Clostridium difficile	in vitro	(12)
Staphylococcus aureus in vitro (11) Clostridium difficile in vitro (12) Bordetella pertussis in vitro (17) Plasma: 37.03 Neisseria meningitidis in vitro (18) µM Escherichia coli in vitro (19) Intracellular: 0.5- Salmonella enterica in vitro (20) 10 mM Haemophilus influenzae in vitro (21) Streptococcus mutans in vitro (22) Streptococcus pneumoniae in vivo (23) Cysteine/ Cysteine Serum: Listeria monocytogenes in vivo (24) Cystine 33.5 µM ystine Serum: Staphylococcus aureus in vitro (11) Escherichia coli in vitro (15) Escherichia coli in vitro (25) Salmonella enterica in vitro (25) Streptococcus mutans in vitro (26) Methionine Serum: 39.8 µM Klebsiella aerogenes in vitro (25) Mycobacterium in vitro (25) tuberculosis Pseudomonas aeruginosa in vitro	S		Campylobacter jejuni	in vitro	(15)
Clostridium difficile in vitro (12) Bordetella pertussis in vitro (17) Plasma: 37.03 Neisseria meningitidis in vitro (18) µM Escherichia coli in vitro (19) Intracellular: 0.5- Salmonella enterica in vitro (20) 10 mM Haemophilus influenzae in vitro (21) Streptococcus mutans in vitro (22) Streptococcus pneumoniae in vivo (23) Cysteine/ Cysteine Serum: Listeria monocytogenes in vivo (24) Cystine 33.5 µM ystine Serum: Staphylococcus aureus in vitro (11) Escherichia coli in vitro (15) Escherichia coli in vitro (25) Salmonella enterica in vitro (25) Streptococcus mutans in vitro (26) Methionine Serum: 39.8 µM Klebsiella aerogenes in vitro (25) Mycobacterium in vitro (25) tuberculosis Pseudomonas aeruginosa in vitro	<u>Glutathione</u>		Francisella tularensis	in vivo	(16)
Bordetella pertussis in vitro (17) Plasma: 37.03 Neisseria meningitidis in vitro (18) μΜ Escherichia coli in vitro (19) Intracellular: 0.5- 10 mM Haemophilus influenzae in vitro (21) Streptococcus mutans in vitro (22) Streptococcus pneumoniae in vivo (23) Cysteine/ Cysteine Serum: Listeria monocytogenes in vivo (24) Cystine 33.5 μΜ ystine Serum: Staphylococcus aureus in vitro (11) Escherichia coli in vitro (25) Salmonella enterica in vitro (25) Salmonella enterica in vitro (25) Streptococcus mutans in vitro (26) Methionine Serum: 39.8 μΜ Klebsiella aerogenes in vitro (25) Mycobacterium in vitro (25) tuberculosis Pseudomonas aeruginosa in vitro		o II	Staphylococcus aureus	in vitro	(11)
Plasma: 37.03 Neisseria meningitidis in vitro (18) µM Escherichia coli in vitro (19) Intracellular: 0.5- Salmonella enterica in vitro (20) 10 mM Haemophilus influenzae in vitro (21) Streptococcus mutans in vitro (22) Streptococcus pneumoniae in vivo (23) Cysteine/ Cysteine Serum: Listeria monocytogenes in vivo (24) Cystine 33.5 µM ystine Serum: Staphylococcus aureus in vitro (11) 62.9 µM Campylobacter jejuni in vitro (25) Salmonella enterica in vitro (25) Streptococcus mutans in vitro (26) Methionine Serum: 39.8 µM Klebsiella aerogenes in vitro (25) Mycobacterium in vitro (25) tuberculosis Pseudomonas aeruginosa in vitro	A A	ОН	Clostridium difficile	in vitro	(12)
μΜ Escherichia coli in vitro (19) Intracellular: 0.5- Salmonella enterica in vitro (20) Haemophilus influenzae in vitro (21) Streptococcus mutans in vitro (22) Streptococcus pneumoniae in vivo (23) Cysteine/ Cysteine Serum: Listeria monocytogenes in vivo (24) Cystine 33.5 μΜ ystine Serum: Staphylococcus aureus in vitro (11) 62.9 μΜ Campylobacter jejuni in vitro (15) Escherichia coli in vitro (25) Salmonella enterica in vitro (25) Streptococcus mutans in vitro (26) Methionine Serum: 39.8 μΜ Klebsiella aerogenes in vitro (25) Mycobacterium in vitro (25) tuberculosis Pseudomonas aeruginosa in vitro	≣ NH₂	0	Bordetella pertussis	in vitro	(17)
Intracellular: 0.5- 10 mM Haemophilus influenzae in vitro (21) Streptococcus mutans in vitro (22) Streptococcus pneumoniae in vivo (23) Cysteine/ Cysteine Serum: Listeria monocytogenes in vivo (24) Cystine 33.5 μΜ ystine Serum: Staphylococcus aureus in vitro (11) 62.9 μΜ Campylobacter jejuni in vitro (15) Escherichia coli in vitro (25) Salmonella enterica in vitro (25) Streptococcus mutans in vitro (26) Methionine Serum: 39.8 μΜ Klebsiella aerogenes in vitro (25) Mycobacterium in vitro (25) tuberculosis Pseudomonas aeruginosa in vitro		Plasma: 37.03	Neisseria meningitidis	in vitro	(18)
Haemophilus influenzae in vitro (21) Streptococcus mutans in vitro (22) Streptococcus pneumoniae in vivo (23) Cysteine/ Cysteine Serum: Listeria monocytogenes in vivo (24) Cystine 33.5 μM ystine Serum: Staphylococcus aureus in vitro (11) 62.9 μM Campylobacter jejuni in vitro (15) Escherichia coli in vitro (25) Salmonella enterica in vitro (25) Streptococcus mutans in vitro (26) Methionine Serum: 39.8 μΜ Klebsiella aerogenes in vitro (25) Mycobacterium in vitro (25) tuberculosis Pseudomonas aeruginosa in vitro		μM	Escherichia coli	in vitro	(19)
Streptococcus mutans in vitro (22) Streptococcus pneumoniae in vivo (23) Cysteine/ Cysteine Serum: Listeria monocytogenes in vivo (24) Cystine 33.5 μM ystine Serum: Staphylococcus aureus in vitro (11) 62.9 μM Campylobacter jejuni in vitro (15) Escherichia coli in vitro (25) Salmonella enterica in vitro (25) Streptococcus mutans in vitro (26) Methionine Serum: 39.8 μΜ Klebsiella aerogenes in vitro (25) Mycobacterium in vitro (25) tuberculosis Pseudomonas aeruginosa in vitro			Salmonella enterica	in vitro	(20)
Streptococcus pneumoniae in vivo (23) Cysteine/ Cysteine Serum: Listeria monocytogenes in vivo (24) Cystine 33.5 μM ystine Serum: Staphylococcus aureus in vitro (11) 62.9 μM Campylobacter jejuni in vitro (25) Salmonella enterica in vitro (25) Streptococcus mutans in vitro (26) Methionine Serum: 39.8 μΜ Klebsiella aerogenes in vitro (25) Mycobacterium in vitro (25) tuberculosis Pseudomonas aeruginosa in vitro			Haemophilus influenzae	in vitro	(21)
Cysteine/ Cystine 33.5 μM ystine Serum: Staphylococcus aureus in vitro (11) 62.9 μM Campylobacter jejuni in vitro (25) Salmonella enterica in vitro (25) Streptococcus mutans in vitro (26) Methionine Serum: 39.8 μΜ Klebsiella aerogenes in vitro (25) Mycobacterium in vitro (25) tuberculosis Pseudomonas aeruginosa in vitro			Streptococcus mutans	in vitro	(22)
Cystine 33.5 μM ystine Serum: Staphylococcus aureus in vitro (11) 62.9 μM Campylobacter jejuni in vitro (25) Escherichia coli in vitro (25) Salmonella enterica in vitro (26) Streptococcus mutans in vitro (26) Methionine Serum: 39.8 μΜ Klebsiella aerogenes in vitro (25) Mycobacterium in vitro (25) tuberculosis Pseudomonas aeruginosa in vitro			Streptococcus pneumoniae	in vivo	(23)
ystine Serum: Staphylococcus aureus in vitro (11) 62.9 μM Campylobacter jejuni in vitro (25) Escherichia coli in vitro (25) Salmonella enterica in vitro (26) Streptococcus mutans in vitro (26) Methionine Serum: 39.8 μΜ Klebsiella aerogenes in vitro (25) Mycobacterium in vitro (25) tuberculosis Pseudomonas aeruginosa in vitro	Cysteine/	Cysteine Serum:	Listeria monocytogenes	in vivo	(24)
Campylobacter jejuni in vitro (15) Escherichia coli in vitro (25) Salmonella enterica in vitro (26) Streptococcus mutans in vitro (26) Methionine Serum: 39.8 μΜ Klebsiella aerogenes in vitro (25) Mycobacterium in vitro (25) tuberculosis Pseudomonas aeruginosa in vitro	<u>Cystine</u>	33.5 µM			
Escherichia coli in vitro (25) Salmonella enterica in vitro (25) Streptococcus mutans in vitro (26) Methionine Serum: 39.8 μΜ Klebsiella aerogenes in vitro (25) Mycobacterium in vitro (25) tuberculosis Pseudomonas aeruginosa in vitro	0	ystine Serum:	Staphylococcus aureus	in vitro	(11)
Escherichia coli in vitro (25) Salmonella enterica in vitro (25) Streptococcus mutans in vitro (26) Methionine Serum: 39.8 μΜ Klebsiella aerogenes in vitro (25) Mycobacterium in vitro (25) tuberculosis Pseudomonas aeruginosa in vitro			Campylobacter jejuni	in vitro	(15)
Streptococcus mutans in vitro (26) Methionine Serum: 39.8 µM Klebsiella aerogenes in vitro (25) Mycobacterium in vitro (25) tuberculosis Pseudomonas aeruginosa in vitro	HS'	ОН	Escherichia coli	in vitro	(25)
MethionineSerum: 39.8 μMKlebsiella aerogenesin vitro(25)Mycobacteriumin vitro(25)tuberculosisPseudomonas aeruginosain vitro	NH ₂		Salmonella enterica	in vitro	(25)
Mycobacterium in vitro (25) tuberculosis Pseudomonas aeruginosa in vitro			Streptococcus mutans	in vitro	(26)
tuberculosis Pseudomonas aeruginosa in vitro	Methionine	Serum: 39.8 μM	Klebsiella aerogenes	in vitro	(25)
tuberculosis Pseudomonas aeruginosa in vitro			Mycobacterium	in vitro	(25)
Pseudomonas aeruginosa in vitro	.s.		tuberculosis		-
<u>.</u>		ОН	Pseudomonas aeruginosa	in vitro	
	NH ₂		-		(25)

Table 1-1 (cont'd)

<u>Taurine</u>	Plasma: 55.5 μM	Enterobacteriaceae	in vitro	(27)
H ₂ N	ОН	Staphylococcus aureus [¥]	in vitro	(28)

^{*} Plasma and serum levels of sulfur-containing metabolites were obtained from the following references: (2, 3, 29–32). Metabolite concentrations in other tissues can be found using the Human Metabolome Database (33).

Organosulfur acquisition

The abundance of organosulfur metabolites in the host makes these potential sulfur sources attractive targets for pathogens. These organosulfur molecules include: Cys, oxidized Cys (referred to as cystine), glutathione (GSH), methionine, and taurine. An advantage of organosulfur utilization is that the molecules are typically more efficiently processed to Cys than inorganic sulfur, requiring only one or two enzymatic steps (Fig. 1-1). In species that use both organic and inorganic sulfur sources, such as Escherichia coli, exogenous Cys is a competitive inhibitor of serine O-acetyltransferase (Fig. 1-1 #10) (25). Transcription of other sulfate assimilation genes is repressed by 0.5 mM cystine and various organosulfur molecules (35, 36). These findings suggest that cells coordinate inorganic and organic sulfur source acquisition strategies. However, numerous pathogens including Listeria monocytogenes, Clostridium perfringens, Legionella pneumophila, Bordetella pertussis, Neisseria gonorrhoeae, S. aureus, and the streptococci are Cys auxotrophs due to incomplete sulfate assimilation pathways (11, 12, 17, 25, 37–40). S. aureus, for example, does not encode ATP sulfurylase, APS kinase, or PAPS reductase and is therefore unable to use sulfate as a source of sulfur. S. aureus is capable of consuming sulfide or thiosulfate as these inorganic sulfur sources can be converted to substrates for the OAS sulfhydrylases (11). Notably, a mutant strain that is limited in its ability to use sulfide

[±] 'in vitro' indicates the cells proliferate in laboratory defined medium when the sulfur-containing metabolite is supplemented as the sole source of sulfur. 'in vivo' denotes those mutant strains lacking sulfur source acquisition systems demonstrate virulence defects in an animal model of infection.

^{*} Conflicting data demonstrating that taurine is not a viable sulfur source for *S. aureus* is reported in references (28, 34).

or thiosulfate as sulfur sources via genetic inactivation of *cysM* is as virulent as WT [11]. This result implies that *S. aureus* does not assimilate these inorganic molecules during infection and supports the hypothesis that the pathogen predominantly acquires organosulfur sources to proliferate within the host (11). In keeping with this hypothesis, the organosulfur sources Cys, cystine, and GSH are viable sources of sulfur for *S. aureus* (11). The fact that many pathogens seem to have lost, or never evolved, the ability to assimilate sulfate underscores the importance of organosulfur metabolites as potential sources of nutrient sulfur during infection.

Cysteine (Cys) and Cystine (CSSC)

Cys is a precursor for a number of sulfur-containing cofactors and many pathogens use it as a sulfur source (Table 1-1) (11, 15, 24, 38, 41). CSSC is also a viable sulfur source for pathogens, but the disulfide bond between the two Cys molecules must be reduced (Fig. 1-1 # 13, Table 1-1 (25, 26)). Cys transporters have been difficult to identify due to the inherent redundancy of amino acid transporters (42). Consequently, assessing the importance of Cys acquisition to pathogenesis has been a challenge. A possible exception is L. monocytogenes, a Cys auxotroph due to a complete lack of the sulfate assimilation pathway (Fig 1-1 #1-4) (41, 43). Mutation of the Cys-transport-associated protein CtaP, a putative substrate binding protein, reduces proliferation in a minimal defined medium [22]. Supplementation of the medium with high concentrations of Cys restores growth of the mutant, providing evidence that CtaP functions in concert with a high affinity Cys importer (24). Consistent with this, a putative ABC-transporter (Imo0136-0137) is encoded adjacent to ctaP (44). Lmo0136-0137 is required for L. monocytogenes replication within Caco-2 cells and the ctaP mutant is attenuated in a murine model of systemic infection (24, 44). CtaP also functions as a host cell adhesin, making it difficult to discern whether the virulence defect of the ctaP mutant is due to loss of a high affinity Cys importer, impaired host cell attachment, or both (24). Although additional biochemical validation

of the CtaP-Lmo0136-0137 transport system is required, it is tempting to speculate that acquisition of Cys is a requirement for intracellular growth and pathogenicity of *L. monocytogenes*.

Methionine (Met)

The other proteinogenic sulfur-containing amino acid, Met, is also an *in vitro* sulfur source for a subset of pathogens. To satisfy the sulfur requirement, Met must undergo sequential recycling reactions that ultimately produce Cys (14). The recycling pathway proceeds from *S*-adenosyl Met, which becomes *S*-adenosyl homocysteine (SAH) after undergoing the methyl transfer reaction. SAH is converted to homocysteine (Fig. 1-1 # 9 and # 16), and through a reverse trans-sulfuration reaction, homocysteine is converted to Cys (Fig. 1-1 #7 and #6) (14, 25, 45). *Klebsiella aerogenes, M. tuberculosis*, and *Pseudomonas aeruginosa* recycle Met, enabling growth on Met as a sole sulfur source (25). Consistent with this, *M. tuberculosis* and *K. aerogenes* import Met *in vitro* and *P. aeruginosa* encodes homologs of Met transporters present in *E. coli* (14, 45–47). However, evidence that the pathogens utilize Met as a source of sulfur during infection is lacking.

Glutathione (GSH)

GSH is a potent antioxidant in host and bacterial cells (2, 48). GSH contains a reactive thiol in the form of Cys, one of the three amino acids that comprise the tripeptide. A glutamate residue is bound to Cys via a unique γ -bond between the R group carboxyl of glutamate and the amino group of Cys. Glycine, the third amino acid, is covalently linked to Cys via a standard peptide bond. GSH functions as a low molecular weight thiol by fluctuating between reduced and oxidized (GSSG) states. In the oxidized state, a disulfide bond adjoins two GSH via the Cys thiols. Within eukaryotic cells, GSH levels range from 0.5-10 mM and are kept at a strict GSH:GSSG ratio (2, 49). On average, human plasma levels of GSH exceed GSSG nearly 30-fold (37.03 μ M and 1.69 μ M, respectively) (Table 1-1) (32). The host spends considerable energy maintaining

GSH levels greater than GSSG. This allows for maximal reactivity of the thiol groups to detoxify reactive oxygen species and other poisons (2, 49).

GSH abundance makes it an ideal source of sulfur and numerous pathogens express transporters that scavenge the plentiful nutrient (Table 1-1). Upon import, liberation of Cys from GSH proceeds via glutamyl-transpeptidase (Ggt) (Fig. 1-1 #14), an enzyme that cleaves the γ-peptide bond releasing glutamate and producing cysteinyl-glycine (2). Cysteinyl-glycine is subsequently processed by peptidases that release Cys from glycine (Fig. 1-1 #15) (2, 50). The unique γ-peptidase activity of Ggt is required to initiate utilization of GSH as a sulfur source and a subset of pathogens encode Ggt (Table 1-1). For example, Ggt is required during *Francisella tularensis* infection as the enzyme cleaves host GSH to produce Cys, fulfilling the sulfur requirement, and driving intracellular proliferation (16).

Taurine

The non-proteinogenic amino acid taurine is abundant in many mammalian tissues but is predominately found complexed to bile salts within the intestines (51). Consequently, members of *Enterobacteriaceae* scavenge taurine for use as a sulfur source (27). Taurine is a substrate for α-ketoglutarate-dependent dioxygenase, an enzyme that produces aminoacetaldehyde and sulfite (Fig. 1-1 #17) which is then processed to sulfide by sulfite reductase (Fig. 1-1 #4) (25). It is unclear whether taurine is a viable sulfur source for non-enteric pathogens such as *S. aureus*. Published findings contradict the capacity of taurine to stimulate *S. aureus* growth in a sulfur deplete medium (28, 34). The fact that *S. aureus* lacks an α-ketoglutarate dependent dioxygenase homologue supports the supposition that taurine is not a viable sulfur source for this pathogen (28).

Frontiers in pathogen nutrient sulfur acquisition

Mammals lack the ability to synthesize Cys from inorganic sulfur; consequently Cys and Met are obtained from the diet (52). Therefore, bacterial sulfate assimilation and Cys synthesis have gained considerable interest as a potential therapeutic strategy to combat infection (53–56) (reviewed in reference (57)). An *in silico* screen identified inhibitors of both *Salmonella* OAS sulfhydrylase isozymes (Fig. 1-1 #5 and #11) as potent *in vitro* antimicrobials (53). OAS sulfhydrylase inhibitors are also being developed for the treatment of infections caused by *M. tuberculosis* (reviewed in reference (58)) and other bacterial pathogens (56, 59–61).

The enzyme APS reductase, which functions in *M. tuberculosis* sulfate assimilation (Fig. 1-1 #14), is also gaining interest as an antibacterial drug target (62). APS reductase inhibitors result in significantly reduced levels of downstream sulfur-containing metabolites, and these compounds display bactericidal activity (62). The *in vivo* efficacy of sulfate assimilation and Cys synthesis inhibitors has yet to be established. As discussed, most pathogens encode redundant nutrient sulfur procurement strategies that exploit host-derived organosulfur metabolites, so inhibiting sulfate assimilation may not be, ultimately, a successful strategy.

Evidence is mounting that some pathogens prefer organosulfur sources, and Cys auxotrophs are isolated from a surprising number of clinical samples derived from patients infected with bacterial species capable of sulfate assimilation (63–66). Prominent examples are Uropathogenic *E. coli* (UPEC), as 1.5 to 2% of clinical isolates are Cys auxotrophs (66), and subsets of *Klebsiella* urinary tract infection isolates are also Cys auxotrophs (65). Loss of Cys synthesis supports the hypothesis that during infection these pathogens have access to reservoirs of host Cys or Cys derivatives, obviating the need for endogenous Cys synthesis via sulfate assimilation. Urine contains a relatively high concentration of free Cys (65.8 µmol mmol⁻¹ creatinine) (67), but Cys auxotrophs are also found among pathogens that colonize different host environments. Sub-populations of *Burkholderia cepacia* isolated from patients afflicted with cystic fibrosis and a subset of *Micrococcus* isolates, a skin commensal, are also Cys auxotrophs (63,

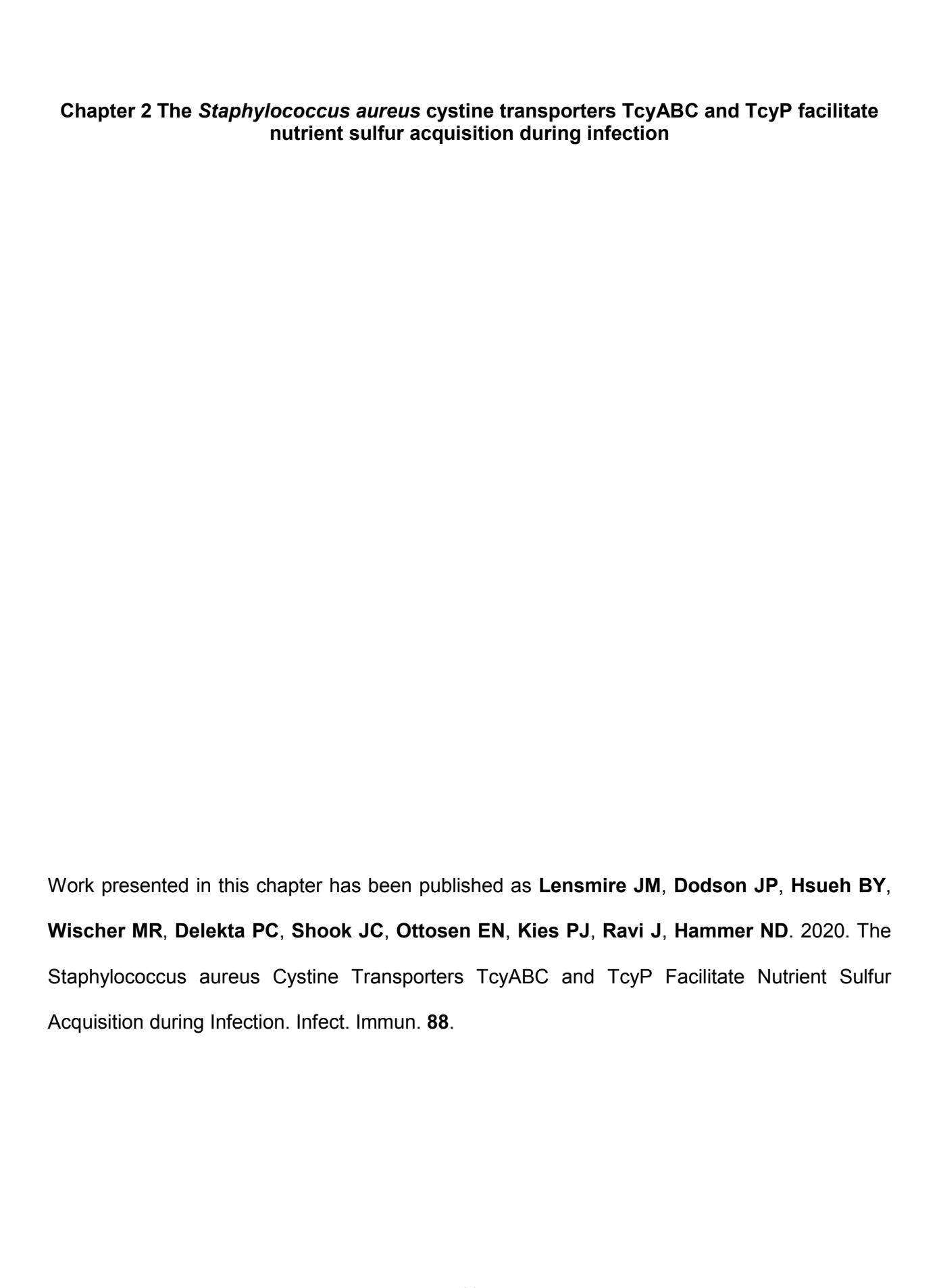
64). The prevalence of Cys auxotrophs and the diversity of sulfur sources available during infection suggests that pathogens will evade therapeutic interventions that exclusively target *de novo* Cys synthesis from inorganic sulfur sources. As the field of pathogen nutrient sulfur acquisition is just beginning to take shape, additional studies are needed to reveal the frequency of Cys auxotroph isolation in other notable bacterial diseases. These findings will define the therapeutic potential and efficacy of targeting *de novo* Cys synthesis and sulfate assimilation to treat bacterial infections.

Concluding remarks

Historically sulfur acquisition has been an understudied area in the field of pathogen nutrient acquisition. Reports described herein have considerably increased our knowledge of nutrient sulfur sources beyond sulfate by revealing that numerous pathogens that lack sulfate assimilation can use organosulfur sources. Future studies focused on defining sulfur source acquisition mechanisms and determining their importance in animal models of infection will elucidate novel avenues for the therapeutic intervention of increasingly antibiotic resistant pathogens.

Acknowledgments

We acknowledge Hammer laboratory members, Dr. Victor DiRita (MSU), and Dr. Chris Waters (MSU) for thoughtful and critical discussion of the manuscript. Funding was provided by Michigan State University and an American Heart Association Scientist Development Grant [16SDG30170026]. We apologize to colleagues whose work was not included due to space restrictions.



Abstract

S. aureus is a significant human pathogen due to its capacity to cause a multitude of diseases. As such, S. aureus efficiently pillages vital nutrients from the host, however, the molecular mechanisms that support sulfur acquisition during infection have not been established. One of the most abundant extracellular sulfur-containing metabolites within the host is Cys, which acts as the major redox buffer in the blood by transitioning between reduced and oxidized (cystine) forms. We therefore hypothesized that S. aureus acquires host-derived Cys and cystine as sources of nutrient sulfur during systemic infection. To test this hypothesis, we used the toxic cystine analogue, selenocystine, to initially characterize S. aureus homologues of the Bacillus subtilis cystine transporters, TcyABC and TcyP. We find that genetic inactivation of both TcyA and TcyP induces selenocystine resistance. The double mutant also fails to proliferate in medium supplemented with cystine, cysteine, or N-acetyl cysteine as the sole sulfur source. However, only TcyABC is necessary for proliferation in defined medium containing homocystine as the sulfur source. Using a murine model of systemic infection, we observe tcyP-dependent competitive defects in the liver and heart, indicating that this sulfur acquisition strategy supports proliferation of S. aureus in these organs. Phylogenetic analyses identified TcyP homologues in many pathogenic species, implying that this sulfur procurement strategy is conserved. In total, this study is the first to experimentally validate sulfur acquisition systems in S. aureus and establish their importance during pathogenesis.

Introduction

Methicillin-resistant *S. aureus* (MRSA) is endemic in hospital and community settings in the United States and is the leading cause of morbidity and mortality resulting from infections with antibiotic resistant bacteria (68–70). This stems from the fact that *S. aureus* infection can lead to wide-ranging disease manifestations, including skin and soft tissue infections, infective endocarditis, sepsis, osteomyelitis, and pneumonia (71, 72). In addition to invasive disease, *S.*

aureus innocuously colonizes the skin and nasal passages of 30% of the population (73–76). Together, these facts highlight the dynamic tissue tropism of this organism.

During infection, pathogens must procure nutrients from host environments. The mechanisms *S. aureus* employs to acquire carbon sources and trace metals during infection are becoming increasingly clear (77–84). However, a complete understanding of the physiology that contributes to the persistence and invasiveness of *S. aureus* is imperative to control infection. Therefore, impairing nutrient acquisition offers potential for therapeutic intervention. *S. aureus* employs a sophisticated metabolism that allows it to both persist during nasal carriage and proliferate to cause systemic disease (85–91). One clear deficiency in our knowledge of *S. aureus* nutrient acquisition is the strategy by which the pathogen scavenges sulfur during infection.

Sulfur is an essential building block for life because it transitions between numerous oxidation states allowing for broad functionality (1). Once sulfur is assimilated to a functional oxidation state, most cells flux sulfur to Cys and Met to generate other sulfur-containing compounds (1, 2, 5). The sulfur demand for a cell is sizable due to the many sulfur-containing compounds required to synthesize proteins and power central metabolism. Consequently, E. coli imports 2.2 mM min⁻¹ of sulfur to support a growth rate of 0.0173 min⁻¹ (92). To fulfill the sulfur requirement some bacteria utilize two broad categories of sulfur-containing substrates: inorganic sulfur sources that include sulfate and thiosulfate or organosulfur sources such as methionine, Cys, and others (93). S. aureus lacks enzymes necessary to assimilate sulfate and consequently it cannot convert sulfate to sulfite (11, 25, 28). Accordingly, S. aureus relies on select inorganic sulfur sources, such as thiosulfate, or organosulfur sources to satisfy its sulfur requirement. Previous studies have shown S. aureus acquires CSSC, Cys, GSH, sulfide, and thiosulfate as sulfur sources in vitro (11), but how S. aureus imports and catabolizes these metabolites is not known. Consistent with this, sulfur transporters have yet to be experimentally validated in S. aureus, despite the fact that it likely encounters many potential sulfur sources during dissemination from the bloodstream to various internal organs (94). For example, human serum

contains CSSC, Cys, homocysteine, cysteinyl-glycine, GSH, sulfate, sulfide, and Met (30, 95), but whether these potential sources of sulfur satisfy the sulfur requirement *in vivo* is not known.

To understand how *S. aureus* fulfills its sulfur requirement we evaluated two putative CSSC transporters encoded by the closely related bacterium *Bacillus subtilis*, TcyABC and TcyP. (26, 42, 96). *B. subtilis* encodes three CSSC transporter systems: TcyP, TcyJKLMN, and TcyABC. TcyABC is a low-affinity ATP-binding cassette (ABC) transporter whereby the lipid anchored substrate-binding protein TcyA delivers substrate to the permease, TcyB, which is then translocated aided by the hydrolysis of ATP by TcyC into the cytoplasm (42). *B. subtilis* TcyP is a high-affinity CSSC and sodium symporter (42). Whether *S. aureus* TcyABC and TcyP act in similar ways to the *B. subtilis* homologues is unknown; though, studies have reported that *tcyABC* and *tcyP* are transcriptionally controlled by the master Cys metabolism regulator CymR in both organisms (28, 97–99).

We hypothesized that TcyABC and TcyP facilitate *S. aureus* CSSC utilization as a sulfur source *in vivo*. To test this hypothesis, we utilized a genetic approach to characterize *tcyA* and *tcyP* mutants in two different strain backgrounds, the laboratory-derived methicillin-resistant strain endemic in the United States, community-acquired USA300 (JE2), and the methicillin-sensitive strain Newman (NWMN) (100, 101). We report the first experimental evidence that *S. aureus tcyABC* and *tcyP* encode CSSC acquisition systems. Additionally, we demonstrate that TcyABC and TcyP are required for growth in media supplemented with Cys or *N*-acetyl cysteine (NAC) as the sole sulfur source. Moreover, TcyABC supports proliferation in medium supplemented with homocystine (hCSSC). Expression of both systems is induced upon sulfur starvation, but *tcyP* expression is stimulated to a greater extent. Notably, our results implicate TcyABC and TcyP as nutrient sulfur acquisition systems that are important during *S. aureus* pathogenesis. This study represents the first-time sulfur source transporters have been experimentally validated and demonstrated to affect *S. aureus* virulence.

Results

Genetic inactivation of tcyA increases resistance to the toxic CSSC analogue selenocystine.

S. aureus encodes homologues of two of the three CSSC transporter systems present in B. subtilis, TcyABC and TcyP (42). Functional characterization of the CSSC transporters in B. subtilis was determined using the toxic CSSC analogue selenocystine (42). In B. subtilis, enhanced resistance to selenocystine correlated with reduced capacity to transport CSSC. We hypothesized the S. aureus tcyABC homologue is a CSSC transporter, and that genetic inactivation would lead to decreased sensitivity to selenocystine. To test this hypothesis, we compared selenocystine sensitivity of a wildtype USA300 methicillin-resistant strain to an isogenic tcyA::Tn mutant using a Kirby Bauer disk diffusion assay. The tcyA::Tn strain demonstrates a reduced zone of inhibition compared to WT, indicating TcyA has a potential role in selenocystine acquisition (Fig. 2-1A). However, the fact that tcyA::Tn displays a zone of inhibited growth, suggests that TcyABC is not the exclusive putative transporter in S. aureus. To test this idea, we incubated the selenocystine plates for an additional amount of time and examined them for the presence of resistant colonies within the zone of inhibited growth. We reasoned colonies able to grow in the zone of inhibition harbor mutations in additional transporters allowing them grow in the presence of the toxic metabolite. After four days of incubation resistant colonies grew within the WT and tcyA::Tn zones of inhibited growth (Fig. 2-1B and C). Colonies generated in the tcyA::Tn mutant background grew closer in proximity to the selenocystine-containing disk than colonies of the otherwise WT background (Fig. 2-1C), indicating that the tcyA::Tn colonies are more resistant than the WT colonies.

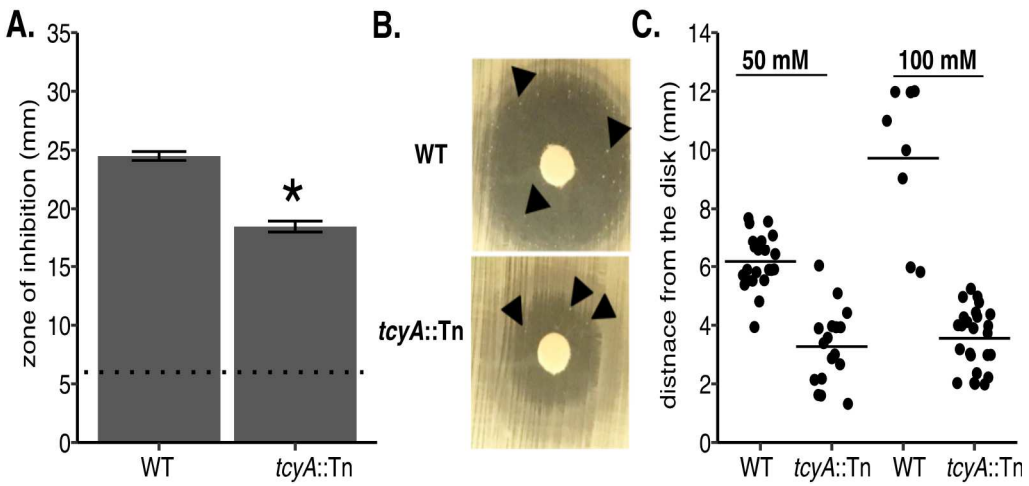


Figure 2-1. A *S. aureus tcyA* mutant demonstrates enhanced resistance to the toxic cystine analogue selenocystine.

(A) WT and *tcyA*::Tn were plated as a lawn on tryptic soy agar (TSA) and a paper disk supplemented with 100 mM selenocystine was added to the plate. The mean zone of inhibition of at least three independent trials is presented. The dotted line represents the disk diameter (6 mm). (B) Colonies develop within the zone of inhibition after 96 hours of growth when WT or *tcyA*::Tn are plated in the presence of 50 mM selenocystine. Arrows point to resistant colonies. (C) Selenocystine resistant WT or *tcyA*::Tn colonies grew the indicated distance from a sterile Whatman paper disk containing 50 mM or 100 mM selenocystine. The bar represents the mean distance from the disk. Error bars represent ± 1 standard error of the mean. * Indicates P<0.05 determined from student's t-test.

Similar selenocystine resistant results were obtained using the methicillin-sensitive strain Newman (NWMN) and an isogenic *tcyA* transposon (*tcyA*::Tn) mutant (Fig. A-1), demonstrating functional conservation between *S. aureus* strains. The JE2 *tcyA*::Tn selenocystine resistant colonies were isolated and tested for selenocystine resistance. All the isolates demonstrate nearly complete resistance to selenocystine, indicating that the strains likely contain inactivating mutations in at least one other transporter (Fig. 2-2A). Next, we tested the effect the secondary mutations had on the ability of isolates to grow in defined medium (PN) containing CSSC. Selenocystine resistant *tcyA*::Tn mutants display reduced growth in medium containing CSSC relative to the parental *tcyA*::Tn mutant (Fig. 2-2B). Together these data suggest that TcyABC is a major contributor to selenocystine sensitivity in *S. aureus* but that another transporter system(s) that is not required for growth in rich medium is also active.

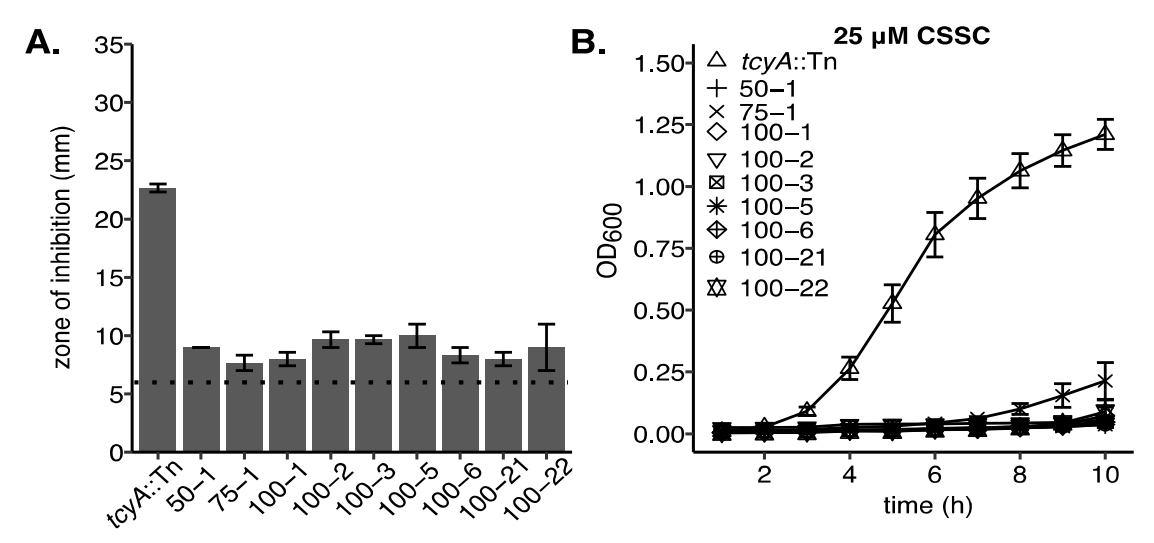


Figure 2-2. Selenocystine resistant colonies in *tcyA*::Tn background maintain resistance to selenocystine.

(A) Representative tcyA::Tn selenocystine resistant colonies were isolated and tested for their resistance in the presence of 100 mM selenocystine. The first number indicates the concentration of selenocystine (50 mM, 75 mM or 100 mM) added to the Whatman disk to the plate the mutants first appeared, and the second number represents the isolate number from that concentration of selenocystine. The dotted line represents the disk diameter (6 mm). (B) Growth of tcyA::Tn selenocystine resistant mutants in 25 μ M cystine. Data represents the mean of at least three independent trials. Error bars represent \pm 1 standard error of the mean.

Table 2-1. Mutations identified in the *tcyP* opening reading frame of *tcyA*::Tn selenocystine resistant mutants.

isolate	mutation	protein effect
50-1	Deletion 580-591 (12bp)	non-frameshift
75-1	G593A	G198E
100-2	Deletion 715-777 (63bp)	non-frameshift
100-3	Deletion 799-802 (4bp)	frameshift

Disruption of both tcyA and tcyP leads to complete selenocystine resistance and reduced growth in a defined medium supplemented with CSSC as the sole sulfur source.

We hypothesized that the selenocystine resistant *tcyA*::Tn mutants harbor mutations in the *tcyP* open reading frame or promoter sequence. To test this, we sequenced the *tcyP* locus in nine of these mutants. All nine harbored WT *tcyP* promoter sequence (data not shown); however, four isolates contained mutations within the *tcyP* open reading frame. The mutation identified in

each isolate was unique and included a nonsynonymous point mutation, two non-frameshift deletions, and a frameshift deletion (Table 2-1).

These mutations likely inactivate TcyP as they promote selenocystine resistance and disrupt the ability of tcyA::Tn to proliferate in medium supplemented with CSSC. (Fig. 2-1 and Fig. 2-2). To further define the contribution of both transporters in S. aureus selenocystine resistance and CSSC acquisition, we generated a tcyA::Tn tcyP::Tn (tcyAP::Tn) double mutant. Compared to WT, the tcyP::Tn single mutant exhibits similar selenocystine sensitivity, but the tcyAP::Tn double mutant demonstrates considerably enhanced resistance (Fig. 2-3A). Comparable selenocystine resistance results were obtained using a tcyAP::Tn generated in strain NMWN (Fig. A-2). These results indicate that tcyABC and tcyP are the dominant selenocystine acquisition systems in S. aureus. To directly test the hypothesis that tcyABC and tcyP are CSSC acquisition systems, we cultured the strains in PN supplemented with 25 μ M CSSC as the sole sulfur source. WT, tcyA::Tn, and tcyP::Tn display similar growth patterns in this medium; however, tcyAP::Tn demonstrates significantly impaired proliferation relative to WT and the single mutants (Fig. 2-3B). Notably, in rich medium the four strains grow similarly, indicating the proliferation defect of tcyAP::Tn is specific to an inability to utilize CSSC as a source of sulfur (Fig. 2-3C). To ensure the selenocystine resistance of tcyAP::Tn is due in part to tcyP or tcyABC inactivation, we constructed complementation vectors encoding tcyP or tcyABC under the control of their native promoters (pKK22 P_{tcvP} ::tcvP or pKK22 P_{tcvABC} ::tcvABC, respectively). The tcvAP::Tn strain harboring pKK22 P_{tcyP}::tcyP or pKK22 P_{tcyABC}::tcyABC demonstrates increased sensitivity to selenocystine (Fig. A-3A). Additionally, ectopic expression of tcyP or tcyABC restores growth of the tcyAP mutant in PN medium supplemented with 25 µM CSSC to WT levels (Fig. A-3B, C). These data validate the roles of TcyP and TcyABC in selenocystine resistance and CSSC utilization.

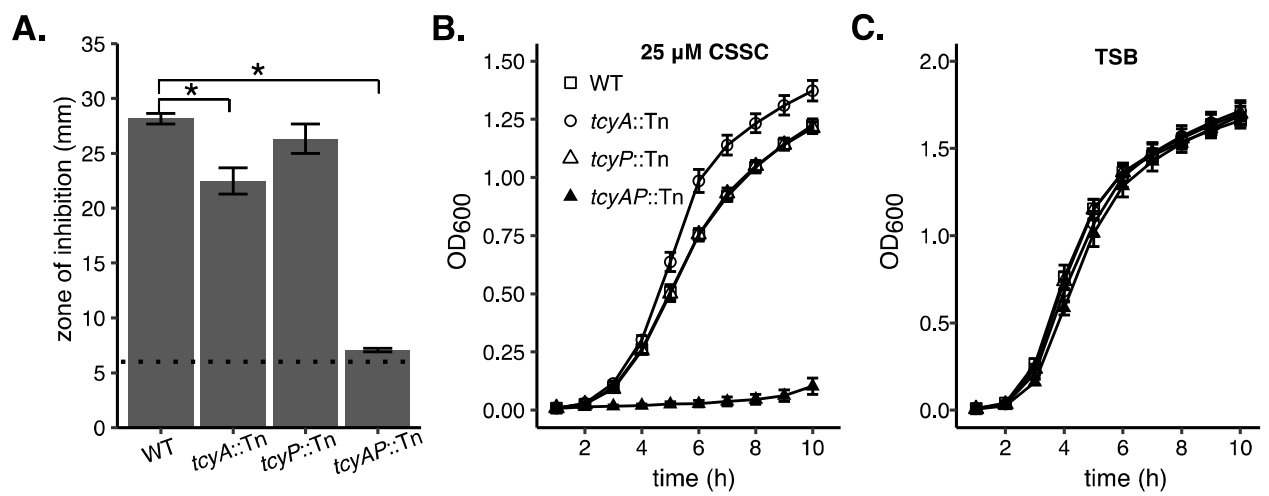


Figure 2-3. TcyABC and TcyP are required for sensitivity to selenocystine and utilization of cystine as a nutrient sulfur source.

(A) WT and *tcyA*::Tn were plated on a lawn on TSA and a disk supplemented with 100 mM selenocystine was added to the plate. The mean zone of inhibition of at least three independent trials is presented. The dotted line represents the disk diameter (6 mm). (B) WT, *tcyA*::Tn, *tcyP*::Tn, and *tcyA tcyP* (*tcyAP*::Tn) double mutant were cultured in PN medium supplemented with 25 μM cystine as the sole sulfur source. (C) WT, *tcyA*::Tn, *tcyP*::Tn, and *tcyAP*::Tn were cultured in TSB. Measurements represent at least three independent trials. Error bars represent ± 1 standard error of the mean. * Indicates *P*<0.05 determined from student's t-test.

S. aureus TcyABC and TcyP support proliferation in medium containing Cys or N-acetyl cysteine as the sole source of sulfur.

Some bacterial ABC-transporters are capable of transporting both dimeric and monomeric substrates (26, 42). For example, in *Streptococcus mutans* TcyABC-mediated import of CSSC is inhibited by Cys, indicating that TcyABC is capable of binding and transporting both substrates (26). To test whether TcyABC and TcyP are important for *S. aureus* utilization of monomeric substrates such as Cys, we quantified growth in media supplemented with Cys as the sole source of sulfur. Because Cys is prone to oxidation in environments containing O₂, quantification of growth was carried out in anaerobic conditions in medium containing the alternative electron acceptor nitrate to stimulate anaerobic respiration. Consistent with the results obtained in aerobic conditions, *tcyAP*::Tn was the only strain that displayed a growth defect relative to WT when CSSC is supplemented as the sole sulfur source (Fig. 2-4A). Similarly, *tcyAP*::Tn exhibits reduced anaerobic growth relative to WT and the two single mutants in PN supplemented with Cys (Fig.

2-4B). This observation indicates that both TcyABC and TcyP support growth on Cys and are functioning redundantly. The capacity of TcyABC and TcyP to support growth on CSSC and Cys implies an extended substrate-binding potential. To test this further, we examined whether both systems support proliferation in medium supplemented with NAC a Cys-containing metabolite present in human blood (102). We cultured *S. aureus* WT and *tcyA*::Tn, *tcyP*::Tn, or *tcyAP*::Tn mutants in PN supplemented with 50 μM NAC. In keeping with the previous CSSC and Cys results, only proliferation of *tcyAP*::Tn is reduced relative to WT (Fig. 2-4C). Notably, WT *S. aureus* achieves a greater maximum OD₆₀₀ in PN medium containing CSSC relative to PN containing Cys or NAC despite the addition of stoichiometrically equivalent levels of sulfur. These results imply that CSSC is the preferred sulfur source of *S. aureus* in these growth conditions.

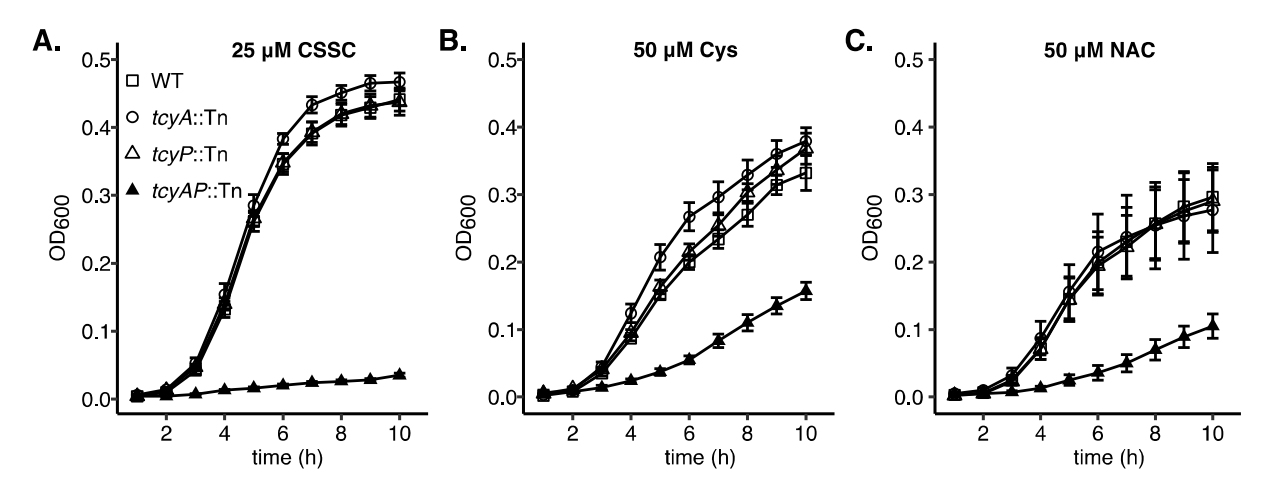


Figure 2-4. TcyABC and TcyP support proliferation in medium supplemented with cysteine (Cys) or *N*-acetyl-cysteine (NAC) as the sole sulfur sources. WT, tcyA::Tn, tcyP::Tn, or tcyAP::Tn were cultured anaerobically in PN medium supplemented with 100 mM sodium nitrate to induce anaerobic respiration and 25 μ M cystine (A), 50 μ M cysteine (B), or 50 μ M *N*-acetyl-cysteine (C) as the sole sulfur source. The mean of at least three independent trials is presented, error bars represent ± 1 standard error of the mean.

TcyABC supports growth on homocystine (hCSSC) but not glutathione.

To further define potential TcyABC and TcyP substrates, we monitored growth of WT, tcyA::Tn, tcyP::Tn, or tcyAP::Tn in PN medium supplemented with hCSSC, the oxidized derivative of homocysteine, a four-carbon compound that is an intermediate in the methionine synthesis pathway. Homocysteine directly enters *S. aureus* sulfur metabolism and can be fluxed to Cys or

methionine (4, 25, 28). Based on the structural similarity between hCSSC and CSSC, we hypothesized that TcyABC supports growth on hCSSC. To test this, 50 μM hCSSC was supplemented in PN medium as the sole sulfur source. In the hCSSC-supplemented medium, *tcyA*::Tn and *tcyAP*::Tn fail to proliferate (Fig. 2-5B), indicating that TcyABC but not TcyP is involved in hCSSC acquisition.

In *S. mutans* import of the Cys-containing tripeptide glutathione (GSH) is mediated by the TcyBC permease and ATP hydrolysis subunits (22). We tested whether *S. aureus* TcyABC could also be involved in the acquisition of GSH as a sulfur source by culturing WT, *tcyA*::Tn, *tcyP*::Tn,

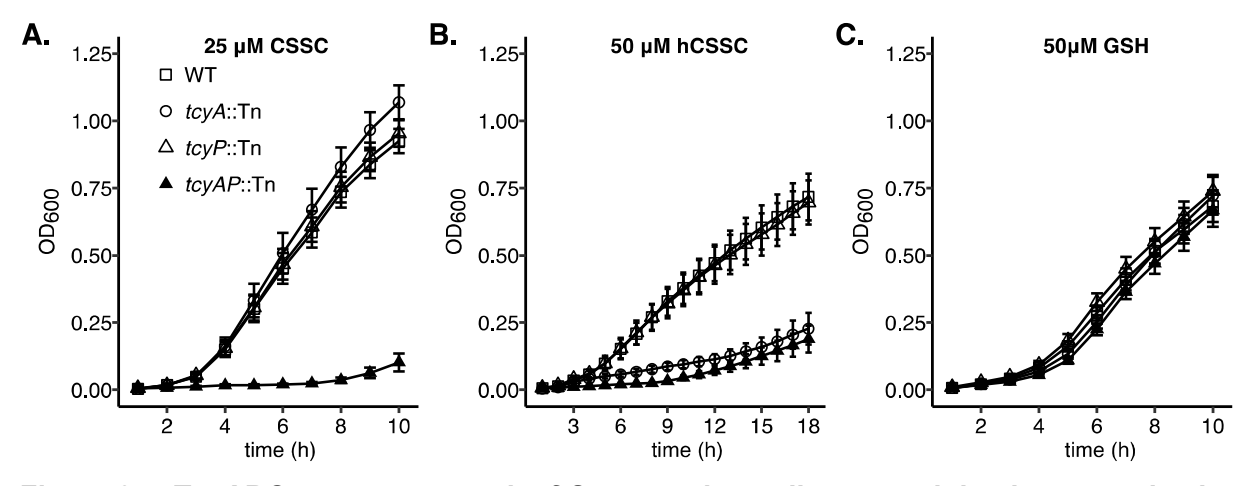


Figure 2-5. TcyABC supports growth of *S. aureus* in medium containing homocystine but not GSH as a sulfur source.

WT, tcyA::Tn, tcyP::Tn, or tcyAP::Tn were cultured in PN supplemented with 25 μ M cystine (CSSC) (A), 50 μ M homocystine (hCSSC) (B), or 50 μ M reduced glutathione (GSH) (C) as the sole source of sulfur. Error bars represent \pm 1 standard error of the mean. The average of at least three independent trials is presented.

or tcyAP::Tn in medium containing 50 μ M GSH. Compared to the differential growth patterns in the other sulfur sources, no difference is observed between WT and mutant growth in PN with GSH (Fig. 2-5C), indicating that neither transporter is required for GSH utilization as a source of sulfur.

tcvP and tcvA are induced in sulfur starvation conditions.

The transcription of *tcyP* and *tcyA* are controlled by the sulfur regulator, CymR (28, 97). A limitation of the previous CymR studies is that they monitored expression in sulfur replete conditions using a *cymR* mutant. To understand how *tcyP* and *tcyA* expression changes in

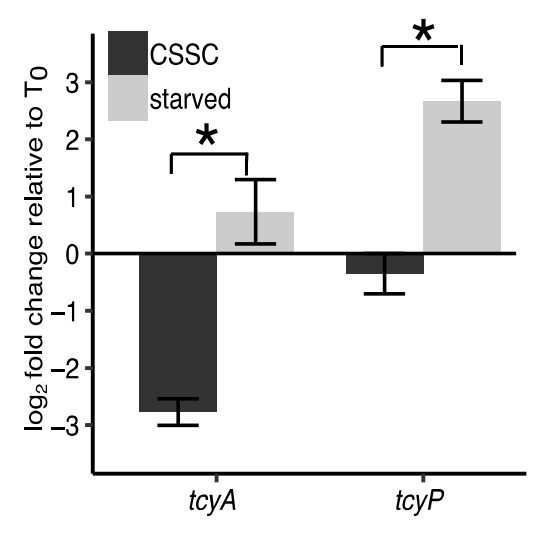


Figure 2-6. *tcyP* and *tcyA* are induced in sulfur starvation conditions.

The comparative $\Delta\Delta C_T$ methodology was used to calculate fold change and *rho* was used as a reference gene. Log₂ fold change of *tcyA* and *tcyP* transcripts relative to T₀ were determined. *S. aureus* was cultured in PN supplemented with 25 μ M CSSC and then transferred to medium containing 25 μ M CSSC or no sulfur source (starved). Bars represent the mean of at least 3 independent trials. The error bars represent \pm 1 standard error of the mean. * Indicates *P*<0.05 determined from student's t-test.

response to sulfur starvation, we sub-cultured cells from a sulfur replete medium to sulfur deplete medium. Specifically, *S. aureus* was cultured in PN supplemented with 25 μ M CSSC (T₀) and then transferred to PN medium supplemented with 25 μ M CSSC (sulfur replete) or a medium devoid of a sulfur source. We found that tcyP and to a lesser extent tcyA are significantly upregulated in response to sulfur starvation relative to sulfur replete medium as determined by a greater log_2 fold change after two hours of incubation (Fig. 2-6). Interestingly, tcyA is repressed when *S. aureus* is transferred from CSSC-supplemented medium into fresh medium containing CSSC (Fig. 2-6). These data demonstrate that tcyP and tcyA expression are responsive to the abundance of sulfur in the environment.

TcyP is required for maximal fitness in the murine liver while TcyABC and TcyP are required for maximal fitness in the murine heart.

The role of sulfur source acquisition systems during *S. aureus* pathogenesis has not been elucidated. Additionally, how TcyP and TcyABC support the proliferation of a bacterial pathogen in any infection model has not been described. We hypothesized that TcyP and TcyABC function cooperatively to satisfy the *S. aureus* sulfur requirement *in vivo*. To test this, we performed competition infections between NWMN WT and isogenic *tcyA*::Tn, *tcyP*::Tn, or *tcyAP*::Tn mutants in a murine model of systemic infection (103). The competitive index in the liver demonstrates that *tcyP*::Tn is outcompeted by WT (Fig. 2-7A, B). *tcyA*:Tn does not display a competitive defect in the heart, liver or kidneys. Neither single utant exhibits reduced fitness in the heart, however,

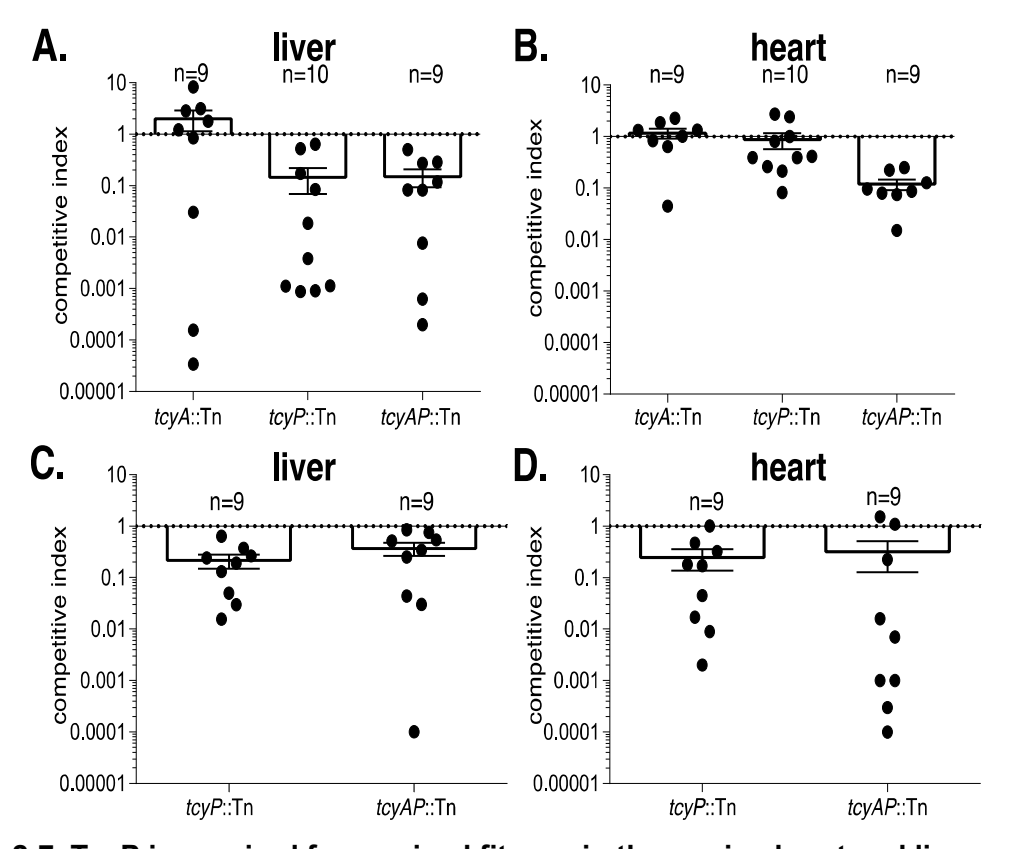


Figure 2-7. TcyP is required for maximal fitness in the murine heart and liver. Balb/c Mice were systemically infected with a 1:1 ratio WT and the indicated mutant strain in Newman (A-B) or JE2 (C-D). Competitive indices were calculated as the output ratio of mutant to WT CFU mL⁻¹ over the input mutant to WT CFU mL⁻¹. The mean competitive index for liver (A and C) and heart (B and D) are presented. Error bars represent ± 1 standard error of the mean.

the tcyAP double mutant displays a competitive defect in this organ. Collectively, these data

indicate that *S. aureus* NWMN sulfur acquisition is mediated predominantly by TcyP in the liver and that TcyABC is capable of compensating for the loss of TcyP in the heart.

To determine if the involvement of TcyP and TcyABC during infection is similar between *S. aureus* strains we repeated the competition infections using the USA300 derivative JE2 (100). Due to the lack of an observed competitive defect for the NWMN *tcyA*::Tn mutant we excluded this mutant from the JE2 competition studies. Consistent with the results using NWMN, the competitive index in the liver demonstrates that *tcyP*::Tn is outcompeted by WT (Fig. 2-7C). Additionally, *tcyP*::Tn demonstrates a competitive defect in the murine heart (Fig. 2-7D). These data demonstrate that *S. aureus* sulfur acquisition in JE2 is mediated by TcyP in both the liver and heart, indicating that sulfur acquisition strategies differ between *S. aureus* strains *in vivo*.

TcyP is conserved across many bacterial phyla.

TcyP is a member of the sodium:dicarboxylate symporter superfamily (IPR036458 specifically, PF00375; IPR001991) with several characteristic transmembrane regions and a C-terminal cytoplasmic tail (Fig. 2-8; top panel). Previous functional characterization of TcyP has only been performed in *E. coli* and *B. subtilis* [28,36]. To determine the conservation of TcyP throughout the bacterial kingdom, we used iterative BLAST (see Methods). We identified *Staphylococcus* TcyP homologues in numerous pathogen-containing bacterial phyla and orders, including enterobacteriaceae within Proteobacteria (Fig. 2-8; orange nodes), and bacillales within Firmicutes (Fig. 2-8; blue nodes). While many homologues are present across bacteria, TcyP sequences form a distinct cluster with the *Staphylococcus*, *Salinococcus*, and a few members of the *Streptococcus*, all of which are Firmicutes. Similarly, the proteobacterial homologues in *Citrobacter*, *Salmonella*, *Enterobacter*, and *Aeromonas* cluster together (Fig. 2-8). These data demonstrate that while many bacterial phyla carry homologues of TcyP, the variations are lineage-specific. We find that there are homologous transporter proteins in other bacterial clades such as Actinobacteria, Fusobacteria, Deinococcus, Thermotogae, and Spirochaetes as well that

belong to TcyP or the broader sodium:dicarboxylate symporter family that includes the aerobic C4-dicarboxylate transporter protein, DctA (Fig. S2-4 and Supplemental file 1). Further experimentation is needed to establish the functional roles of these homologues in CSSC or Cys acquisition and pathogenesis.

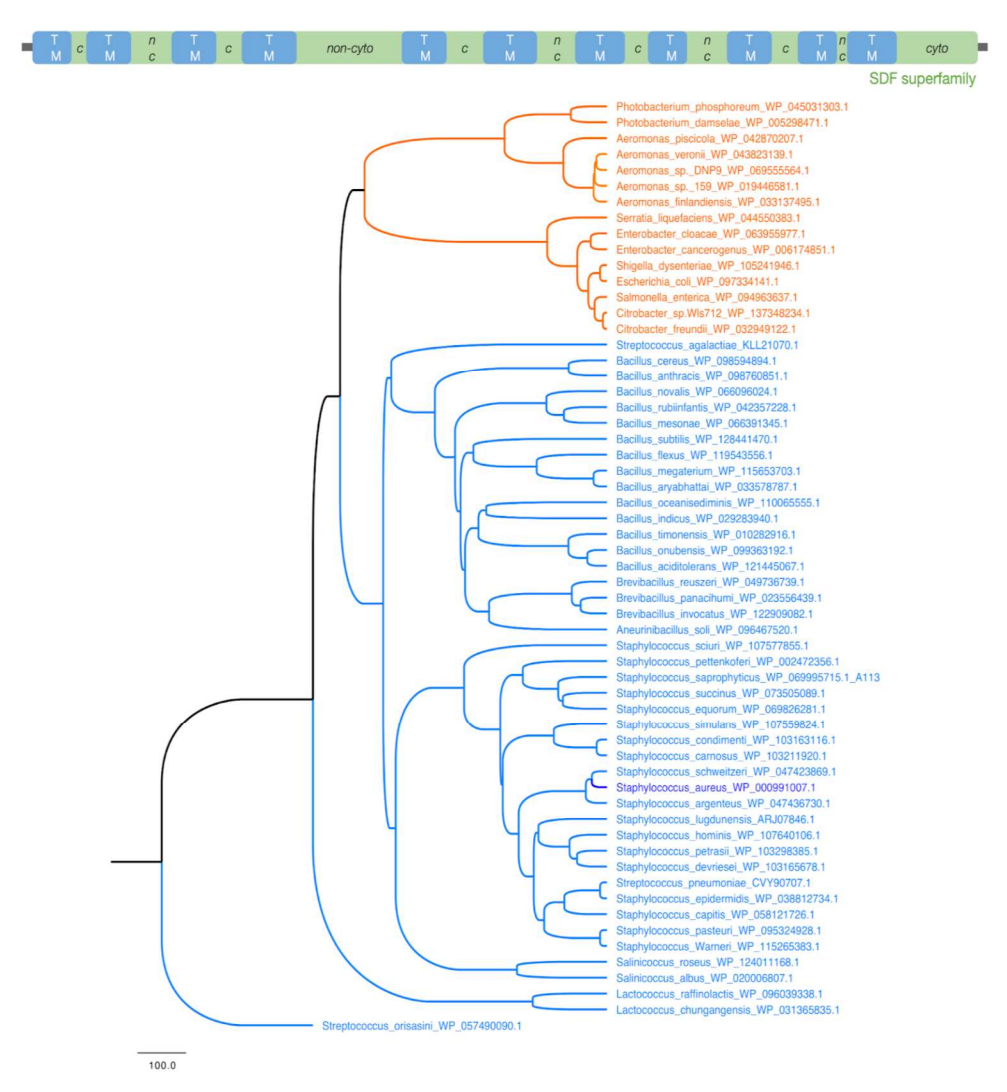


Figure 2-8. TcyP is broadly conserved in bacteria.

Top panel: Domain architecture and cellular localization of the S. aureus TcyP protein (462aa; WP_000991007.1), as characterized by Interproscan, Phobius (see Methods). The predominant domain, sodium:dicarboxylate symporter superfamily is indicated in green with the transmembrane (TM) regions shown in blue. The predicted cytoplasmic (c) and non-cytoplasmic (nc) regions are labeled for the loop residues. Bottom panel: Homologues of TcyP in Firmicutes (blue) and Proteobacteria (orange) using the S. aureus TcyP as the guery are shown. S. aureus is highlighted in dark blue.

Discussion

Acquisition of nutrient sulfur is essential for all organisms; however, we lack a basal understanding of sulfur sources *S. aureus* uses and the proteins necessary to facilitate their acquisition. To synthesize critical metabolites required for cell proliferation organisms have evolved assimilatory processes that exploit both inorganic or organic sulfur sources (5, 25, 104, 105). *S. aureus* sulfur catabolism is limited due to the inability to convert sulfate, a fully oxidized and highly abundant plasma sulfur source, into a reduced and utilizable form (3, 11, 25, 28). In the current study, we examined CSSC acquisition by *S. aureus* through the characterization of TcyABC and TcyP. Human serum levels of CSSC have been reported to be as high as 62.9 μM (30). While the ability of *S. aureus* to use CSSC as a sulfur source *in vitro* was previously described (11), the transporters involved in this process have not been experimentally validated.

Our results demonstrate that TcyP and TcyABC support growth on a wide range of Cys analogues. We exploited this fundamental aspect to determine whether the respective mutant strains demonstrated enhanced resistance to selenocystine, which differs from CSSC by the replacement of the sulfur atoms with selenium atoms. The ability to transport Cys and CSSC by the same transporters has been previously speculated in other organisms (26, 42). Evidence presented here demonstrates that disruption of both *tcyA* and *tcyP* impairs growth in medium supplemented with Cys relative to WT *S. aureus*. This data suggests TcyP and TcyABC are capable of importing both Cys and CSSC and previous investigations provide precedent for the observed substrate promiscuity of TcyP and TcyABC (26, 42).

Broadly, ABC-transporters can be categorized into three types (106, 107). Type I encompasses transporters that translocate metabolites a cell needs in bulk quantities including amino acids and sugars (106–108). Type I ABC-transporters and their corresponding substrate-binding proteins contain a substrate binding and recognition pocket that is surrounded by flexible loops whereas type II substrate-binding proteins are confined by a non-flexible helix (107). Consequently, type II ABC-transporters have a higher affinity for substrates than type I (107).

TcyABC likely belongs to the Type I group of ABC-transporters due to the speculated low-affinity for CSSC and the fact its cognate metabolite is needed in large quantities (42). These facts could explain why TcyABC might be able to accommodate both CSSC and Cys in its substrate-binding site. Further studies will provide insight to the flexible substrate binding site of TcyABC, but TcyA has been crystalized and the structure has been determined with either CSSC or Cys bound to the binding site revealing that it has affinity for both derivatives (109).

Additional studies in B. subtilis have also shown that TcyP transport of CSSC is inhibited by Cys, indicating Cys competes with CSSC for access to the channel of the transporter (42). Similar findings have been reported in S. mutans TcyABC (26). Our data agrees with these previous studies showing TcyP and TcyABC display substrate promiscuity in transporting CSSC and Cys analogues. We show that while TcyABC and TcyP support growth on Cys and derivatives, WT S. aureus does not grow to the same levels when these sulfur sources are present at equivalent sulfur levels to CSSC. Calculations in E. coli reveal that a cell contains as much as 230 µmol sulfur atoms and this amount of sulfur can be provided by the transport of 115 µmol of CSSC (92). Assuming that S. aureus has a similar sulfur demand to E. coli, theoretically equimolar concentrations of CSSC, Cys, or NAC would lead to equivalent levels of growth; however, this is not observed. In fact, S. aureus growth in CSSC-containing medium exceeds growth when either NAC or Cys is present, indicating CSSC must be more efficiently acquired by S. aureus relative to NAC or Cys. Both the S. mutans and B. subtilis studies show a moderate decrease in CSSC transport in the presence of Cys, but a limitation of these studies is that Cys transport was measured through the ability to inhibit radiolabeled CSSC import (26, 42). Based upon prior results and data presented here, both transporters appear to have greater affinity for CSSC but can likely transport Cys with some efficiency (28). Therefore, as a consequence of decreased efficiency, the same sulfur molar concentration of NAC or Cys does not lead to the same intracellular concentration of sulfur and ultimately a greater environmental sulfur concentration is

required to support the same level of growth. Our study provides more resolution due to our examination of TcyABC- and TcyP-mediated growth on Cys and derivatives.

We next wanted to broaden our studies to investigate transport of structurally similar intermediates in the sulfur assimilation pathway and show for the first time that *S. aureus* utilizes hCSSC as a sulfur source. Prior studies established reduced homocysteine as a viable sulfur source for *S. aureus* but did not examine growth on the oxidized form (28). hCSSC is the disulfide, oxidized form of homocysteine, a four-carbon compound that is an intermediate in the pathway that produces methionine using Cys. Cys is a substrate for a condensation reaction with *O*-acetyl-homoserine that generates cystathionine (4, 25). Cystathionine is then cleaved to generate homocysteine (25, 96). We hypothesize that homocysteine directly enters *S. aureus* sulfur metabolism and can be fluxed to Cys or methionine (4, 25, 28). We demonstrate that genetic inactivation of *tcyABC* leads to a failure to grow in medium supplemented with hCSSC as the sole sulfur source. This data further implies that the TcyA substrate-binding domain is promiscuous, as it must act as a receptor for multiple sulfur-containing metabolites including CSSC, Cys, NAC, hCSSC, and selenocystine.

While it is known that CymR represses TcyP and TcyP, we wanted to determine the responsiveness of *tcyA* and *tcyP* expression to the abundance of sulfur in the environment. Our results demonstrate that sulfur-deplete environments induce *tcyP* expression and to a lesser greater extent *tcyA* expression. Previous studies showed *tcyP* and *tcyA* are transcriptionally repressed by CymR, the master Cys metabolism regulator in Firmicutes (28, 97). In *cymR* mutants, *tcyP* transcript levels increase 25-fold relative to WT (28, 97). Furthermore, gel shift assays demonstrated that CymR directly binds the *tcyP* promoter (28). Enhanced transcriptional control of *tcyP* likely has several physiological implications. First, *B. subtilis* TcyP is predicted to have a greater affinity for CSSC than TcyABC (42). Induction of TcyP by *S. aureus* in sulfur deplete environments is an adept strategy to accrue CSSC because of the greater affinity relative to TcyABC. Second, upon expression, the increased affinity of TcyP for CSSC likely ensures the

sulfur requirement is satisfied by CSSC in sulfur deplete environments. Third, increased CSSC import leads to a greater intracellular Cys pool which potentiates Fenton-chemistry and oxidative damage in *E. coli* (92, 110). Additionally, studies have shown growth of a *cymR* mutant in *B. subtilis* in the presence of CSSC is severely impaired further suggesting the necessity to control CSSC levels (98). Therefore, strict transcriptional control of *S. aureus tcyP* likely reduces a potentially toxic accumulation of intracellular Cys. An interesting observation from our transcriptional analysis of *tcyA* and *tcyP* is the apparent *tcyA* repression that occurs when the cells are cultured in CSSC and sub-cultured into the same medium. This finding seems counterintuitive as it appears the cell is repressing transporters necessary to obtain the only viable sulfur source in the medium; however, given the potential toxicity associated with Cys accumulation (92, 110) repression of TcyABC could be a tactic to modulate CSSC import to limit toxicity.

This work and others suggest that there are at least two different strategies for bacterial Cys and CSSC import. Some organisms encode mechanisms supported by high-affinity CSSC transporters that are also capable of transporting Cys at a reduced efficiency while others have evolved strategies in which dedicated Cys and CSSC importers are specific for their cognate metabolite (26, 42, 111). One model predicts that the strategy employed is dependent on the oxygenic environments in which the organism resides (112). For instance, some anaerobes and facultative anaerobes have homologues of a distinct Cys transporter present in *Campylobacter jejuni* (111, 112). In an anaerobic environment, Cys will likely be reduced, while CSSC is the dominant form in aerobic environments. *E. coli* has evolved a strategy in which CSSC is imported and converted to Cys intracellularly; however, excess Cys is exported and subsequently rapidly oxidized in the external environment (92). This strategy suggests that *E. coli* predominantly encounters CSSC in its environment and has evolved to target CSSC. *S. aureus* does not encode a predicted Cys specific transporter. Based on data presented here, *S. aureus* employs a strategy that utilizes dedicated CSSC transporters that also transport Cys with lower affinity and efficiency.

The preference for CSSC over Cys is also interesting due to the fact that the cell must invest energy in reducing the CSSC disulfide bond to liberate Cys. Cys, on the other hand, can be directly incorporated into the translational or cofactor synthesis pathways. Evolutionarily the preference for CSSC might provide some insights into the environments in which *S. aureus* primarily resides and the state of Cys in these environments. An integral aspect of *S. aureus* pathogenesis is the upregulation of secreted proteases (113, 114). Protease-null strains demonstrate pronounced growth reductions in peptide-rich environments including serum (115). Protease secretion likely increases Cys abundance at the host-pathogen interface. Additionally, the reactive Cys thiol is sensitive to effects of the host oxidative burst, increasing CSSC, or other Cys-containing thiol adducts that result from the formation of mixed disulfides (116). These conditions could enhance the importance of Cys and CSSC metabolism to *S. aureus* pathogenesis. Future work will further characterize TcyABC and TcyP by examining their role in the transport of Cys-containing mixed disulfides.

A previous study has noted a potential link between Cys acquisition and pathogenesis. The *Listeria monocytogenes* protein CtaP is required for *in vitro* proliferation in low Cys conditions and *ctaP* mutants demonstrate reduced colonization in the livers and spleens of mice following intravenous challenge. A direct correlation between Cys acquisition and *L. monocytogenes* pathogenesis is difficult due to the fact that CtaP was also shown to be involved in host cell adhesion (24). Using a murine model of systemic infection, we show that in *S. aureus* strain JE2 TcyP is sufficient for proliferation of *S. aureus* in the heart and liver. However, in strain NWMN TcyP is required for maximal fitness in the liver but both TcyP and TcyABC are important for proliferation in the heart. While prior studies demonstrate a mutant strain of *S. aureus* inactivated for thiosulfate assimilation is as virulent as the corresponding WT strain in a murine skin lesion infection model (11), these data represent for the first time that sulfur source acquisition systems support *S. aureus* infection. The fact that TcyABC and TcyP are required for growth in medium containing different sulfur sources makes it challenging to define the exact sulfur-containing

metabolite that is acquired *in vivo*. Due to the competitive defect observed for JE2 *tcyP*::Tn in murine liver and heart, we can narrow the acquired sulfur source to CSSC, Cys, or NAC. Similarly, we can conclude NWMN could be catabolizing CSSC, Cys, or NAC during liver colonization. In contrast, due to the observation that inactivation of both *tcyA* and *tcyP* in *S. aureus* strain NWMN is necessary for a colonization defect in murine heart, we can only conclude the catabolism of sulfur sources occurring could include CSSC, Cys, NAC, and hCSSC. The different *in vivo* phenotypes observed between the two strains could be due to regulatory factors present in JE2 but not in NWMN. JE2 harbors the staphylococcal cassette chromosome (SCCmec) and the arginine catabolism mobile element (ACME) (72, 117), and previous work has shown that ACME and SCCmec mutants differentially regulate a subset of genes which includes some annotated but uncharacterized transporters (117). The presence of ACME and SCCmec in JE2 may cause a differential sulfur requirement during proliferation in the heart compared to NWMN due to transcriptional changes. This might explain why the JE2 *tcyP* mutant demonstrates heart colonization phenotype while inactivation of both *tcyP* and *tcyABC* are required to observe a virulence defect in strain NWMN.

An interesting observation from the infection experiments is that loss of TcyABC and TcyP does not completely ablate the capacity of the strains to compete with WT, as *tcyAP* double mutants are still recovered from the organs. This result suggests that other sulfur sources are likely present that support proliferation in the absence of cognate TcyP- and TcyABC-dependent metabolites. Our data indicate that TcyABC and TcyP do not support growth on GSH as a sulfur source. Therefore, GSH present in the heart and liver could allow the *tcyAP* mutants to establish infection in these organs. Further investigation into the sulfur catabolism of *S. aureus* is necessary to determine the identity and abundance of TcyP- and TcyABC-dependent and independent sulfur sources present within host organs. Additionally, the identification of GSH acquisition systems will support direct investigation into the importance of GSH acquisition during infection.

We found that many bacteria encode TcyP homologues and that the homologues predominantly cluster into groups based on their lineages. Whether these transport systems are unique to CSSC, and whether they are functional and relevant to pathogenesis in the other phyla remains to be explored. Based on the homology to *S. aureus* TcyP and the data presented here showing that TcyP is involved in CSSC, Cys, and NAC transport, these results provide a platform to characterize TcyP-dependent sulfur transport in other pathogenic bacteria.

Materials and methods

Bacterial strains.

Strains used in this study are described in Table A-1. JE2 is derived from the community-acquired methicillin-resistant (CA-MRSA) *S. aureus* clinical isolate USA300 LAC (100). Strain Newman is a methicillin-sensitive strain (101). Mutants were created by transducing the transposon (Tn) inactivated gene insertion provided by the Network on Antimicrobial Resistance in *S. aureus* (NARSA) for distribution by BEI Resources into the desired strain using previously described transduction methodology (100, 118). For the *tcyA tcyP* double mutant, the erythromycin resistance cassette in *tcyP*::Tn was replaced with a tetracycline resistance cassette using a previously described allelic replacement strategy (119). Tn insertion was confirmed by PCR.

Generation of complementation vectors.

The plasmid pKK22 was used for complementation studies (120). Integration of inserts was achieved using Gibson assembly methodology and employed HiFi assembly master mix (New England Biosciences, Ipswich, MA). The tcyP or tcyABC open reading frame sequence, including its native promoter, was amplified from JE2 genomic DNA and pKK22 was amplified from plasmid DNA using primers listed in Table A-2. HiFi assembly was used to construct pKK22 P_{tcyP} ::tcyP or P_{tcyABC} ::tcyABC, and the constructs were transformed into a pir^+ Escherichia coli

strain. The P_{tcyP} ::tcyP and P_{tcyABC} ::tcyABC sequence was verified by Sanger sequencing. Plasmid was isolated from E. coli and transformed into RN4220, and the RN4220 passaged plasmid was transduced into the final recipient strains.

Growth Analysis.

Strains were cultured in trypic soy broth (TSB) overnight, washed with phosphate buffered saline (PBS), and normalized to an OD_{600} = 1. Cells were then added to 96-well round-bottom plates at a starting OD_{600} of 0.01. Growth was monitored by measuring OD_{600} at hourly time points using a BioTek plate reader set at 37°C with continuous, linear shaking. Growth analysis was carried out with PN-medium supplemented with 5 mg mL $^{-1}$ glucose and indicated sulfur sources. PN medium was prepared as previously described and contained seventeen amino acids, excluding Cys, asparagine, and glutamine (121). Cys was omitted to test the ability of *S. aureus* to grow on various sulfur sources. Blank measurements were subtracted from measurements and experiments were performed in triplicate that were subsequently averaged. To fully ensure Cys and NAC were maintained reduced, chemicals were weighed aerobically, and immediately transferred to a Coy anaerobic chamber with a 95:5 N_2 :H $_2$ atmosphere (Grass Lake, MI) where it was dissolved in a degassed solution of 1N HCI. Anaerobic growth analysis was carried out in the presence of 100 mM sodium nitrate as an alternative electron acceptor.

Selenocystine disk diffusion assays and isolation of resistant mutants.

Overnight cultures grown in TSB at 37° C were swabbed onto 20 mL trypic soy agar (TSA) plates to generate a lawn of bacterial growth. A volume of 10 μ L of 50 mM, 75 mM, or 100 mM selenocystine dissolved in 1N HCl was added to a sterile Whatman paper disk and was transferred to the TSA plate. Plates were incubated at 37° C for 24 h. The zone of inhibition was measured in millimeters and was defined as the diameter between bacterial lawn growth.

Colonies arising in the zone of inhibition after 96 hrs were restreaked onto TSA plates, subsequently cultured in TSB, and archived at -80°C.

Genomic DNA isolation and gene sequencing.

Selenocystine resistant mutants were cultured in TSB. Cells were centrifuged and resuspended in buffer containing 60 µg mL⁻¹ lysostaphin from ABMI (Lawrence, NY) and were incubated for 1 h at 37°C to remove the cell wall. Genomic DNA was isolated using a Promega Wizard genomic DNA purification kit (Madison, WI) following the manufacturer's directions. The *tcyP* ORF and promoter were amplified using GoTaq polymerase (Promega Madison, WI). The amplicon was purified using Wizard PCR cleanup kit following manufacturer's instructions (Promega Madison, WI). Sanger sequencing was performed by the Michigan State University Research Technology Support Facility (East Lansing, MI).

qRT-PCR analysis.

Overnight cultures of JE2 were grown in TSB at 37° C and sub-cultured 1:100 into 50 mL of PN supplemented with 5 mg mL⁻¹ glucose and $25 \,\mu\text{M}$ CSSC in three 250 mL Erlenmeyer flasks for three hours at 37° C. A volume of 50 mL was centrifuged for 10 min at 4,700 rpm at room temperature, washed once in PBS, and centrifuged a second time. One sample was processed as the T₀ and was lysed. Upon resuspension in the indicated growth medium, PN supplemented with 5 mg mL⁻¹ glucose and $25 \,\mu\text{M}$ CSSC or PN supplemented with 5 mg mL⁻¹ glucose lacking a sulfur source. Cells were incubated for 2 hours at 37° C in 250 mL Erlenmeyer flasks. A volume of 50 mL was centrifuged for 10 min at 4,700 rpm at room temperature, and the cell pellet was resuspended in 750 μ L LETS buffer containing 0.1 M LiCl, 10 mM EDTA, 10mM Tris-HCl (pH 7.4) and 1% SDS. Cells were transferred to a 2 mL bead beating tube with 500 μ L volume of 0.1 mm zirconia/silica beads (BioSpec Bartlesville, OK). The lysates were incubated at 55°C for 5 min and

centrifuged for 10 min at 13,700 rpm and at 4°C. Supernatant was transferred to 1 mL Trizol. RNA was precipitated using chloroform phase separation and isopropanol, and then purified using an RNAeasy kit following manufactures instructions. Contaminating DNA was removed via treatment with an on-column DNase treatment. RNA was treated with Turbo DNase and cDNA was synthesized using SuperScript III reverse transcriptase (ThermoFisher Waltham, MA) following manufacturer instructions and random hexamer methodology (Invitrogen Carlsbad, CA). qRT-PCR was set up using SYBR Green master mix with 20 μ L reactions containing 10 μ L SYBR Green master mix, 2 μ L of 10 μ M forward primer, 2 μ L of 10 μ M reverse primer, and 50 ng cDNA. Primers used for each gene are presented in Table A-2. qRT-PCR was performed on a QuantStudio 3 Real-Time pcr thermocycler (ThermoFisher Waltham, MA) and was performed in technical triplicate with minus reverse transcriptase controls to determine genomic DNA contamination. Comparative $\Delta\Delta$ C_T methodology was used to compare transcript levels using *rho* as a reference target (122–124).

Competition in murine model of systemic infection.

WT and mutant strains were grown in TSB overnight at 37° C, sub-cultured 1:100, and grown in TSB for 3 h at 37° C and 225 rpm. Strains were washed in PBS and normalized to an OD₆₀₀ equal to 0.4. The competitions were prepared by mixing equal volumes of WT and mutant strain. To quantify the input ratio, the mixture was serially diluted and plated onto TSA and TSA supplemented with 10 μ g mL⁻¹ erythromycin (erm¹⁰) to discern between WT and mutant (erythromycin resistant). The mutant strains utilized in these experiments harbored at least one erm resistance cassette. WT CFUs were calculated by subtracting CFUs generated on TSA-erm¹⁰ from CFUs present on TSA. Ten female eight-week old BALB/c mice were retro-orbitally infected with 100 μ L of 10^{7} CFUs of the WT and mutant mixture. After 96 hours, the heart, and liver were collected and homogenized in 1 mL PBS. Homogenates were serially diluted and plated onto TSA

or TSA-erm¹⁰. Competitive indices were calculated as dividing the mutant:WT output CFU ratio by the mutant: WT input CFU ratio. Infections were performed at Michigan State University under the principles and guidelines described in the Guide for the Care and Use of Laboratory Animals. Animal work was followed as approved by Michigan State University Institutional Animal Care and Use Committee (IACUC) approved protocol number (12/16-205-00).

Phylogenetic analyses of TcyP.

The TcyP amino acid sequence (WP_000991007.1 from *S. aureus* USA300_FRP3757, assembly GCF_000013465.1) was used as the query sequence for a position-specific iterative BLAST (PSI-BLAST) for two iterations against the NR database. The protein sequences of select representative homologues from pathogen-containing clades, Proteobacteria and Firmicutes, were aligned *S. aureus* TcyP sequence using ClustalO (125, 126). A phylogenetic tree was generated from the alignment using FigTree (127). The protein domain and localization predictions were done using CDD (128), Interproscan (129), and Phobius (130). For the supplemental analyses, *S. aureus* TcyP (WP_00991007.1) was used as the query for one iteration of PSI-BLAST across all bacteria using the RefSeq protein database (to limit redundancy). The results from the top 3000 hits in the similarity search were used to identify TcyP-like proteins in other bacterial clades (Supplemental File 1). To include representative members across diverse genera, matches with closely related *S. aureus* strains and multispecies were filtered out followed by selection of the top hit (based on percent identity) per genus. The resulting data were used to construct the phylogenetic tree, as described above.

Acknowledgements

The following reagents were provided by the Network on Antimicrobial Resistance in *S. aureus* (NARSA) for distribution by BEI Resources, NIAID, NIH: *S. aureus* subsp. *aureus* Strain JE2, *tcyA* transposon mutant (NE1592), and *tcyP* transposon mutant (NE625). We thank Dr.

Jeffery Bose's laboratory at the University of Kansas Medical Center for supplying the pKK22 complementation vector. Jack Dodson is supported by American Society for Microbiology Undergraduate Research Fellowship This work is funded by the American Heart Association 16SDG30170026, start-up funds provided by Michigan State University, and the National Institutes of Health R01 Al139074.

Chapter 3 The glutathione import system expands <i>Staphylococcus aureus</i> nutrient sulfur acquisition and promotes interspecies competition.

Abstract

Sulfur is an indispensable element vital for proliferation of bacterial pathogens within the host. Prior studies indicated that the human pathogen, S. aureus utilizes the sulfur-containing molecule glutathione (GSH) as a source of nutrient sulfur; however, mechanisms employed by S. aureus to acquire GSH are not defined. GSH is abundant in humans and has been established as a source of nutrient sulfur for other pathogens. These facts support the hypothesis that S. aureus acquires host GSH to satisfy the requirement for sulfur during infection. To tests this hypothesis, we sought to identify genetic determinants that promote GSH acquisition and catabolism in S. aureus. A genetic screen revealed that a five-gene locus comprising a putative ABC-transport system and γ-glutamyl transpeptidase (Ggt) promotes S. aureus proliferation in medium supplemented with either reduced or oxidized (GSSG) GSH as the sole source of sulfur. Based on these phenotypes we named the transporter the glutathione import system or GisABCD. Biochemical characterization of Ggt indicates that S. aureus Ggt cleaves both GSH and GSSG and suggests Ggt is localized in the staphylococcal cytoplasm, a localization distinct from other bacterial Gqt enzymes. Though qis mutants lacked a virulence phenotype, bioinformatic analyses demonstrate that only species closely related to S. aureus encode GisABCD homologues. GisABCD is not conserved in S. epidermidis. Consequently, we demonstrate that GisABCD-Ggt provides a competitive advantage for S. aureus over S. epidermidis upon GSH or GSSG supplementation. Overall, this study describes a new sulfur acquisition system in S. aureus that targets host GSH and promotes competition against other staphylococci.

Author summary

S. aureus is an important human pathogen that causes considerable morbidity and mortality. A requirement of S. aureus pathogenesis is acquisition of essential nutrients from host tissues. While mechanisms by which some nutrients are acquired during infection are well established, knowledge of how pathogens satisfy the sulfur requirement is limited to only a handful

of pathogens. This work focuses on *S. aureus* acquisition of glutathione (GSH), a sulfur-containing metabolite that promotes redox homeostasis. We expand the number of viable *S. aureus* sulfur sources by presenting for the first time that oxidized GSH promotes proliferation and determine that the GisABCD-Ggt transport system supports utilization of both GSH and GSSG as sources of nutrient sulfur. Also, we reveal that GisABCD-Ggt is not conserved in closely related *Staphylococcus epidermidis*. In keeping with this, GisABCD-Ggt system affords an interspecies competitive advantage to *S. aureus* over *S. epidermidis* in medium containing GSH and GSSG. In total, this work demonstrates that GisABCD-Ggt supports *S. aureus* GSH and GSSG acquisition, provides mechanistic details for their import and catabolism, and reveals, through conservation studies, that GisABCD-Ggt may shape intra-genus competition in environments containing GSH or GSSG.

Introduction

Sulfur is an essential element for all domains of life due to its chemical versatility. Sulfur atoms take on a range of redox states, -2 to +6, facilitating many cellular functions including electron transfer reactions (1, 131). Additionally, as a constituent of the amino acid Cys, sulfur provides structural complexity through formation of uniquely stable disulfide bonds (1, 131). Ultimately, Cys synthesis serves as the critical intermediate for synthesis of methionine (Met) and other sulfur-containing cofactors including FeS clusters (1, 4, 5, 25). To satisfy the sulfur requirement, organisms have evolved strategies to acquire inorganic and organic sources of sulfur. Inorganic sulfur sources are compounds including sulfate, sulfite, and sulfide where the sulfur is in a highly oxidized state (25, 105). Inorganic sulfur is reduced to sulfide prior which reacts with o-acetyl serine to generate Cys (25, 105). On the other hand, organosulfur sources satisfy the sulfur requirement through catabolism or conversion of the sulfur-containing compound because the sulfur is predominantly complexed to carbon and in a more reduced state (25, 28, 42, 92).

The ability of bacterial pathogens to scavenge nutrient sulfur from host environments is paramount to the ability to proliferate and cause disease. An abundant nutrient targeted by pathogens for use as a sulfur source during infection is the antioxidant tripeptide glutathione (GSH) which consists of glutamate, Cys, and glycine. GSH is abundant within the human body, reaching intracellular concentrations of 0.5-10 mM (2, 49). In addition to humans, some bacterial species also utilize GSH as a low molecular weight thiol to protect against aberrant oxidative damage resulting from aerobic metabolism (48). GSH abundance in host tissues represents a significant reservoir of nutrient sulfur for invading pathogens (2, 16, 132). In fact, GSH is an established source of sulfur for *Streptococcus mutans, Streptococcus pneumoniae, Haemophillus influenzae, Salmonella enterica* serovar Typhimurium, *Escherichia coli, Bordetella pertussis, Clostridium difficile*, and *Francisella tularensis* (12, 16, 17, 19–23, 132, 133).

Liberation of the Cys residue is critical for utilization of GSH as a source of nutrient sulfur, a process requiring cleavage of the γ-peptide bond between glutamate and Cys. However, γ-peptide bonds are remarkably stable against cellular proteolytic enzymes and therefore specialized proteases are required, one of which, γ-glutamyl transpeptidase (Ggt), cleaves GSH, generating glutamate and cysteinyl-glycine. Cysteinyl-glycine then becomes a substrate for other cellular peptidases leading to liberation of Cys (2, 50, 134–136). Subcellular localization of Ggt is species specific. In humans, Ggt is peripherally localized to the plasma membrane. In Gramnegative bacteria, Ggt can be expressed in the periplasm or in the cytoplasm, while some Grampositive bacteria secrete the enzyme (137–139). Ggt localization has implications for how organisms maintain internal redox homeostasis. As GSH is an established source of sulfur for select pathogens during infection, it is not surprising that Ggt can be a virulence factor during infection. For instance, Ggt is critical for intracellular survival of *F. tularensis* in macrophages (16). Ggt has been shown to promote virulence of *Helicobacter pylori* and *Acinetobacter baumanni* (140, 141). In both organisms, Ggt induces host cell damage, though a role in nutrient sulfur

acquisition has not been established (141–143). Putative Ggt enzymes are encoded in many pathogens; however, only a minority of Ggt homologues have been studied in detail.

The important human pathogen *S. aureus*, which causes significant invasive disease such as osteomyelitis, endocarditis, prosthetic join infections, and skin and soft tissue infections, encodes a putative Ggt (71, 72, 74, 76, 144). However, its role in catabolizing exogenous GSH as a source of nutrient sulfur has not been determined. Notably, *S. aureus* is not capable of synthesizing GSH (145, 146). These facts support the hypothesis that *S. aureus* Ggt promotes utilization of host GSH as a source of nutrient sulfur. Previous work established that GSH supplied as a source of nutrient sulfur promotes growth of *S. aureus*, however, GSH acquisition and catabolism has not been explored further in *S. aureus* or other members of the *Staphylococcus* genus (11).

Nutrient sulfur sources targeted by *S. aureus* in the host has been an understudied area. Prior work *in vitro* defined sulfide, thiosulfate, Cys, cystine (CSSC), and GSH as sulfur sources that promote *S. aureus* growth (11, 28). Our previous work further characterized mechanisms of Cys and CSSC acquisition by focusing on two transporters, TcyP and TcyABC (147). TcyP promotes growth on CSSC, Cys, and *N*-acetyl Cys as sulfur sources whereas TcyABC supports proliferation on hCSSC in addition to the sulfur sources supported by TcyP (147). Disruption of *tcyP* in the USA300 strain JE2 led to decreased heart and liver colonization in the systemic model of infection but only when a *tcyP* mutant was competed with WT. This organ specific fitness defect likely indicates that *S. aureus* is capable of acquiring alternative sulfur sources during infection (147).

S. aureus utilizes reduced GSH as a source of sulfur but whether oxidized GSH (GSSG) is a viable source of sulfur, as well as, the mechanisms that support GSH sulfur source utilization are not defined (11). In this study, we demonstrate GSSG promotes S. aureus growth and performed a genetic screen to identify genes required for GSSG utilization. This analysis led to the discovery of a putative ATP-binding-cassette (ABC) transporter system encoded within the

SAUSA300 0200-SAUSA300 0203 locus. Mutating these genes impairs S. aureus proliferation in medium supplemented with either GSH or GSSG. Based on these growth phenotypes and bioinformatics domain predictions, we named this system the glutathione import system (gisABCD). We show that GisA is an ATPase suggesting that GSH and GSSG import is ATP dependent and that GisABCD is a bona fide ABC-transporter. The SAUSA300 0204 gene encodes a putative Gqt and is predicted to be operonic with the gisBCD genes that encode annotated permeases and substrate-binding protein. Strains harboring a transposon within ggt display significant proliferation defects in GSH- or GSSG-supplemented media. We determine that Gqt is cell associated and lacks a signal sequence suggesting it resides on the interior of the cell. We also show that recombinant Gqt cleaves both GSH and GSSG. Collectively, findings presented here demonstrate that GisABCD supports growth in GSH- and GSSG-containing environments, presumably by importing these host-derived, sulfur-containing metabolites. Based cell associated and likely internal location of Gqt, we propose that GSH and GSSG are imported intact into the cytoplasm where they are cleaved to glutamate and cysteinyl-glycine eventually leading to liberation of Cys and synthesis of downstream sulfur-containing metabolic cofactors. Intriguingly, we find that the GisABCD system is not conserved throughout staphylococci but is present in only a subclade of species closely related to S. aureus. In keeping with this, S. aureus outcompetes S. epidermidis, a member of the staphylococci that does not encode homologues to the complete Gis system, in GSSG- or GSH-supplemented environments. This work expands nutrient sulfur sources available to S. aureus within the host, provides evidence for Gisindependent transport of GSH, and provides avenues to explore metabolic niche specialization between invasive and non-invasive staphylococci.

Results

S. aureus proliferates in medium supplemented with GSSG as a sole source of nutrient sulfur.

A previous study qualitatively reported that S. aureus generates colonies in a chemically-

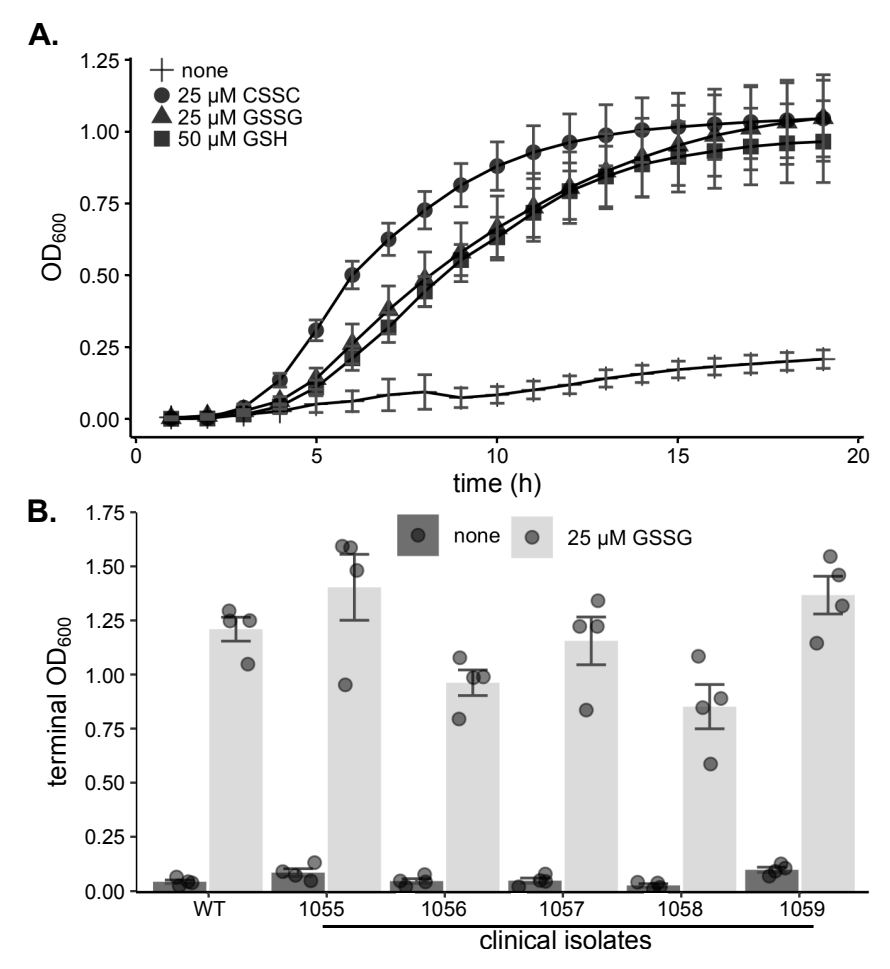


Figure 3-1. Supplementation of GSSG as sole sulfur source supports growth of Staphylococcus aureus.

(A) WT JE2 S. aureus was cultured in PN medium lacking a viable sulfur source. CSSC, GSSG, or GSH were added to the medium at the indicated concentrations. (B) WT S. aureus and both MSSA or MRSA clinical isolates were cultured in chemically defined medium supplemented with no sulfur added (none) or 25 μM GSSG and grown for 19 h. The bars depict the mean terminal OD600, and the dots represent the individual trials terminal OD600. The mean of at least three independent trials and error bars representing \pm 1 standard error of the mean are presented in A and B.

defined medium supplemented with GSH as the sulfur source, indicating that the abundant host metabolite is a viable source of nutrient sulfur (11). However, this study did not examine *S. aureus* proliferation in a medium supplemented with GSSG as the sulfur source. We employed a

chemically-defined medium, referred to as PN, to investigate growth of *S. aureus* on GSSG as the source of nutrient sulfur (121). PN contains sulfate and met, but as *S. aureus* lacks the capacity to assimilate sulfate or otherwise grow on Met as a sole sulfur source, CSSC is added as the source of nutrient sulfur (11, 28). In keeping with this, *S. aureus* fails to proliferate in PN devoid of CSSC (Fig. 3-1A). Supplementation of PN with either 50 µM GSH or 25 µM GSSG promotes *S. aureus* growth (Fig. 3-1A). The finding that GSSG supports *S. aureus* growth in a sulfur source specific manner expands sulfur-containing metabolites present in host tissues that can be used by *S. aureus* as a source of nutrient sulfur. To determine whether utilization of GSSG is conserved throughout the species, we examined proliferation of clinical isolates in medium containing GSSG. Growth of methicillin-sensitive and methicillin-resistant clinical isolates was quantified in PN supplemented with GSSG as the sole sulfur source. Compared to PN lacking a viable sulfur source, GSSG supplementation considerably increased terminal OD₆₀₀ (Fig. 3-1B). Clinical isolates show varying lag phases in medium containing GSSG, but GSSG stimulated growth of all strains (Fig. B-1).

SAUSA300_0200-0204 encodes a putative ABC-transporter and predicted Ggt that supports proliferation on both GSH and GSSG.

To determine genetic factors that facilitate *S. aureus* utilization of GSSG as a sulfur source, we screened the Nebraska Transposon Mutant Library (NTML) for mutants that fail to proliferate in PN medium supplemented with 25 µM GSSG as the sole source of sulfur (119). Five GSSG proliferation impaired mutants were identified in the screen, and each harbored a transposon insertion in one of five genes present in a single locus, SAUSA300_0200-*ggt* (Fig. 3-2A). Backcrossing the transposons into an otherwise WT, isogenic JE2 strain, resulted in substantially reduced growth in medium supplemented with 25 µM GSSG (Fig. 3-2B). Transposon inactivation also impaired *S. aureus* proliferation in PN supplemented with 50 µM GSH (Fig. 3-2C). However, the backcrossed mutants displayed WT-like growth in medium supplemented with

25 µM CSSC or in rich medium (Fig. 3-2D, E). Based on the failure of the mutants to proliferate

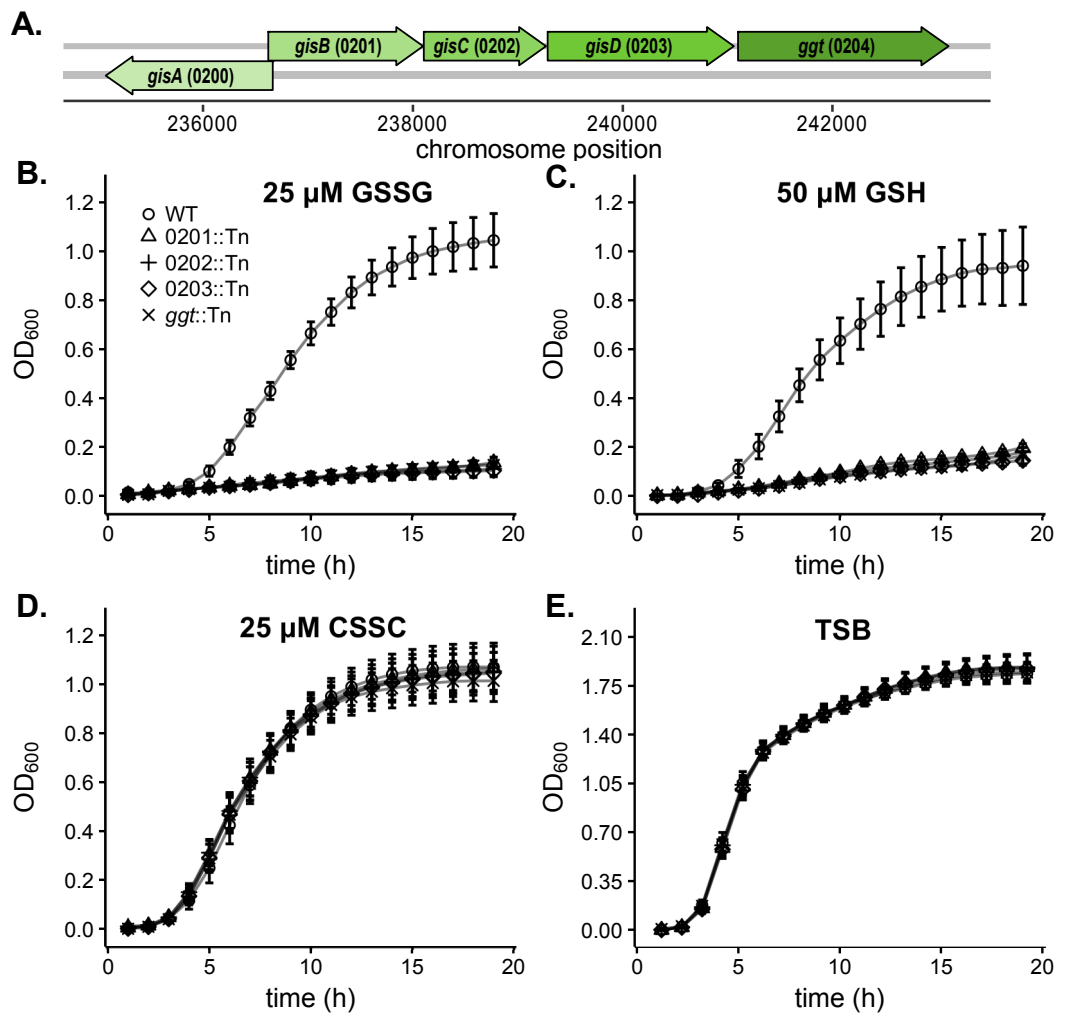


Figure 3-2. SAUSA300_0200-ggt supports growth on GSH and GSSG as sulfur sources.

(A) Location of SAUSA300_0200-ggt within the *S. aureus* genome. Strains cultured in PN supplemented with 25 μ M GSSG (B), 50 μ M GSH (C), 25 μ M CSSC (D), or TSB (E). Presented is the mean of at least three independent trials and error bars represent \pm 1 standard error of the mean.

in GSH- or GSSG-supplemented PN medium and the fact that SAUSA300_0200-SAUSA300_0203 encodes a putative ABC-transporter with a predicted Ggt (SAUSA300_0204), we propose to name these genes the **g**lutathione **i**mport **s**ystem (*gisABCD-ggt*) (Fig. 3-2A). The system encodes a predicted ATPase, GisA, two permease subunits, GisBC, a substrate-binding lipoprotein, GisD and a putatitive γ-glutamyl transpeptidase, Ggt (Fig. 3-2A). Domain architecture analysis of the GisABCD-Ggt system shows GisA is predicted to contain ATP binding cassette

domains, GisB and GisC are transmembrane permeases with 9 transmembrane segments, and GisD contains a signal peptide and contains a predicted lipid attachment site (Fig. B-2). Pfam confirms that Ggt is predicted to be a γ-glutamyl transpeptidase (Fig. B-2). In aerobic environments, GSH can be oxidized resulting in disulfide bond formation and generation of GSSG. To ensure GSH was not being abiotically oxidized to GSSG, we examined growth of WT, *gisB*, and an in-frame Δ*gisABCD-ggt* deletion mutant in anaerobic conditions where CSSC, GSH or GSSG were supplemented as sulfur sources. In anaerobic conditions, *gisB* and *gisABCD-ggt* grow to WT levels in CSSC but show reduced proliferation in PN supplemented with GSH or GSSG, further confirming that GisABCD-Ggt supports proliferation when either reduced or oxidized GSH are supplemented as sources of nutrient sulfur (Fig. B-3).

Recombinant GisA displays ATPase activity.

GisABCD is a predicted ABC-transport system. Consistent with this, ProSITE predicts GisA to have 2 ATP-binding cassettes implying that import of GSH and GSSG is an ATP-dependent process (Fig. B-2). GisA also harbors two sets of the canonical ATP binding Walker A and B boxes as well as an ATP binding motif (Fig. 3-3A). To validate the GisABCD ABC-transporter prediction, ATPase activity of recombinant GisA (rGisA) was monitored. rGisA was expressed and purified from *E. coli* using nickel NTA chromatography (Fig. 3-4). SDS-PAGE of purified rGisA demonstrated an approximate mass of 60 kDa, which is consistent with its 60 kDa predicted size. Purified protein liberated inorganic phosphate upon incubation with ATP in the presence of MgCl₂, indicating GisA hydrolyzes ATP (Fig. 3-3B). These data demonstrate that GisA is an ATPase, suggesting that import of GSH and GSSG through GisABCD is an ATP driven

process.

rGgt liberates glutamate from both GSH and GSSG.

To gain a better understanding of S. aureus GSH and GSSG catabolism, we next focused

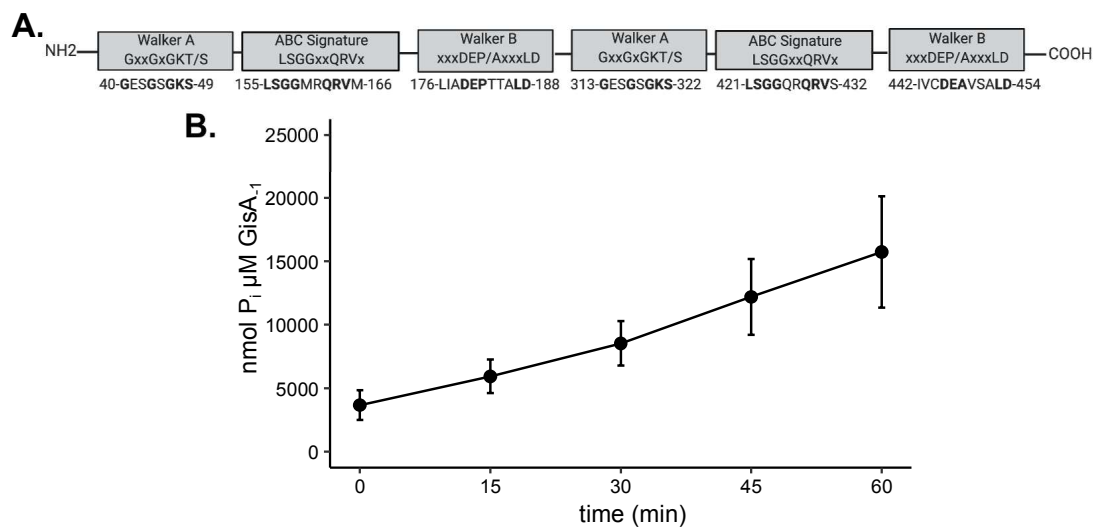


Figure 3-3. GisA harbors ATPase domain signatures and has demonstrates ATPase activity.

(A) GisA contains a pair of Walker A motifs, Walker B motifs, and ABC Signature motifs. The numbers correspond to the codon position of the first amino acid in the motif. Domain structure figure was created with BioRender. (B) Time course analysis of ATP activity of GisA incubated at $37^{\circ}C$ for 1 h with 400 μ M ATP. Samples were taken at time points indicated. Presented is the mean of nine independent trials and error bars represent \pm 1 standard error of the mean. Each trial used a new purification of GisA.

on the putative γ–glutamyl transpeptidase encoded by *ggt*. Pfam analysis revealed *S. aureus* Ggt has a γ-gamma glutamyl transpeptidase domain, which belongs to the larger N-terminal nucleophile hydrolase protein family, proteins that are autocatalytically processed and cleave amide bonds (Fig. B-2) (148, 149). First, complementation experiments tested whether growth of a *ggt* mutant cultured in PN medium supplemented with GSH or GSSG could be restored by providing WT or a C-terminal His-tagged *ggt* encoded on a plasmid. WT-like growth *was* displayed by *ggt* mutant strains harboring either plasmid, indicating that failure to proliferate in GSSG- or GSH-supplemented medium is due to genetic inactivation of *ggt* and that the His-tag does not interfere with the activity of the enzyme (Fig. B-5). Next, C-terminal His-tagged recombinant Ggt

(rGgt) was expressed and purified from *E. coli* (Fig. B-6). Ggt enzymes are produced as an inactive polypeptide that is auto-catalytically cleaved to generate approximate 40 kDa and 35 kDa subunits (149, 150). We observe a tripartite banding pattern consisting of the 75 kDa, full-length pro-Ggt as well as smaller, 40 kDa and 35 kDa polypeptides representing subunits of the mature enzyme (Fig. B-6). Active Ggt cleaves GSH by attacking the glutamyl residue, transferring it to the enzyme, and ultimately water enters to hydrolyze glutamate (151). To investigate whether *S. aureus* Ggt cleaves GSH and GSSG, purified rGgt enzyme was incubated with increasing concentrations of GSH and GSSG and glutamate release was quantified by mass spectrometry. We reasoned that because glutamate was an established and conserved product released by Ggt enzymes the release of glutamate was an adequate measurement for Ggt hydrolysis activity. Glutamate was detected in reactions containing rGgt incubated with either GSH or GSSG (Fig. 3-4). Importantly, glutamate could not be detected in reactions lacking substrate or rGgt, indicating

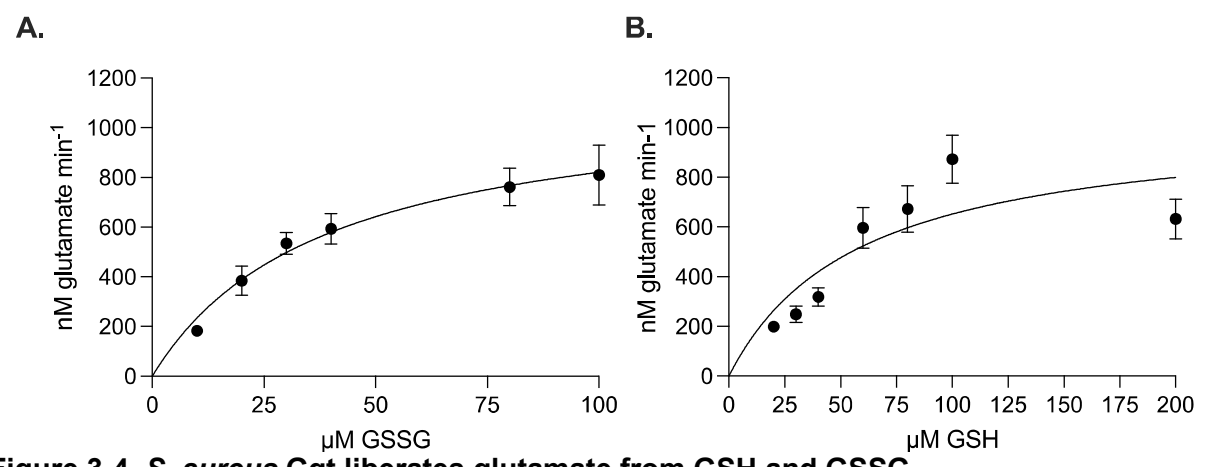


Figure 3-4. S. aureus Ggt liberates glutamate from GSH and GSSG. rGgt was incubated in the presence of the indicated concentrations of GSH and GSSG.

Glutamate released per min was calculated and the data was fit with the Michaelis Menten equation using GraphPad Prism. Presented is the mean of glutamate released per min for reactions set up using 4 independent protein purifications. Error bars represent ± standard error of the mean. Some error bars are smaller than the symbol size.

glutamate release resulted from enzymatic activity (data not shown). K_m values of Ggt for GSSG and GSH are 38.56 μ M (95% confidence interval 20.31 to 76.07) and 58.54 μ M (95% confidence interval 26.70 to 122.9), respectively. These measures are similar to previously reported Ggt homologues expressed in other organisms. For example, *E. coli* Ggt has a K_m value for GSH at

29 μ M (152). Additionally, Ggt V_{max} for GSSG and GSH are similar at, 1137 nM min⁻¹ (95% confidence interval 886 to 1572) and 1033 nM min⁻¹ (95% confidence interval 762 to1478), respectively.

Ggt is cell associated in S. aureus.

Ggt localization varies depending on the organism but has implications as it pertains to the substrate of GisABCD. Some Bacillus species secrete Ggt, and secreted Ggt suggests the substrate of GSH transporters is the Ggt degradation product of GSH or GSSG. However, cytoplasmic Ggt implies the GSH transporter substrate is GSH or GSSG. We used the previously described His-tagged Ggt expression vector (Ggt-His) to determine the subcellular localization of the enzyme. S. aureus cells expressing native or Ggt-His were cultured in PN supplemented with 25 μM GSSG, collected and separated into supernatant and whole cell lysate (WCL). An α-6x His primary antibody was used to immunoblot and monitor the presence or absence of Ggt within each fraction. rGgt served as a size comparison control. Bands corresponding to Ggt-His were not detected in the supernatant fractions; however, a band at ~35kDa was observed in both the Ggt-His WCL and rGgt samples. This band was specific to Ggt-His as it was not present in WCL collected from cells expressing Ggt lacking the His tag. This result suggests Ggt is cell associated (Fig. 3-5). Hemolysin A (Hla) was used as a supernatant fractionation control, and a greater intensity band corresponding to the molecular weight of Hla was observed in supernatants of cells expressing either His-tagged or native Ggt than in the WCL indicating proper fractionation of supernatants from whole cells (Fig. 3-5). To enrich Ggt present in supernatant or WCL fractions, the fractions isolated from cells expressing either His-tagged or native Ggt cultures were incubated with Ni-NTA. In keeping with previous results, a ~35kDa band was present exclusively in the His-tagged WCL (Fig. 3-5). SignalP-5.0 predicts very low likelihoods of signal peptide, twinarginine translocation (TAT) signal peptide, and lipoprotein signal peptide, 0.007, 0.003, 0.008, respectively, and TatP 1.0 also does not predict a signal peptide (153, 154). Additionally, no signal

peptide is predicted in the domain architecture analysis (Fig. B-3). The absence of bands corresponding to Ggt in the supernatant, as well as the lack of signal sequence predictions,

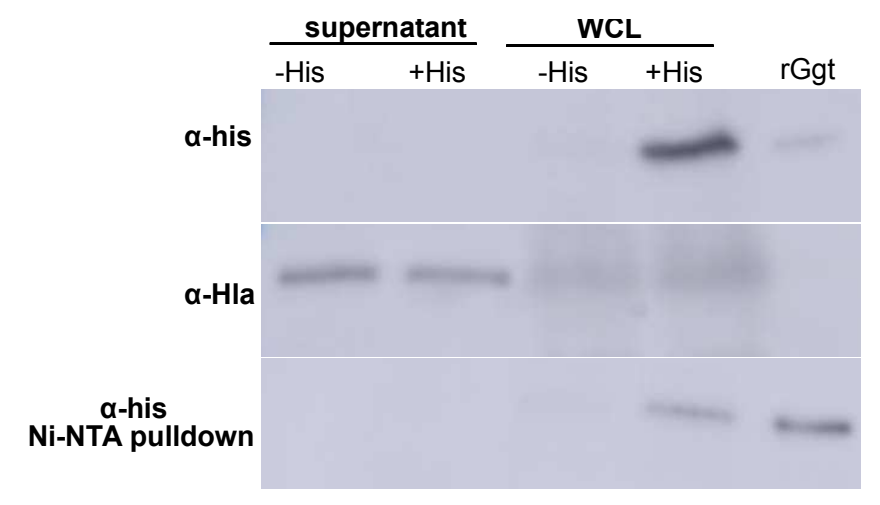


Figure 3-5. S. aureus Ggt is cell associated. Fractions of S. aureus ggt::Tn pOS1 P_{lgt} ::ggt and pOS1 P_{lgt} ::ggt-His probed with an α -His antibody or an α -hemolysin A antibody (Hla). ggt::Tn pOS1 P_{lgt} ::ggt is denoted by -His and ggt::Tn pOS1 P_{lgt} ::ggt-His is denoted by +His.

suggests Ggt is cell associated and likely localizes to the *S. aureus* cytoplasm. Further fractionation studies are in progress that remove the peptidoglycan, isolate membranes, and cytoplasmic fractions.

GisABCD-Ggt independent utilization of physiological concentrations of GSH.

We next tested whether GisABCD-Ggt was important for *in vivo* proliferation of *S. aureus* using a systemic mouse model of infection; however, organs of mice infected with a *gisB* mutant contained equivalent bacterial burdens as organs harvested from mice infected with WT. This result indicates that GisABCD-Ggt is dispensable for *S. aureus* pathogenesis in this model (Fig. B-7A). A possible explanation is that *S. aureus* acquires other sources of nutrient sulfur present in the host. In fact, previous work indicated the Cys and CSSC transporter TcyP was required for maximal fitness in murine heart and liver. Consequently we quantified bacterial burdens in murine organs after infection with a *gisB*::Tn *tcyP*::Tn double mutant. Again, no significant difference was

observed between bacterial burdens generated in cohorts of mice infected with the double mutant or WT strains (Fig. B-7B). The lack of a virulence phenotype was perplexing due to the abundance of GSH in host cells and the observation that GSH catabolism mutants in other pathogens display virulence defects (16, 132). However, while gisABCD mutants are impaired for growth in medium supplemented with micromolar concentrations of GSH, GSH accumulates to 0.5-10 mM in host cells (2). Therefore, we wanted to test proliferation of *gisABCD-qqt* mutants at concentrations of GSH and GSSG that more closely mimic those present in the host. The ΔgisABCD-ggt mutant displays significantly increased proliferation in PN media supplemented with 500 µM and 750 µM GSH relative to 50 µM GSH (Fig. 3-6). There is no statistical difference between terminal OD₆₀₀ achieved by WT and that of $\Delta gisABCD$ -ggt in medium containing 500 μ M GSH or 750 μ M GSSG. Intriguingly, we do not observe equivalent growth enhancement in 375 µM GSSG and furthermore the slight increases in terminal OD₆₀₀ reached by ΔgisABCD-ggt in medium with 375 μM GSSG are not significantly different from the terminal OD600 in medium with 25 µM GSSG (Fig. 3-6). Increased concentrations of GSH and GSSG do not alter the lag phase but only effect terminal OD₆₀₀ (Fig. B-8). These findings indicate S. aureus acquires GSH independent of the GisABCD-Ggt system, suggesting another GSH utilization system is active in this pathogen.

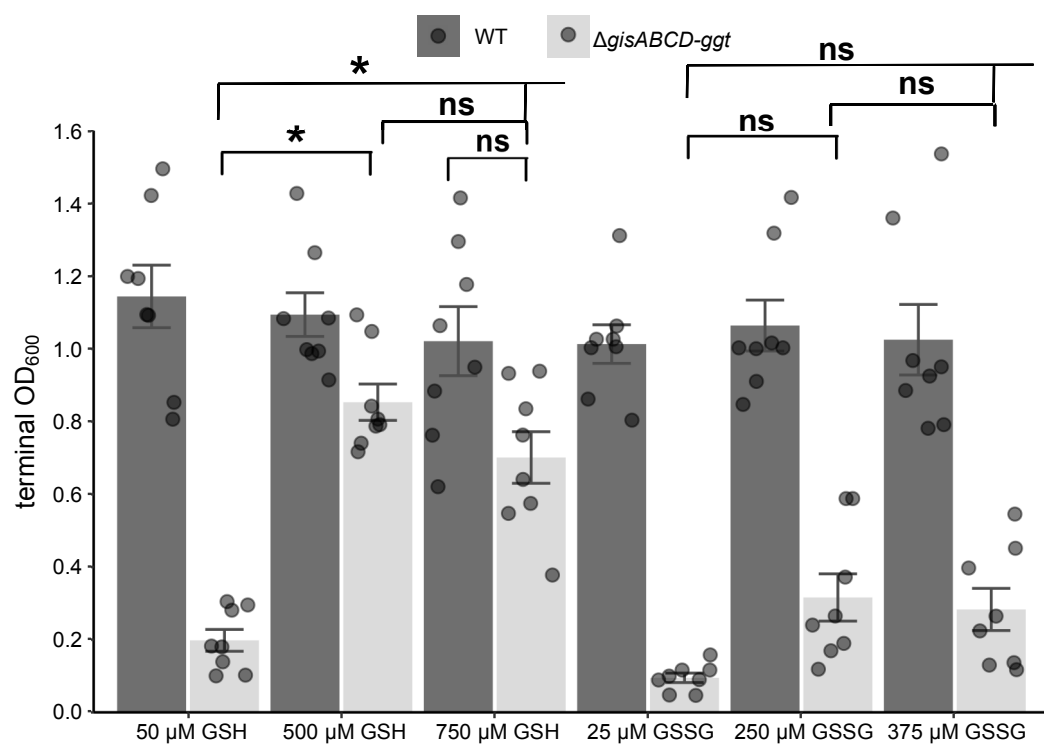


Figure 3-6. S. aureus encodes another transporter that supports growth on physiologically relevant concentrations of GSH.

WT and $\Delta gisABCD$ -ggt were grown in the presence of 50 μ M GSH, 500 μ M GSH, 750 μ M GSH, 25 μ M GSSG, 250 μ M GSSG, and 375 μ M GSSG. Bars depict the mean of the terminal OD₆₀₀ after 19 h of growth. Dots represent the terminal OD₆₀₀ from each individual trial. Error bars represent \pm 1 standard error of the mean. * Indicates p-value <0.05 by one way ANOVA with Tukey's multiple comparison correction.

Ggt homologues are present across Firmicutes.

The fact that *gisB* and *gisB tcyP* mutants failed to display a virulence phenotype in a systemic model of infection prompted an inquiry into the conservation of the GisABCD-Ggt system throughout Firmicutes. We looked for GisABCD-Ggt like proteins across Firmicutes to identify species that carry the entire operon. Since the ABC-transporter proteins are ubiquitous across bacterial lineages, we centered our homolog searches fon Ggt-like proteins. Consequently, we used *S. aureus* Ggt as the initial query and then searched for GisABCD homologues in the Firmicute species containing Ggt homologues (Fig. B-9). Many of the Firmicutes encode Ggt homologues including *Bacillus*, *Gracilibacillus*, *Lysinbacillus*, and *Brevibacterium*; however, these

species do not contain homologues to the complete GisABCD-Ggt system. The distribution of homologues of the GisABCD-Ggt proteins within firmicutes reveals six distinct clusters. Other Firmicutes contain only Ggt homologs (cluster 3), GisB/GisC homologues (cluster 2/4) while others contain GisBC and Ggt homologues (cluster 5) (Fig. B-9). Cluster 6 containing *Bacillus*, *B. subtilis*, *Ctyobacillus*, *and Lysinibacillus acetophenoni* have homologues to the complete GisABCD-Ggt system and exhibit a greater percent similarity than other Firmicutes (Fig. B-9).

GisABCD-Ggt promotes interspecies competition in a GSH-specific manner.

We predicted that GisABCD-Ggt would be widespread throughout Staphylococcus. However, only species in the S. aureus-related cluster complex, Staphylococcus argenteus and Staphylococcus schweitzeri encode homologues to a complete GisABCD-Ggt, as does the next closely related staphylococci, Staphylococcus simiae (157, 158). However, conservation rapidly diverged as the next closely related species, S. epidermidis only encodes apparent GisA, GisC, and Ggt homologues with excessively low percent similarities below the cutoff for the heatmap (30% similarity) (158). Taken together the study of the conservation of Gis-Ggt-like proteins across Firmicutes suggests that S. aureus is inefficient at utilizing GSH as a source of nutrient sulfur. To test this, proliferation of a clinical S. epidermidis isolate was monitored in modified PN medium (PN_{mod}) where MgSO₄ was replaced with MgCl₂ and Met was omitted. Supplementation of 25 µM GSSG failed to stimulate comparable proliferation of S. epidermidis to S. aureus while supplementation of 50 µM GSH leads to severely delayed growth of S. epidermidis relative to S. aureus (Fig. B-10A-F). Notably, S. epidermidis displays a similar growth phenotype in 750 µM GSH to S. aureus, and S. epidermidis does not show enhanced growth in 375 µM GSSG relative to 25 µM GSSG (Fig. B-10E). Together these data indicate potential conservation of the unknown GSH transport system. Next, the capacity of GisABCD-Ggt to provide a fitness advantage to S. aureus in competition with S. epidermidis was determined. To test this, we monitored output ratios of S. aureus to S. epidermidis after a 24 h co-culture in PN_{mod} supplemented with different sulfur

sources. *S. aureus* outcompeted both a *S. epidermidis* clinical isolate and the laboratory RP62a strain in minimal medium supplemented with 25 µM GSSG and 50 µM GSH (Fig. 3-6, Fig. B-10G). Conversely, h *S. epidermidis* strains outcompeted *S. aureus* in medium with 50 µM Met (Fig. 3-6, Fig. B-10G). *S. aureus* demonstrated a fitness advantage over *S. epidermidis* in 750

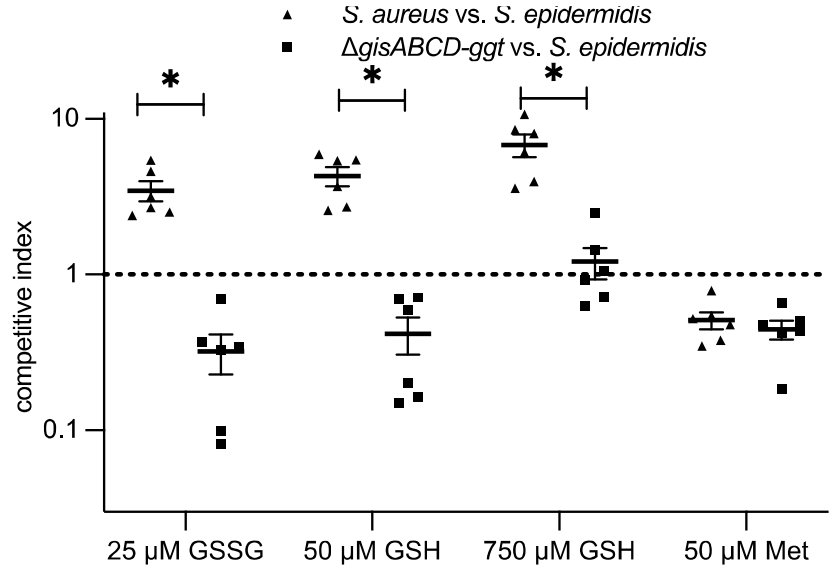


Figure 3-7. GisABCD promotes competition in GSH- or GSSG-supplemented media.

In vitro competition experiments between *S. aureus* and *S. epidermidis* strain RP62a. Presented is the competitive index from each individual trial and the line represents the mean. Error bars represent ± 1 standard error of the mean. * Indicates p-value <0.05 as determined by one-way ANOVA with Tukey's multiple test correction.

 μ M GSH despite equivalent *S. epidermidis* proliferation in monoculture in this concentration (Fig. 3-6, Fig. B-10F). Both *S. epidermidis* strains outcompeted $\Delta gisABCD$ -ggt in 25 μ M GSSG and 50 μ M GSH, indicating that GisABCD-Ggt is essential for *S. aureus* outcompeting *S. epidermidis* in environments containing this host-derived metabolite. Disruption of $\Delta gisABCD$ -ggt reduces the fitness advantage of *S. aureus* in medium with 750 μ M GSH further suggesting the Gisindependent transport system could be conserved between *S. aureus* and *S. epidermidis*.

Discussion

Sulfur is essential for life. Consequently, invading pathogens must procure sulfur during infection and are restricted to sulfur-containing metabolites present in host tissues to fulfill this

requirement. To date CSSC, Cys, *N*-acetyl Cys, hCSSC, sulfide, thiosulfate, and GSH have been shown to be viable sulfur sources for *S. aureus* (11, 28, 147). In this study we expand the number of possible sulfur sources to include GSSG and show that *S. aureus* utilizes the ABC-transporter system, GisABCD, and a γ-glutamyl transpeptidase, Ggt, to import and catabolize GSH and GSSG as sources of nutrient sulfur.

Data presented here supports a model for how GisABCD-Ggt functions to support S. aureus acquisition of GSH and GSSG (Fig. B-11). Bioinformatic evidence predicts GisD is a substrate binding protein and GisBC are transmembrane permeases (Fig. B-2). Our model predicts GisD is sufficiently versatile to support capture of both GSH and GSSG, which represents a 2-fold difference in mass. Prior studies in *Haemophilus influenzae* established a precedent for a substrate binding protein capable of seizing both GSH and GSSG (21). Additionally, the GshT GSH transporter expressed by *S. mutans* transports γ-glutamyl containing mixed disulfides, and studies have specifically examined homocysteine conjugated to GSH (22, 159). In keeping with these results, the authors speculated that the y-glutamyl residue is the lynchpin for substrate recognition, which is a potential mechanism for GisD substrate recognition (159). Future studies employing proliferation assays, transport efficiency measurements, and three-dimensional structural analysis of GisABCD will define the substrate binding capacity of this transporter in S. aureus. The fact that gisACBD mutants fail to proliferate when either GSSG or GSH are supplied as the sole source of nutrient sulfur supports the conclusion that GisABCD imports these metabolites. ATP hydrolysis powers ABC-transporters, and we show that rGisA is capable of hydrolyzing ATP, supporting the bioinformatic annotation that GisABCD is an ABC-transporter. Based on the subcellular localization of Ggt, the model predicts that GSH and GSSG are imported intact and cleaved in the cytoplasm, generating glutamate and cysteinyl-glycine in the case of GSH or glutamate and cysteinyl-glycine disulfide in the case of GSSG. Liberation of cysteine from cysteinyl-glycine represents the finals step of fulfilling the sulfur requirement and in E. coli this process occurs via the amino peptidases A, B, and N, and the dipeptidase D (50). A critical

difference in GSSG acquisition compared to GSH is reduction of the cysteinyl-glycine disulfide. Whether reduction occurs prior to or after proteolysis of cysteinyl-glycine is not known. Future studies probing the identities of the cysteinyl-glycine proteases and cysteinyl-glycine disulfide reductase will resolve the order of these steps.

Cytoplasmic localization of Ggt is consistent with fact that S. aureus does not synthesize GSH and therefore does not utilize GSH as a primary, endogenous low molecular weight thiol. S. aureus and other Firmicutes use bacillithiol as a low molecular weight thiol (145, 160). Consequently, intracellular expression of Gqt will not perturb redox homeostasis as it pertains to the abundance of bacillithiol, the low molecular weight thiol used by S. aureus (145, 160). GSH is the low molecular weight thiol in E. coli and Ggt is expressed in the periplasmic space where it contributes aides in the hydrolysis of GSH to allow the cell to import cysteinyl-glycine (48, 137). Cytoplasmic localization of Ggt is rare in bacteria. In Neisseria meningitidis Ggt is localized to the membrane on the cytoplasmic face (139). Future experiments will determine further fractionate the S. aureus cell and investigate whether it interacts with the membrane. The conclusion that Ggt is localized within the cell indicates that the substrates for GisABCD import are GSH and GSSG. Furthermore, these findings reveal that catabolism occurs inside of the cell unlike other bacterial species such as E. coli and F. tularensis where Ggt cleavage occurs in the periplasmic space followed by import of cysteinyl-glycine via dipeptide transport systems (16, 132, 137, 161). The strategy S. aureus employs to import and cleave GSH and GSSG leaves open the possibility that GSH and GSSG may persist in the cytoplasm in-tact (48, 146). It is currently not known how rates of GSH import compare to Ggt kinetics. Also, whether GSH is imported and degraded when other sources of nutrient sulfur are available has not been addressed. Therefore, GSH accumulation in the cytoplasm is possible. Our study does not preclude the notion that GSH could serve another function in S. aureus in addition to being a source of nutrient sulfur. Streptococcus pneumoniae, Streptococcus pyogenes and H. influenzae highjack exogenous GSH to protect against oxidative stress and metal toxicity (23, 133, 162). Our methodology exclusively examined

use of GSH as a sulfur source; though in complex environments containing GSH and other sources of nutrient sulfur, GSH could serve alternative functions for *S. aureus*. Future work investigating accumulation of GSH and GSSG intracellularly when *S. aureus* is cultured in the presence of multiple viable sulfur sources will determine whether GSH and GSSG serve alternative roles in *S. aureus* physiology.

gis mutants do not display virulence defects in a murine model of systemic infection; however, clinical isolates of S. aureus maintain the ability to utilize GSSG as a source of sulfur. Emergence of Cys auxotrophs after adaptation to the host environment suggests that nutrient sulfur acquisition is dispensable in some cases (63-66). Consequently, the observation that S. aureus clinical isolates maintain the ability proliferate in medium supplemented with GSSG implies that trait might be important in the host. A confounding observation that obstructs direct quantitation of the importance of GSH utilization to S. aureus pathogenesis is the presence of another GSH acquisition system. The finding that gis mutants proliferate in physiologically relevant concentrations of GSH reveals that S. aureus likely encodes at least one other GSH transporter. Proliferation of gis mutants was restored upon supplementation with 750 µM GSH but supplementation with 375 µM GSSG resulted in low levels of proliferation that were not significantly different than observed using 25 µM GSSG. This result suggests the transporter is specific for GSH. Growth restoration in the gis mutant at greater GSH concentrations also implies that S. aureus expresses another peptidase capable of cleaving the y-peptide bond in GSH. The identity of this system remains unknown. Ggt-independent cleavage of GSH has been reported in yeast species by DUG enzymes and by the ChaC homologue present in F. tularensis (132, 163). Dug2p and Dug3P, members of the Ntn superfamily, are known to form a heterodimer and cleave the y-peptide bond in GSH, while ChaC, predominantly present in eukaryotic cells, are yglutamyl cyclotransferases where cysteinyl-glycine and 5-oxoproline not glutamate is released (164, 165). Perhaps, S. aureus follows a strategy of secreting the other enzyme capable of cleaving GSH and transports cysteinyl-glycine through one of the 6 putative oligopeptide or

dipeptide transport systems expressed by *S. aureus* (132, 166–168). Nevertheless, identifying proteins responsible for GisABCD-Ggt-independent transport and cleavage of GSH will allow for a complete investigation into whether *S. aureus* imports and catabolizes GSH during infection.

Ggt cleavage of the γ-bond proceeds when the catalytic threonine attacks the glutamate residue leading to an enzyme-glutamate intermediate and releasing cysteinyl-glycine. Ultimately water enters, hydrolyzing the glutamate from the enzyme (151). Our data shows *S. aureus* Ggt cleaves both GSH and GSSG liberating glutamate. The ability to cleave both substrates has been shown by *Proteus mirabilis* Ggt and *H. pylori* Ggt (169, 170). *S. aureus* can use Ggt to cleave both substrates instead of relying on a thiol reductase to reduce GSSG to GSH. Additionally, glutamate is released by Ggt from both GSH and GSSG; consequently, we predict that the products of hydrolysis are glutamate, cysteinyl-glycine when GSH is the substrate or cysteinyl-glycine disulfide when GSSG is the substrate. We surmise that cysteinyl-glycine disulfide is reduced prior to cleavage by another protease liberating Cys (151, 171).

Phylogenetic analysis of Staphylococcus using 16S rRNA sequence revealed that *S. aureus* forms the *S. aureus*-related complex with *S. argenteus* and *S. schweitzeri*. This complex is closely related to *S. simiae* (157, 158). GisABCD-Ggt conservation studies revealed that the *S. aureus*-related complex and *S. simaei* encode GisABCD-Ggt homologues while the next closely related species *S. epidermidis* encodes only GisA, GisC and Ggt homologues (158). *S. schweitzeri* colonizes the nasopharynx of African wildlife such as bats and primates with limited reports of human isolates and no resulting disease, while *S. argenteus* is reported to colonize fruit bats and monkeys while also causing significant infections in humans including skin and soft tissue infections, bone and joint infections, and sepsis (172–179). A correlation between the ability to cause systemic disease and encoding a complete GisABCD-Ggt is not apparent. Both *S. aureus* and *S. argenteus* encode GisABCD-Ggt and are systemic pathogens but *S. schweitzeri* also encodes the system but is not readily associated with systemic disease. Consistent with these results is the lack of a virulence phenotype displayed by the *gisB* mutant in a systemic

model of infection. Overall, these observations suggest GisABCD-Ggt plays important roles in aspects of staphylococcal physiology beyond those needed for systemic infection. Furthermore, *S. aureus, S. epidermidis, and S. schweitzeri* can be found in the nasal passages of humans or closely related primates but the observation that GisABCD-Ggt is not conserved completely in *S. epidermidis* suggests GisABCD-Ggt is not an essential system for nasal colonization (73, 76, 157, 180). Both *S. aureus* and *S. epidermidis* are residents of the skin microflora of humans, while we do not know the levels of GSH present on human skin, this niche could be further explored to determine if GisABCD-Ggt provides a competitive advantage to *S. aureus* when proliferating on the skin. Future work investigating functional homology between *S. aureus* GisABCD and GisABCD homologues, as well as examining the operonic structure of GisABCD-Ggt homologues in staphylococci will determine if the system functions together or whether Ggt homologues function with an alternative import system. Additionally, testing whether heterologous expression of *S. epidermidis* GisA and GisC homologues in corresponding *S. aureus* mutants functionally complement the strains will provide further mechanistic details and possibly the function of the *S. epidermidis* proteins.

Only select Firmicutes encode homologues to each component of GisABCD-Ggt; however, our current analysis did not investigate the genomic location and organization of the homologues. Perhaps these homologues are present in distinct chromosome locations and do not function together. Future studies can investigate the genomic location of GisABCD-Ggt homologues, and this would inform us whether the homologues function together. Our bioinformatic analysis used the presence of a glutamyl hydrolase domain as the filtering metric; however, many Ggt enzymes have been reported to exhibit substrate promiscuity (181–183). Structural studies comparing *S. aureus* Ggt and other Ggt homologues will define substrate preferences and provide insights into the origins of *S. aureus* Ggt.

We found that numerous Firmicutes encode Ggt homologues, but conservation of GisABCD is limited in the same bacteria. The apparent lack of conservation suggests that these

organisms evolved mechanisms of GSH transport distinct from GisABCD. Based on the seemingly similar growth phenotypes displayed by *S. aureus* and *S. epidermidis* in medium supplemented with 750 uM GSH, genome wide protein domain architecture bioinformatic comparisons between these species may identify candidate transport systems capable of importing GSH. Additional work could examine the conservation of genomic context and operonic structure of the Ggt homologues present across Firmicutes to determine whether *ggt* is located near genes encoding novel GSH transporters.

In summary, we show *S. aureus* utilizes GSSG as a sulfur source and provide a model into *S. aureus* import and catabolism of GSSG and GSH. Prior to this work, sources of nutrient sulfur were described, but the mechanisms *S. aureus* employed to acquire and catabolize these metabolites were not defined. We identified a transporter system, GisABCD-Ggt that supports proliferation of *S. aureus* when micromolar concentrations of GSSG or GSH are supplied while Gis mutants can proliferate in high micromolar concentrations of GSH but not GSG. We demonstrate that GisABCD-Ggt is conserved in select *Staphylococcus* species related to *S. aureus* but the whole system is not conserved in *S. epidermidis*. Furthermore, GisABCD-Ggt provides a fitness advantage to *S. aureus* over *S. epidermidis* when grown in medium containing GSH.

Materials and Methods

Bacterial strains used in this study.

The WT *S. aureus* strain used in these studies was JE2, a laboratory derivative from the community-acquired USA300 LAC (100). SAUSA300_0200-ggt mutants strains were generated via transduction of the transposon inactivated gene from the Nebraska Transposon Mutant Library (NTML) into JE2 using transduction methodology (100, 118). The bacterial strains used in this study are presented in Table B-1.

A strain harboring an in-frame deletion of *gisABCD-ggt* was achieved using a previously described allelic exchange methodology for *S. aureus* (184). One kb upstream of SAUSA300_0200 and one kb downstream of *ggt* were amplified using primers listed in Table B-2 and cloned into pKOR1-mcs. pKOR1-mcs was confirmed to have both correct 1kb homology sequences by Sanger sequencing. The deletion strain was screened for hemolysis on blood agar plates and displayed WT level hemolysis.

Growth analysis.

Chemically defined (PN) medium was prepared as previously described (121). PN contains 17 amino acids and lacks asparagine and glutamine. CSSC was also omitted in order to determine the capacity of *S. aureus* to grow in PN supplemented with various sulfur sources (121). PN medium was supplemented with 5 mg mL⁻¹ glucose for this work. Prior to inoculation in PN, *S. aureus* was cultured in TSB overnight, washed with PBS, and resuspended in PN medium to an OD₆₀₀ equal to 1. Round-bottom 96-well plates containing PN with 5 mg mL⁻¹ glucose supplemented with the listed sulfur sources were inoculated with *S. aureus* strains at an initial inoculum of OD₆₀₀ of 0.01. Growth analysis was carried out at 37°C with continuous shaking for the indicated timeframe.

Isolation and growth of clinical isolates.

Deidentified clinical isolates of *Staphylococcus aureus* were obtained from a regional hospital clinical laboratory. Three isolates were MRSA isolated from abscesses (1055-1057) and the other two were MSSA isolated from bone (1058 and 1059). Identification and minimum inhibitory concentration assays were performed by the parent laboratory following Clinical and Laboratory Standards Institute approved methods. After initial isolation, subcultures were grown on TSA overnight. One colony was then suspended in 5 mL of TSB for overnight growth at 37 °C and archived at -80 °C. WT JE2 and clinical isolates were grown in TSB overnight at 37 °C and

shaking at 225 rpm. Overnight cultures were washed with PBS and normalized to an OD_{600} equal to 1. A 96-well plate containing PN supplemented with 25 μ M CSSC or 25 μ M GSSG was inoculated at OD_{600} equal to 0.01 and the cells were incubated for 19 h at 37 °C with continuous shaking. OD_{600} was measured, blank corrected, and triplicate wells were averaged.

Anaerobic growth.

To ensure CSSC, GSH and GSSG were maintained in their respective reduced or oxidized forms, stocks were prepared by weighing the appropriate amount of the chemical aerobically and immediately transferring it to an anaerobic chamber (Coy) with a 95:5 % nitrogen:hydrogen atmosphere. Sulfur sources where then resuspended in either anaerobically acclimated water (GSH and GSSG) or anaerobically acclimated 1 N HCl (CSSC). Cultures were grown in TSB, washed with PBS, and diluted to an OD600 equal to 1 with PN after which they were transferred to the anaerobic chamber. The 96-well plate contained 150 μ L PN with 100 mM sodium nitrate supplemented with 25 μ M CSSC, 25 μ M GSSG, or 50 μ M GSH and strains were added at a starting OD600 equal to 0.01. The plate was incubated statically at 37 °C for 24 h, and the OD600 was measured. The absorbance of uninoculated medium was subtracted from the cell culture derived OD600 values and triplicates averaged.

Domain prediction of GisABCD-Ggt.

The USA300_FPR3757 (assembly GCF_000013465.1) reference was used to determine domain prediction for GisA (ABD21741.1), GisB (ABD21022.1) GisC (ABD20640.1), GisD (ABD22752.1), and Ggt (ABD22038.1). Protein sequences were analyzed with custom scripts using InterProScan, TMHMM, Phobius, Pfam, and PROSITE to identify domains and secondary structures (129, 185–189). Domain architectures were visualized using custom R scripts and the R package gggenes (190).

Construction of pET28b::ggt and pET28b::gisA and purification of tagged protein.

The ggt and gisA open reading frames prior to the stop codon were amplified with primers sets listed in Table S2. The expression vector pET28-b was digested with Ncol-HF and Xhol-HF. Plasmid assembly was performed using Gibson assembly and the NEB HiFi assembly kit (NEB, New England, MA). The assembly mixture was transformed into E. coli, cells were recovered in lysogeny broth (LB), and plated onto LB agar containing 50 mg mL⁻¹ kanamycin and 5 mg mL⁻¹ glucose. Plasmids were confirmed using Sanger sequencing and transformed into a NEB strain 3016 slyD mutant. Transformed E. coli were cultured in LB with 50 mg mL⁻¹ kanamycin overnight at 37 °C with shaking at 225 rpm, sub-cultured 1:50 into 500 mL LB with 50 mg mL⁻¹ kanamycin in a 2 L flask and grown to an OD600 of 0.4-0.5. Ggt or GisA protein expression was induced by addition of 200 μM isopropyl-1-thio-β-D-galactopyranoside (IPTG) and the culture was separated into 5, 500 mL flasks containing 100 mL of culture and incubated for 4 h at 27 °C and 225 rpm shaking. After induction, cells were centrifuged at 10,000 x g for 10 mins at 4 °C and washed with PBS. Resulting GisA and Ggt induction pellets were resuspended in 40 mL of buffer containing 50 mM tris, 200 mM KCl, 20 mM imidazole at pH 8-, or 40-mL buffer containing 50 mM tris, 500 mM NaCl, 20 mM imidazole at pH 8, respectively. Cells were lysed using a fluidizer set to 20,000 psi and samples were run through 5 times. Lysates were then centrifuged at 15,000 x g for 15 mins to remove intact cells and the resulting supernatant was retained. To purify the target proteins, Ni-NTA chromatography was used. Purification was performed by incubating the cleared lysate with 1 mL Ni-NTA resin (Qiagen, Hilden, Germany) on a rotating platform at 4 °C for 2 h. Protein was eluted with 50 mM tris 400 mM imidazole. Buffers used to purify GisA contained 200 mM KCI while buffers used to purify Ggt contained 500 mM NaCl. Each buffer contained 1x protease inhibitor cocktail (Millipore-Sigma). The GisA elutant was dialyzed using 10 mM tris, 200 mM KCl at pH 7.5 as the dialysis buffer for 18 h. The Gqt elutant was dialyzed using 10 mM tris, 150 mM at pH 7.0 as the dialysis buffer for 18 h. Both the elutions were concentrated using 10

kDa molecular weight cutoff protein concentrators. Purification was confirmed via electrophoresis using 12% SDS-PAGE gels. Protein concentrations were determined with the bicinchoninic acid (BCA) protein kit (BioRAD).

ATPase activity of GisA.

ATPase activity of purified recombinant GisA was monitored using the malachite green phosphate assay (Millipore-Sigma). Recombinant GisA was diluted to 2.5 μ g per reaction. Diluted GisA, 250 μ M MgCl₂, and 400 μ M ATP were incubated for 1 h at 37 °C and samples were taken at 0, 15, 30, 45, and 60 mins. At the indicated time points samples were flash frozen in a dry-ice ethanol bath and stored at -80 °C (191). Samples were thawed at room temperature, malachite green reagent was added, and P_i release was determined following the manufacturer's instructions. Each biological replicate was an independent protein purification.

Quantitation of Ggt enzyme kinetics.

Reactions were set up as follows: 10 mM tris with 150 mM NaCl containing 5 µg recombinant Ggt and indicted concentrations of GSH and GSSG dissolved in the reaction buffer. Reactions proceeded for 30 mins at 37°C after which the reaction was incubated at 80 °C for 5 mins to stop the reaction. Samples were dried using a roto-vac speed vacuum and stored at -80 °C until further processing. Samples were resuspended in water, derivatized with carboxybenzyl (CBZ), and samples were run on a Waters Xevo TQ-S triple quadrupole mass spectrometer using previously described methodologies (192). Signal was normalized to a ¹³C-glutamine internal standard. A glutamate standard curve was run using the same chromatographic conditions and the fit equation was employed to quantitate glutamate. Glutamate released per min was calculated and data were fit to the Michaelis-Menten equation using GraphPad Prism. Data is the average of glutamate quantified from four independent protein purifications.

Western blotting analysis of S. aureus Ggt.

The ggt ORF, his tag, and stop codon were amplified from pET28b::ggt and cloned into pOS1 P_{lgt} digested with Ndel and HindIII using Gibson assembly. Additionally, the *ggt* ORF was amplified from JE2 and pOS1 P_{lat} digested with Ndel and HindIII using Gibson assembly. Plasmids were confirmed by Sanger sequencing and transformed from E. coli DH5a into S. aureus RN4220 via electroporation. His-tagged Ggt encoding plasmid was purified from RN4220 and transformed into JE2 ggt::Tn. The empty vector control strain were generated by transforming JE2 and ggt::Tn with pOS1 P_{lat}::ggt and ggt::Tn pOS1 Plat::ggt-His cultures were prepared as described in growth analysis and subcultured into 3, 250 mL flasks each containing 100 mL PN with 25 µM GSSG, and 10 µg mL⁻¹ chloramphenicol at a starting OD₆₀₀ equal to 0.1, and grown for 4 h at 37 °C and 225 rpm shaking. Cells were recovered via centrifugation, supernatant was retained, and the pellet washed with PBS. Fifty mL of the initial supernatant was precipitated with trichloracetic acid (final percent of 10 % v/v) (TCA), incubated at least 2 h at 4 °C, pelleted, and the resulting pellet was washed twice with 95 % ethanol. Medium supernatant and lysed WCL were incubated with Ni-NTA resin overnight at 4 °C after which the resin was pelleted and washed with PBS. Samples were mixed with laemmli buffer, incubated at 95 °C for 10 min, run on a 12% SDS-PAGE gel using tris-glycine running buffer, and transferred at 65 volts for 1 h at 4 °C to pvdf membrane. Membranes were incubated overnight in phosphate buffered saline tween-20 (PBST) with 5% bovine serum albumin (BSA) at 4 °C with agitation. An α-His mouse antibody was used as the primary antibody at a 1:4000 dilution in PBST-5% BSA and incubated for 1 h with shaking. The membrane was washed 3 times with PBST. Secondary antibodies were either goat α-mouse IgG conjugated to horseradish peroxidase (HRP) or goat α-rabbit IgG conjugated to HRP used at 1:4000 and 1:1000 respectively (Sigma-Aldrich). To assess proper fractionation a rabbit α-hemolysin A (Hla) antibody used at 1:8000. Membranes were washed 3 times PBST after secondary antibody incubations.

Membranes were developed using the ECL Prime kit (Cytiva, Marlborough, MA) and imaged using Amersham Imager 600 (GE Healthcare, Amerhsam, Buckinghamshire, UK).

Murine systemic infections.

WT, *gisB*::Tn, and *gisB*::Tn *tcyP*::Tn were grown in TSB overnight at 37°C, diluted 1:100 into TSB and grown for 3 h at 37 °C at 225 rpm shaking. Cultures were pelleted, washed with PBS, and normalized to OD₆₀₀ equal to 0.4. Female C57B6 or BALB/c mice were retrorbitally infected with 10⁷ CFUs and infection proceeded for 96 h after which heart, liver and kidneys were collected and homogenized in 1 mL PBS. Organ homogenates were dilution plated onto TSA and CFUs mL⁻¹ were determined. Infections were performed at Michigan State University under the principles and guidelines described in the Guide for the Care and Use of Laboratory Animals (193). Animal work was followed as approved by Michigan State University Institutional Animal Care and Use Committee (IACUC) approved protocol number 12/16-205-00.

Resolving of GisABCD-Ggt homologs across bacteria.

The USA300_FPR3757 (assembly GCF_000013465.1) Ggt protein sequence (ABD22038.1) was used as the query protein for homology searches (using DELTA-BLAST) using the NCBI RefSeq database (194–196). Data was filtered to include only members of the Firmicutes that had Ggt homologues containing a glutamyl transpeptidase domain. This dataset was used as the subject to query USA300_FPR3757 GisABCD using blastP. Percent similarity was used to generate a heatmap. The heatmap was created and hierarchical clustering was performed using the R package pheatmap.

In vitro S. aureus and S. epidermidis competitions.

Because S. epidermidis encodes the genes in the sulfate assimilation pathway and the ability of S. epidermidis to utilize Met as a sulfur source was unknown, we wanted to modify the PN medium to fully test sulfur utilization with S. aureus and S. epidermidis. PN medium was tailored by replacing MgSO₄ with MgCl₂ and omitting Met generating PN_{mod} (197–199). S. epidermidis and S. aureus displayed little growth in PN_{mod}. S. aureus and S. epidermidis growth curves were performed as described above in PN_{mod} supplemented with the listed sulfur sources for 25 h. For in vitro competition experiments, S. aureus, S. aureus ΔgisABCD-ggt, and S. epidermidis were cultured overnight in TSB, pelleted, wash in PBS, and normalized to the same OD₆₀₀ in PN medium. Strains were mixed in a 1:1 ratio (v/v) and inoculated into 5 mL PN_{mod}. PN_{mod} was supplemented with 25 µM GSSG, 50 µM GSH, 750 µM GSH, or 50 µM Met. GSH solutions were freshly prepared prior to each trial to limit oxidation. Dilution plating of the original mixture was plated onto mannitol salt agar (MSA) to quantify the initial counts of each organism. Cultures were incubated for 24 h at 37°C with 225 rpm shaking after which the cultures were dilution plated onto MSA and allowed to grow for 48 h at 35 °C. S. aureus ferments mannitol and appears yellow on MSA, while S. epidermidis does not and maintains a pink color; consequently, yellow, and pink colored colonies were enumerated to assess quantities of each organism. Competitive indices (CI) were calculated by dividing the S. aureus to S. epidermidis output ratio by the S. aureus to S. epidermidis input ratio. CI greater than one indicate more S. aureus than S. epidermidis while CI less than one signify greater quantities of *S. epidermidis* compared to *S. aureus*.

Acknowledgements

The following reagents were provided by the Network on Antimicrobial Resistance in Staphylococcus aureus (NARSA) for distribution by BEI Resources, NIAID, NIH: Nebraska Transposon Mutant Library (NTML) Screening Array NR-48501 SAUSA300 0200-

SAUSA300_0204 transposon mutants. We thank the laboratory of Taeok Bae at Indiana University for supplying the plasmid, pKOR1-mcs, and we thank the DiRita and Crosson laboratories at Michigan State University for technical support. This work is funded by the National Institutes of Health R01 Al139074 and R21 Al142517.

Chanter 4 Defining Stanbylococcus aureus transcriptional adaptation to sulfur starvation
Chapter 4 Defining Staphylococcus aureus transcriptional adaptation to sulfur starvation and distinct sources of nutrient sulfur.

Abstract

Staphylococcus aureus causes significant disease but also innocuously colonizes nasal passages and of a subset of the human population. S. aureus infection begins when the organism breaches protective barriers, gaining access to the vasculature ultimately colonizing distinct host organs. To colonize the host, S. aureus must sense and adapt to nutrient availability in distinct tissue environments. Successful adaptation allows the pathogen to scavenge nutritional resources required for proliferation. An understudied aspect of S. aureus nutrient acquisition is how it obtains the essential element sulfur. Sulfur is essential for life and a nutritional requirement for *S. aureus* pathogenesis. To fulfill the sulfur requirement, *S. aureus* relies on the transcriptional repressor, CymR, which previous studies have shown represses expression of genes encoding sulfur acquisition systems and cysteine synthesis. This study defines S. aureus sensing of nutrient sulfur by examining CymR-dependent and -independent transcriptional responses to sulfur starvation. Adaptation to inorganic nutrient sulfur and different sources of organic nutrient sulfur are also presented. We found genetic inactivation of CymR in sulfur replete culture conditions lead to upregulation of 46 genes and these genes are enriched for sulfur transporters. Sulfur starvation also leads to upregulation of genes associated with iron acquisition and oxidative stress. We also observe upregulation of genes encoding sulfur acquisition systems that are controlled by CymR when S. aureus is cultured in GSH or thiosulfate, conditions in which models suggest CymR repression should be active. This study presents the S. aureus gene expression changes to sulfur starvation, provides further insight into the CymR regulon, and defines sulfur source specific transcripts.

Importance

Staphylococcus aureus is an important pathogen of human concern due to its ability to cause disease in numerous body sites. Successful colonization of the host by *S. aureus* requires acclimation to changing environments within the host. The nutrient sulfur is essential for *S. aureus* to grow in the host and cause disease; however how *S. aureus* acclimates to distinct sulfur environments has not been monitored. Here we define the sulfur starvation response of *S. aureus*. Different types of sulfur sources are available in the environment and assimilation of the different types requires different energy input, but how *S. aureus* changes gene expression in the presence of specific sources of sulfur has not been defined. We also studied the gene expression of *S. aureus* grown on various specific sulfur sources. Overall, studies presented here characterize how *S. aureus* senses and responds to changing sulfur environments.

Introduction

Bacterial pathogens sense external stimuli and respond by altering gene expression to thrive in constantly changing host environments. *Staphylococcus aureus* is capable of infecting nearly every vertebrate organ, causing considerable morbidity and underscoring this pathogen's capacity to thrive in diverse host environments. (68–71). For example. *S. aureus* is a resident of the nasal microbiota of 30% of the population and a resident of the skin microbiota in 4% of the population (72, 200). Carriage of *S. aureus* is a risk factor for post-operative infections (144). *S. aureus* pathogenesis is initiated by damage to the skin either through trauma or surgical intervention (75). Upon gaining access to the vasculature, *S. aureus* rapidly disseminates into peripheral organs (94). To successfully transition between these different host environments *S. aureus* senses and acquires essential nutrients from the host environments, but an understudied nutritional requirement of *S. aureus* pathogenesis is sulfur.

Sulfur is essential due to its redox potential which is harnessed by multiple cofactors and amino acids (1, 2, 5, 135, 201, 202). Cysteine (Cys) is the critical focal point of sulfur metabolism

as it is a substrate for the generation of proteins and numerous cofactors. Within biological systems sulfur is available in organic or inorganic metabolites. Organic sulfur sources include Cys, glutathione (GSH), and methionine and in these compounds the sulfur is complexed to carbon allowing for assimilation via direct import or liberation of the sulfur containing moiety. The sulfur in inorganic sulfur sources, such as sulfate or thiosulfate, is highly oxidized, and requires reductive processes to assimilate to Cys (25, 105). In humans Cys and GSH act as low molecular weight thiol redox buffers in serum and within cells, respectively. Consequently, Cys and GSH represent abundant organic sources of sulfur for invading pathogens. Prior studies have shown S. aureus utilizes GSH, oxidized GSH, Cys, cystine (CSSC), homocystine, N-acetyl Cys, sulfide, and thiosulfate as sulfur sources (11, 147). How S. aureus responds to a sulfur depleted environment, regulates utilization of inorganic versus organosulfur sources, and changes cellular physiology in response to specific sulfur sources are questions that remain unanswered.

Control of nutrient sulfur acquisition systems and Cys synthesis in *S. aureus* and other Firmicutes is regulated by CymR. CymR responds to intracellular Cys levels by forming a complex with CysM, the enzyme that catalyzes the reaction of OAS and sulfide, when Cys levels are high (28, 99). The CymR-CysM complex acts as a repressor, impeding expression of genes involved in nutrient sulfur acquisition and metabolism (28). Repression is relieved when the CymR-CysM interaction is disrupted by high levels of OAS, the carbon backbone necessary for synthesis of Cys from inorganic sulfur such as sulfate (4, 25, 203). OAS levels increase in the cell as the Cys level decreases because the enzyme responsible for OAS synthesis, serine acetyltransferase (CysE) is negatively controlled by Cys. Consequently, environments depleted for Cys cause increased CysE activity, resulting in accumulation of OAS and signaling a need for nutritional sulfur (4, 25, 203). Alternatively, CymR has also been shown to respond to oxidation. An internal Cys residue, Cys-25, senses the oxidation state of the cell and when oxidized relieves CymR repression by causing a protein conformational change that decreases the affinity of the protein for DNA (204). Previous work has characterized transcriptional alterations that occur in a *S*.

aureus cymR mutant, however, transcriptional changes that result from sulfur starvation in an otherwise WT cell have not been reported.

The type of sulfur source acquired by *S. aureus* likely affects metabolism. Inorganic sulfur sources shift cellular metabolism by depleting OAS pools needed to synthesize Cys and the necessary input of reducing power. However, assimilation of organosulfur sources predominantly involves liberation of the sulfur-containing compound instead of synthesis (4, 25). These facts support the hypothesis that organic sources of nutrient sulfur will elicit different transcriptional responses than inorganic sulfur sources.

This study defines the sulfur starvation response in *S. aureus* and establishes potential CymR-dependent and -independent transcriptional targets in sulfur replete and deplete growth conditions. Furthermore, transcriptional changes that occur when *S. aureus* adapts to different sulfur sources is investigated. Our findings are consistent with previous reports that identified genes upregulated in a *cymR* mutant. We observe upregulation of iron transporter and oxidative stress genes during sulfur starvation. Adaptation to inorganic thiosulfate as the sulfur source leads to differential expression of 566 genes of which 238 genes are upregulated and 328 are downregulated compared to *S. aureus* grown on CSSC as a sulfur source. Upregulation of sulfur source transporters under CymR control is observed when GSH or thiosulfate are supplied as sulfur sources. However, these conditions are sulfur replete and CymR repression should be active. This suggests CymR is responsive to additional, unknown stimuli (28). Overall, work presented here outlines links between sulfur starvation, iron homeostasis, and the oxidative stress response, and provides evidence for additional stimuli of sulfur import and catabolism related gene regulation.

Results and discussion

Sulfur starvation and the CymR response.

Currently, there are two models for CymR regulation (Fig. 4-1A). First, CymR complexes with CysM when intracellular Cys is high, but this complex is disrupted upon OAS accumulation when intracellular Cys levels are low (Fig. 4-1A) (28). In the second model, a redox sensitive Cys

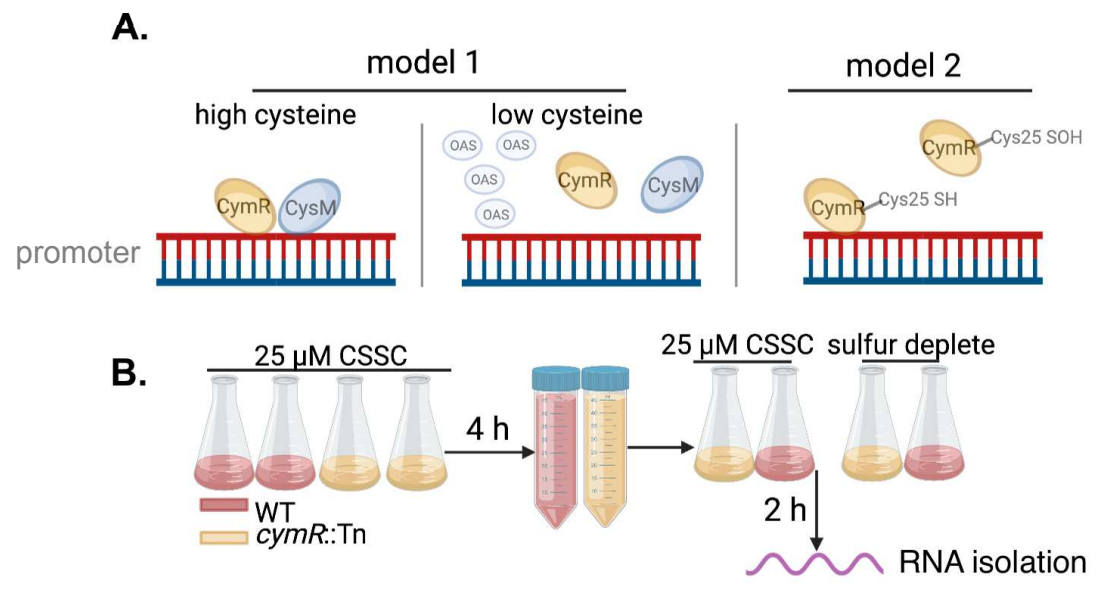


Figure 4-1. Experimental design employed to define the CymR-dependent and –independent response to sulfur starvation in *S. aureus*.

(A) Schematic depicting control of CymR regulation in *S. aureus*. (B) Illustration depicting the culture conditions. WT and *cymR*::Tn *S. aureus* were cultured in PN with 25 μ M CSSC (CSSC) to mid-exponential phase. Cultures were pelleted, washed, and resuspended at the same cell density in medium with (sulfur replete) or without CSSC (sulfur deplete).

residue in CymR responds to the oxidation state of the cell and upon oxidation elicits a conformation change in CymR, alleviating repression (Fig. 4-1A) (204). This study sought to establish the transcriptional response of *S. aureus* to sulfur starvation and investigate the CymR regulon. *S. aureus* strain JE2 and an isogenic *cymR* mutant (*cymR*::Tn) were incubated in chemically defined PN medium supplemented with 25 μ M CSSC as the sole source of nutrient sulfur. Cells were cultured to mid-exponential phase. Next, WT and *cymR*::Tn cells were collected, washed, and resuspended at the same cell density into PN supplemented in sulfur replete (25 μ M CSSC) or sulfur deplete (no added sulfur source) 2 h (Fig. 4-1B). This experimental design reveals

the CymR response with a robust methodology and examines the overlap of the sulfur starvation response and CymR regulon. Comparisons between the culture conditions and total number of

Table 4-1. Culture conditions comparing sulfur starvation and the CymR regulon.

culture conditions	abbreviated	description	compar ator	total differentiall y regulated genes	upregulated genes	downregulate d genes
<i>cymR</i> ::Tn	cymR-	CymR	WT	112	46	86
+CSSC	replete	dependent changes	+CSSC			
sulfur	WT-deplete	starvation	WT	989	499	490
starved WT		induced changes	+CSSC			
sulfur	cymR-	starvation	cymR	344	169	175
starved	deplete	induced	+CSSC			
<i>cymR</i> ::Tn		changes				
		independent				
		of CymR				

genes differentially regulated greater than 2-fold are outlined in Table 4-1.

CymR is the fulcrum of the sulfur transcriptional response (28). Consequently, CymR regulation was investigated from two perspectives. The first surveys genes upregulated when CymR is disrupted in a medium supplemented with CSSC (cymR-replete) and the second surveys transcriptional responses to sulfur depletion. Prior studies by Soutourina et al. employed microarray technology to examine the CymR response using a cymR mutant grown in rich medium (28). This study identified 46 genes upregulated in the cymR mutant, 16 genes were associated with sulfur acquisition and metabolism and 30 were associated with the cell-envelope (28). We sought to expand upon the study of CymR-dependent genes using RNA-seq and defining the CymR regulon in a derivative of the current strain endemic in the United States USA300, JE2 (Fig. 4-1B). The cymR-replete condition mimics those used by Soutourina et al., with the exception that the chemically defined PN minimal medium was employed. Similar to the Soutourina et al. study, 46 genes were upregulated (Table 4-1 and Table 4-2), including genes encoding 12 hypothetical proteins and 12 predicted transporter proteins.

Table 4-2. Sulfur status independent CymR regulon.

locus	gene name	product	log₂ ratioª	adj p-value ^b	COG °
SAUSA300 RS00910	-	hypothetical protein	3.414	1.24E-06	S
Table 4-2 (cont'd)					
SAUSA300_RS10985		YeeE/YedE family protein	3.392	5.27E-07	S
SAUSA300_RS10980		oxidoreductase	3.262	1.24E-06	0
SAUSA300_RS00925	ssuC	ABC-transporter permease	3.131	1.71E-06	Р
SAUSA300_RS00930		acyl-CoA dehydrogenase	3.037	5.27E-07	1
SAUSA300_RS13915	isaA	transglycosylase IsaA	2.783	1.32E-03	М
SAUSA300_RS02035	tcyP	L -cystine transporter	2.683	1.49E-04	U
SAUSA300_RS05050		hypothetical protein	2.361	6.94E-04	S
SAUSA300_RS02045		hypothetical protein	2.283	1.69E-04	Α
SAUSA300_RS01055		ABC-transporter ATP-binding protein	2.247	3.75E-03	Р
SAUSA300_RS01170		glycerophosphoryl diester phosphodiesterase	2.243	8.12E-03	С
SAUSA300_RS02340	gmp C	ABC-transporter substrate- binding protein	2.187	7.48E-03	Р
SAUSA300_RS12610	sdp C	lysostaphin resistance protein A	2.099	2.39E-03	S
SAUSA300_RS00915	ssuB	sulfonate ABC-transporter ATP-binding protein	2.054	1.80E-02	Р
SAUSA300_RS05345		cell-wall-binding lipoprotein	2.048	1.21E-02	L
SAUSA300_RS02635	cysK	Cys synthase	2.033	1.44E-02	Е
SAUSA300_RS09440	crcB 2	camphor resistance protein CrcB	2.013	1.54E-02	D
SAUSA300_RS02325	mcc B	cystathionine gamma-synthase	1.998	1.52E-02	Е
SAUSA300_RS02335	met P2	ABC-transporter permease	1.990	2.18E-02	Р
SAUSA300_RS01875		hypothetical protein	1.968	9.99E-03	S
SAUSA300_RS13605		lantibiotic ABC-transporter ATP-binding protein	1.941	1.44E-02	V
SAUSA300_RS02330	met N2	methionine import ATP-binding protein MetN 1	1.903	2.10E-02	Р
SAUSA300_RS12685		alpha/beta hydrolase	1.901	1.10E-02	I
SAUSA300_RS01060		ABC-transporter permease	1.859	3.42E-02	EP
SAUSA300_RS04485		hypothetical protein	1.830	4.28E-02	S
SAUSA300_RS13940		hypothetical protein	1.828	3.51E-02	S
SAUSA300_RS02855		N-acetyl- L, L -diaminopimelate deacetylase	1.816	1.33E-02	Е
SAUSA300_RS00920	ssuA	hypothetical protein	1.796	2.63E-02	Р
SAUSA300_RS13025	tcyA	amino acid ABC-transporter substrate-binding protein	1.764	2.09E-02	ET
SAUSA300_RS12500	sdpB	CPBP family intramembrane metalloprotease	1.734	2.68E-02	S
SAUSA300_RS13320		hypothetical protein	1.689	2.68E-02	S
SAUSA300_RS05415		hypothetical protein	1.673	4.79E-02	S
SAUSA300_RS10230		hypothetical protein	1.662	3.73E-02	S

Table 4-2 (cont'd)					
SAUSA300_RS00605	sirA	iron ABC-transporter substrate-binding protein	1.644	2.19E-02	Р
SAUSA300_RS05540	isdA	iron-regulated surface determinant protein A	1.642	2.81E-02	M
SAUSA300_RS12705		TetR family transcriptional regulator	1.641	3.28E-02	K
SAUSA300_RS11450		hypothetical protein	1.618	4.28E-02	S
SAUSA300_RS12440		CHAP domain-containing protein N-	1.600	2.68E-02	S
SAUSA300_RS03340	tagA	acetylmannosaminyltransferas e	1.585	3.81E-02	M
SAUSA300_RS04060	clpP	ATP-dependent Clp protease proteolytic subunit	1.523	2.68E-02	OU
SAUSA300_RS00985	brnQ 1	branched-chain amino acid transporter II carrier protein	1.520	4.28E-02	Е
SAUSA300_RS07465	cmk	cytidylate kinase	1.507	3.05E-02	F
SAUSA300_RS07075	brnQ 3	branched-chain amino acid transport system II carrier protein	1.491	3.51E-02	Е
SAUSA300_RS15260		hypothetical protein	1.463	4.28E-02	S
SAUSA300_RS09900		PTS transporter subunit IIC	1.449	4.28E-02	S
SAUSA300_RS13625		membrane protein	1.447	4.28E-02	S

^a Expression ratio of *cymR*::Tn grown in medium containing CSSC relative to WT grown in same medium.

Gene Ontology (GO) predictions using PATHER GO analysis of transcripts upregulated in *cymR*-replete demonstrate that genes encoding sulfur metabolic enzymes and sulfur-associated transporters are significantly enriched (Fig. 4-2). Included in this analysis are sulfur-associated transporters, sulfur compound transporters, sulfur amino acid transporters, and L-amino acid transporters (Fig. 4-2). Compared with Soutourina *et al.* 10 of 16 upregulated sulfur-associated genes are shared between the datasets (Table 4-2 grey) (28). These 10 genes include the Cys and CSSC transporters, *tcyP* and *tcyA*, the putative methionine import protein (SAUSA300_RS02330, *metN2*), acyl-coA dehydrogenase (SAUSA300_RS00930), two ABC-

^bAdjusted p-value from DESeg2 output.

^cA: RNA processing and modification B: chromatin structure and dynamics C: energy production and conversion D:cell cycle control and mitosis E: amino acid metabolism and transport F: nucleotide metabolism and transport G: carbohydrate metabolism and transport, H: coenzyme metabolism, I: lipid metabolism, J: translation, K: transcription, L: replication and repair, M: cell wall/membrane/ envelope biogenesis, N: cell motility, O: post-translational modification, protein turnover, chaperone function, P: inorganic ion transport and metabolism, Q: secondary structure, T: signal transduction, U: intracellular trafficking and secretion, Y: nuclear structure, Z: cystosekeleton, S: function unknown. Genes highlighted in gray indicate results overlapping with Soutourina *et al*.

transporters for which the substrate has not been experimentally determined (SAUSA30_RS10985 and SAUSA30_RS01055) (Table 4-2 grey). Of the 30 upregulated cell-envelope associated genes observed in Soutourina *et al.*, only 2 were also captured in the upregulated in *cymR*-replete data set (Table 4-2 grey). Both genes encode hypothetical proteins. Our data demonstrates enrichment of sulfur compound transport genes in *cymR*::Tn grown in sulfur replete conditions relative to WT grown in the same conditions, confirming that CymR

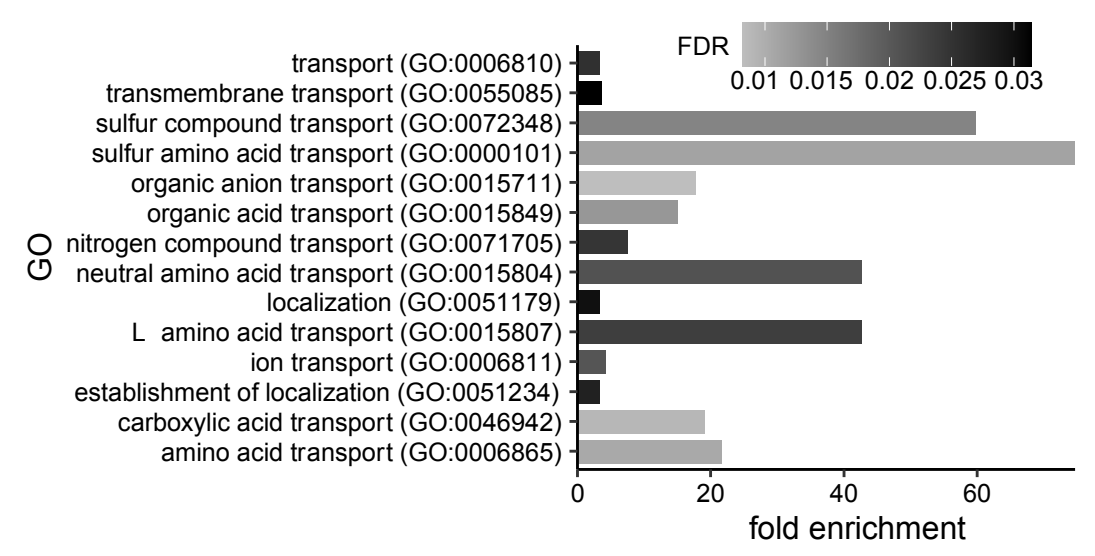


Figure 4-2. *cymR*-replete dataset is enriched for genes involved in amino acid and sulfur compound transport.

The dataset of genes upregulated when cymR is disrupted in sulfur replete conditions relative to WT in sulfur replete conditions was input into PANTHER and the enrichment test was performed on the GO terms. Present in the GO terms that are significantly enriched and the color depicts the false discovery rate (FDR).

controls sulfur transporter. Additionally, we observe upregulation of sulfur metabolism genes such as *cysK*, encoding Cys synthase, and *mccB*, encoding cystathionine gamma synthase. Slight differences observed between our data and Soutourina *et al.* can be attributed to increased sensitivity of RNAseq compared to microarray technology, use of a chemically defined medium as opposed to a rich medium, and genetic variance between JE2 and strain SH1000.

S. aureus transcriptional response to sulfur starvation.

Based on current models of CymR regulation, we reasoned that the CymR-dependent

sulfur starvation response parallels the sulfur replete CymR regulon (*cymR* replete). To assess the *S. aureus* sulfur starvation response, WT *S. aureus* was cultured in medium containing CSSC, pelleted, and resuspended at the same cell density in either medium containing CSSC (WT-

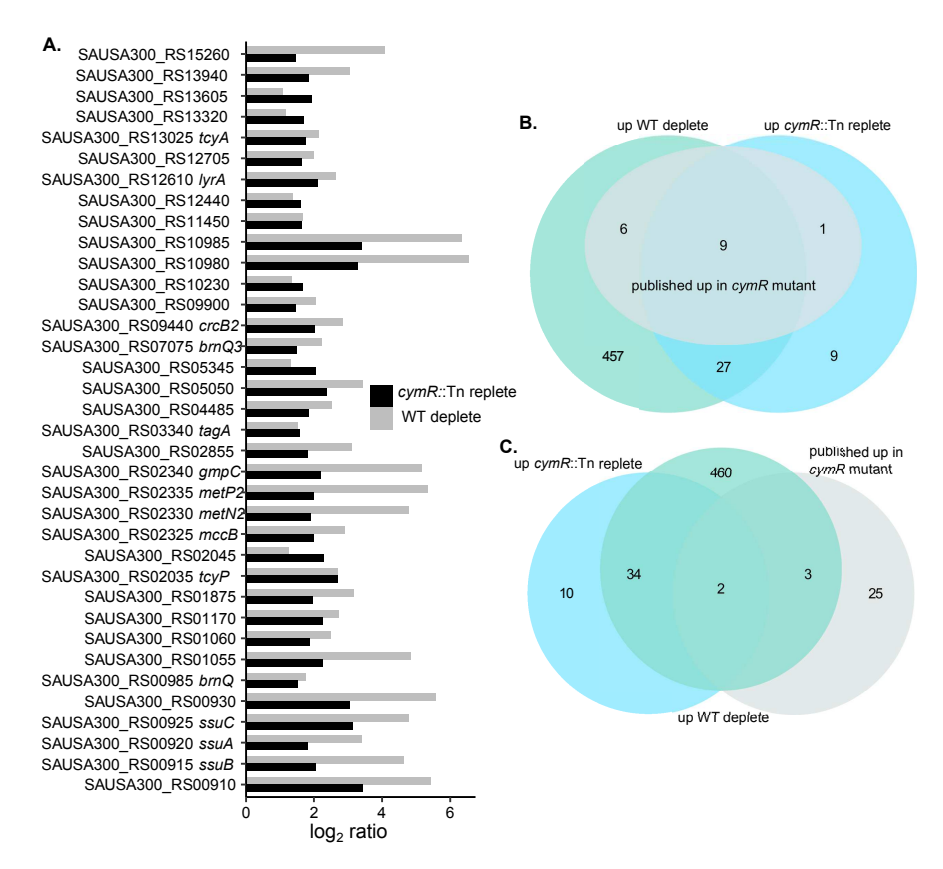


Figure 4-3. Comparison of the *S. aureus* sulfur starvation transcriptional response to the CymR regulon.

(A) Depicted is the intersection between genes upregulated in *cymR*-replete and WT-deplete. (B) Venn diagram comparing genes upregulated in WT-deplete and genes upregulated *cymR*-replete, and a published *cymR* mutant sulfur data set (28). (C) Comparison of the same datasets with a published *cymR* mutant cell enveloped associated gene dataset (28).

replete) or no added sulfur (WT-deplete) (Fig. 4-1B). Compared to WT-replete, WT-deplete displayed upregulation of 499 genes (Table 4-1, dataset S1). Compared to the 46 genes upregulated in *cymR*-replete, 36 of these transcripts are also upregulated in WT-deplete (Fig. 4-3A). Within this dataset were genes known to be involved in sulfur import and catabolism including cystathionine gamma-synthase (SASUSA300_RS02325), and components of the sulfonate and methionine transporter systems (SAUSA300_RS00915 and SAUSA300_02330). Comparison

between WT-deplete, *cymR*-replete, and published dataset revealed 9 out of 16 genes were shared between the three datasets (Fig. 4-3B, Table C-1) (28). These nine genes include the Cys and CSSC transporters, *tcyP* and *tcyA*, the putative methionine import protein (SAUSA300_RS02330), acyl-coA dehydrogenase (SAUSA300_RS00930), two ABC-transporters for which the substrate is unknown (SAUSA30_RS10985 and SAUSA30_RS01055) (Fig. 4-3B, Table C-1). Genes upregulated in WT-deplete share 15 out of 16 genes with the Soutourina *et al.* published dataset (Fig. 4-3B, Table C-1) (28).

Based on their microarray results, Soutourina *et al.* proposed a consensus sequence for CymR binding; however, the sequence is present at 11 loci across the genome, only 3 of which are present in predicted promoter regions (28). The observation that genes upregulated in the WT-deplete dataset are jointly upregulated in *cymR*-replete suggests these genes are under CymR control. The number of genomic locations possessing the CymR binding consensus sequence and the number of genes differentially regulated in *cymR*::Tn suggests the binding site for CymR is promiscuous. Further studies could use refined methodologies to study CymR

Table 4-3. Genes encoding transcriptional regulators that are differentially regulated in response to sulfur starvation.

locus	gene name	product	log₂ ratio ^a	adj p-value ^b
		upregulated		
SAUSA300_RS04840	spxA	regulatory protein Spx	2.73	1.81E-09
SAUSA300_RS05125		MarR family transcriptional regulator	2.71	9.76E-07
SAUSA300_RS07905	fur	transcriptional repressor	2.71	5.02E-11
SAUSA300_RS10675		transcriptional activator RinB	2.54	5.81E-04
SAUSA300_RS08020	argR	arginine repressor	2.35	3.08E-07
SAUSA300_RS12240	sarV	transcriptional regulator	2.34	5.11E-06
SAUSA300_RS11435		transcriptional regulator	2.15	6.44E-07
SAUSA300_RS13510	sarT	transcriptional regulator	2.04	3.91E-02
SAUSA300_RS10810		XRE family transcriptional regulator	2.03	1.49E-06
SAUSA300_RS03330	mntR	DtxR family transcriptional regulator	2.02	3.01E-06
SAUSA300_RS13930		TetR family transcriptional regulator	2.01	7.32E-06

Table 4-3 (cont'd)				
SAUSA300_RS12705		TetR family transcriptional	1.97	4.38E-05
SAUSA300_RS00495		regulator LysR family transcriptional	1.94	2.25E-03
SAUSA300 RS07955	malR	regulator LacI family transcriptional	1.93	6.41E-04
3A03A300_R307933	man	regulator	1.93	0.416-04
SAUSA300_RS13640	mhqR	MarR family transcriptional regulator	1.93	1.12E-04
SAUSA300 RS00590	sarS	transcriptional regulator	1.82	1.05E-04
SAUSA300_RS03500	rbf	AraC family transcriptional	1.72	1.58E-04
_		regulator		
SAUSA300_RS14305	argR	ArgR family transcriptional regulator	1.68	1.80E-02
SAUSA300 RS09835		transcriptional regulator	1.65	2.50E-03
SAUSA300 RS03085		transcriptional regulator	1.52	2.70E-02
SAUSA300_RS02375	gltC	LysR family transcriptional	1.51	5.12E-03
_	J	regulator		
SAUSA300 RS01375		GntR family transcriptional	1.50	4.19E-04
_		regulator		
SAUSA300_RS08905	nrdR	transcriptional regulator	1.48	7.00E-04
_		NrdR		
SAUSA300_RS08625	cymR	Rrf2 family transcriptional	1.48	1.34E-03
_	•	regulator		
SAUSA300_RS06710	<i>lexA</i>	LexA repressor	1.38	1.34E-03
SAUSA300 RS00335	argR	ArgR family transcriptional	1.35	4.40E-02
_	J	regulator		
SAUSA300 RS03605	mgrA	MarR family transcriptional	1.24	7.12E-03
_	J	regulator		
SAUSA300 RS10800		transcriptional regulator	1.23	1.53E-02
SAUSA300_RS02780	sigH	RNA polymerase sigma	1.22	1.39E-02
_	_	factor		
SAUSA300_RS12855	rsp	transcriptional regulator	1.20	2.51E-02
SAUSA300_RS14275	arcR	transcriptional regulator	1.18	1.46E-02
SAUSA300_RS10970	scrR	Lacl family transcriptional	1.09	3.77E-02
		regulator		
SAUSA300_RS12730	tcaR	transcriptional regulator	1.05	2.21E-02
		downregulated		
SAUSA300_RS06065	fapR	transcription factor	-2.50	1.58E-08
SAUSA300_RS14035		TetR/AcrR family	-2.28	2.86E-06
		transcriptional regulator		
SAUSA300_RS03250	sarA	transcriptional regulator	-2.28	1.26E-06
SAUSA300_RS06480	glnR	MerR family transcriptional	-2.05	6.24E-07
		regulator		
SAUSA300_RS12480		transcriptional regulator	-2.02	9.26E-06
SAUSA300_RS13560		MerR family transcriptional	-1.85	4.82E-05
		regulator		
SAUSA300_RS14240	nsaR	DNA-binding response	-1.61	1.32E-03
		regulator		
SAUSA300_RS01420	rbsR	Lacl family transcriptional	-1.43	6.36E-03
		regulator		

Table 4-3 (cont'd)				
SAUSA300_RS06330		GntR family transcriptional	-1.05	2.81E-02
		regulator		
SAUSA300 RS11555	czrA	transcriptional regulator	-1.03	2.26E-02

^a Expression ratio of WT grown in sulfur deplete conditions relative to WT grown in sulfur replete conditions.

promoter binding propensities and establish a more predictive consensus binding sequence.

Sulfur starvation induces changes in numerous transcriptional regulators.

To define transcriptional changes in sulfur starvation due to sulfur depletion, the WT-deplete dataset was examined further focusing on transcriptional regulators. Overall, 989 genes were differentially regulated in WT-deplete (Table 4-1). Of this cohort of genes 499 were upregulated and 490 were downregulated (Table 4-1). Due to the essentiality of sulfur to *S. aureus* metabolism, growth in sulfur deplete conditions should lead to considerable transcriptional changes, and the observation the sulfur starvation response is larger than the CymR regulon suggests expression of transcriptional regulators may be occurring. We filtered the WT-deplete dataset for genes with a predicted regulator function. A total of 44 genes encoding transcriptional regulators are differentially expressed in WT-deplete, 34 are upregulated and 10 downregulated (Table 4-3). Upregulated genes include genes encoding the regulators SpxA, AgrR, SarV, SarT, MntR, MalR, and SarS (Table 4-3). Surprisingly, *cymR* and *fur*, the gene encoding the master iron regulator, were also upregulated (Table 4-3). The upregulation of *fur* was previously observed when CymR is disrupted and *S. aureus* is grown in rich medium (97). The data was probed further to identify patterns that could explain *fur* upregulation.

Genes associated with iron transport and acquisition and the oxidative stress response are upregulated in response to sulfur starvation.

^bAdjusted p-value from DESeq2 output.

Many enzymes require iron sulfur clusters (Fe-S) for their function (205, 206). However, a delicate balance is required between intracellular sulfur levels and iron to decrease the potential of generating reactive intermediates through Fenton chemistry (92, 110). Prior studies in *B. subtilis* and *S. aureus* reported that *cymR* mutants display increased sensitivity to oxidative stress, suggesting dysregulation of intracellular thiols or iron homeostasis (97, 98). In keeping with this, the WT-deplete dataset was examined for genes associated with iron import and acquisition. In fact, strong upregulation of several iron acquisition systems and ferritin was revealed (Table 4-4).

Table 4-4. Sulfur starvation induces expression of iron import and oxidative stress genes.

locus	gene name	product	log₂ ratioª	adj p- value ^b
		metal/iron acquisition		
SAUSA300_RS10250	ftnA	non-heme ferritin	4.87	1.93E-36
SAUSA300_RS03875	sstC	iron ABC transporter ATP-binding	3.67	4.11E-10
		protein		
SAUSA300_RS12340	fhuD2	ferrichrome ABC transporter	3.65	9.31E-15
		substrate-binding protein		
SAUSA300_RS05570	isdG	monooxygenase Isdl	3.62	3.27E-13
SAUSA300_RS00650	sbnl	siderophore biosynthesis protein	2.84	1.25E-11
		SbnI		
SAUSA300_RS00885	isdl	monooxygenase Isdl	2.73	1.54E-09
SAUSA300_RS11755	hstB	iron ABC transporter permease	2.56	6.65E-10
SAUSA300_RS13820	feoA	ferrous iron transporter A	2.55	2.54E-03
SAUSA300_RS03865	sstA	iron ABC transporter permease	2.45	1.76E-06
SAUSA300_RS05410	mntH	divalent metal cation transporter	2.42	4.98E-09
SAUSA300_RS14545		heme ABC transporter ATP-binding	2.41	2.70E-08
		protein		
SAUSA300_RS03400	fhuB	iron ABC transporter permease	2.36	1.56E-08
SAUSA300_RS00620	sbnC	lucA/lucC family siderophore	2.13	5.89E-04
		biosynthesis protein		
SAUSA300_RS00615	sbnB	2,3-diaminopropionate biosynthesis	2.05	2.34E-02
		protein SbnB		4 00= 0=
SAUSA300_RS04915		alanine:cation symporter family	2.04	1.32E-05
041104000 5004000		protein	4.00	0.005.00
SAUSA300_RS01830	efeB	deferrochelatase/peroxidase EfeB	1.89	2.02E-02
SAUSA300_RS11750	htsC	iron-dicitrate ABC transporter	1.83	1.09E-05
CALICASOO DOOSO	4D	permease	4.04	0.505.00
SAUSA300_RS03870	sstB	iron ABC transporter permease	1.81	8.50E-03
SAUSA300_RS13050	:10	cation transporter	1.71	5.27E-05
SAUSA300_RS05545	isdC	iron-regulated surface determinant	1.65	2.15E-03
CVIICV3UU DCU443U	sufB	protein C	1.61	2.33E-04
SAUSA300_RS04430	fhuD1	Fe-S cluster assembly protein SufB	1.51	2.33E-04 3.36E-02
SAUSA300_RS10865	ו עטווו	ferrichrome-binding protein FhuD	1.31	3.30⊏-02

Table 4-4 (cont'd)				
SAUSA300_RS05535	isdB	iron-regulated surface determinant protein B	1.26	1.96E-02
SAUSA300 RS08270	znuB	metal ABC transporter permease	1.12	1.59E-02
SAUSA300_RS03405	fhuG	iron ABC transporter permease	1.07	1.39E-02
SAUSA300_RS00600	sirB	iron ABC transporter permease	1.03	4.39E-02
		oxidative stress		
SAUSA300_RS02020	ahpF	alkyl hydroperoxide reductase subunit F	2.91	5.73E-11
SAUSA300_RS02025	ahpC	alkyl hydroperoxide reductase subunit C	2.87	9.92E-13
SAUSA300_RS06680	katA	catalase	2.16	5.53E-08
SAUSA300_RS14205	gpxA2	glutathione peroxidase	2.05	1.39E-05
SAUSA300_RS06465	bsaA	glutathione peroxidase	1.25	5.91E-03
		unique <i>cymR</i> -deplete		
SAUSA300_RS00625	sbnF	lucA/lucC family siderophore	3.81	1.44E-07
	sbnF	siderophore biosynthesis protein	2.81	9.42E-05
SAUSA300_RS00640		SbnG		
SAUSA300_RS11775	sfaB	lucA/lucC family siderophore	2.66	1.04E-06
		biosynthesis		
SAUSA300_RS04425		iron-sulfur cluster assembly scaffold	2.16	4.17E-04
		protein		
SAUSA300_RS00415	sufD	Fe-S cluster assembly scaffold protein SufD	1.52	1.30E-02

^a Expression ratio of WT grown in sulfur deplete conditions relative to WT grown in sulfur replete conditions.

In addition, upregulation of the Isd system (*isdBC*, *isdI* and *isdG*) which encodes enzymes involved in acquisition of iron from heme was detected (82). Upregulation of iron acquisition genes suggests an imbalance in intracellular iron levels, and dysregulation of iron can lead to oxidative stress. Previous work established that *cymR* mutants are sensitive to oxidative stress; therefore, whether sulfur starvation leads to upregulation of oxidative stress response genes was investigated further. Upregulation of genes encoding alkyl hydroperoxide reductase subunit C and F, catalase, and two GSH peroxidases was revealed (Table 4-4). Upregulation of *ahpC* and *ahpF* was also reported in *cymR* mutant cultured in rich medium (97). To investigate possible CymR independent responses to sulfur starvation, genes that are uniquely differentially expressed in a cymR cultured in a sulfur depleted medium (*cymR*-deplete) were compared to WT-deplete. Overall, *cymR*-deplete displays differential expression of 344 genes of which 169 are upregulated

bAdjusted p-value from DESeq2 output.

and 175 are downregulation (Table 4-1, dataset 1). Of the 169 genes upregulated, 48 are unique to the *cymR*-deplete dataset as are 72 of the 175 that are downregulated. Some of the unique upregulated genes include additional siderophore production encoding genes, SAUSA300_RS00625, SAUSA300_RS00640, and SAUSA300_RS11775, and iron sulfur cluster assembly encoding genes, SAUSA300_04425 and SAUSA300_00415 (Table 4-4).

The observation that the *cymR*-deplete dataset contains limited uniquely differentially expressed genes suggests much of the sulfur starvation response could be due to release of CymR repression. Based upon our observations, 499 genes are upregulated due to sulfur starvation, but the genes upregulated in *cymR*-deplete is only 48 unique genes suggesting only approximately 10% of the sulfur starvation response is due to changes independent of CymR. In prior experiments, a *cymR* mutant cultured in rich medium shows induction of an iron-compound ABC-transporter, Fur, and PerR, a regulator that controls oxidative stress and iron storage proteins (97, 207). These data suggest an interplay between CymR repression and iron homeostasis. Similarly, sulfur depleted conditions presented here represent growth environments where CymR repression is released, and upregulation of *fur* and induction of iron acquisition genes is also observed, suggesting Fur repression is relieved. Intriguingly, a link between sulfur and iron regulation has been established in *Pseudomonas aeruginosa* where the sulfur regulator, CysB, binds to the promoter of *pvdS*, an alternative sigma factor involved in the iron response, positively regulating expression (208). Together these results demonstrate that sulfur starvation increases transcription of iron acquisition and oxidative stress pathways.

Comparison of S. aureus transcriptional adaptation to specific sources of nutrient sulfur.

Whether *S. aureus* acquires and catabolizes organic or inorganic sulfur sources has implications for the physiology of the cell. Genes differentially expressed when *S. aureus* is cultured in the presence of thiosulfate, Cys, GSSG, and GSH were identified using CSSC as the baseline control condition. In total 631 genes are differentially expressed when *S. aureus* is grown

on Cys, GSH, GSSG or thiosulfate compared to expression when S. aureus is grown on CSSC (dataset S2). S. aureus cultured in medium supplemented with Cys resulted in downregulation of a single gene, SAUSA300 RS04580, an annotated pyridine nucleotide disulfide oxidoreductase. SAUSA300 RS04580 is also downregulated in media supplemented with GSSG, GSH or thiosulfate. Proliferation in environments containing oxidized, inorganic thiosulfate requires input of more energy than the other organic sulfur sources due to the requirement for OAS. Consequently, genes uniquely differentially expressed in a thiosulfate-supplemented medium were examined. Compared to the organic sulfur sources, thiosulfate supplementation demonstrated the greatest number of differentially expressed genes across the sulfur sources, resulting in upregulation of 238 genes and downregulation of 328 genes (Fig. 4-4A) with 135 and 196 genes uniquely upregulated and downregulated, respectively (Fig. 4-4B, C). Supplementation with GSH or GSSG resulted in 208 total genes upregulated and 232 genes downregulated (Fig. 4-4A) with 30 total genes uniquely upregulated and 17 total genes uniquely downregulated (Fig. 4-4B, C). The total differentially expressed dataset was queried for genes encoding predicted transcriptional regulators. Twenty-one regulators are differentially expressed in total when S. aureus is grown on thiosulfate, GSH or GSSG (Fig. 4-4D). Twelve of the twenty-one regulators are uniquely differentially expressed in thiosulfate, 8 of the remaining 9 regulators are differentially expressed between GSH or GSSG (Fig. 4-4D). One regulator, SAUSA300 RS07955 (malR), is upregulated in GSH, GSSG, and thiosulfate, and three regulators, SAUSA300 RS10185 (vraR), SAUSA300 RS10800, and SAUSA300 RS12480, are downregulated in GSH, GSSG, and

thiosulfate (Fig. 4-4D). The dramatic transcriptional reprogramming in response to thiosulfate suggests that the overall metabolism and nutritional requirements of the cell changed. Growth on thiosulfate requires OAS, and OAS synthesis requires serine acetyltransferase to convert serine and acetyl-coenzyme A, two nutrients vital for thiosulfate assimilation, to OAS and coenzyme A. Proliferation using GSH requires no additional metabolite input and growth on GSSG requires only reducing power (25). Consequently, assimilation of thiosulfate has the potential to

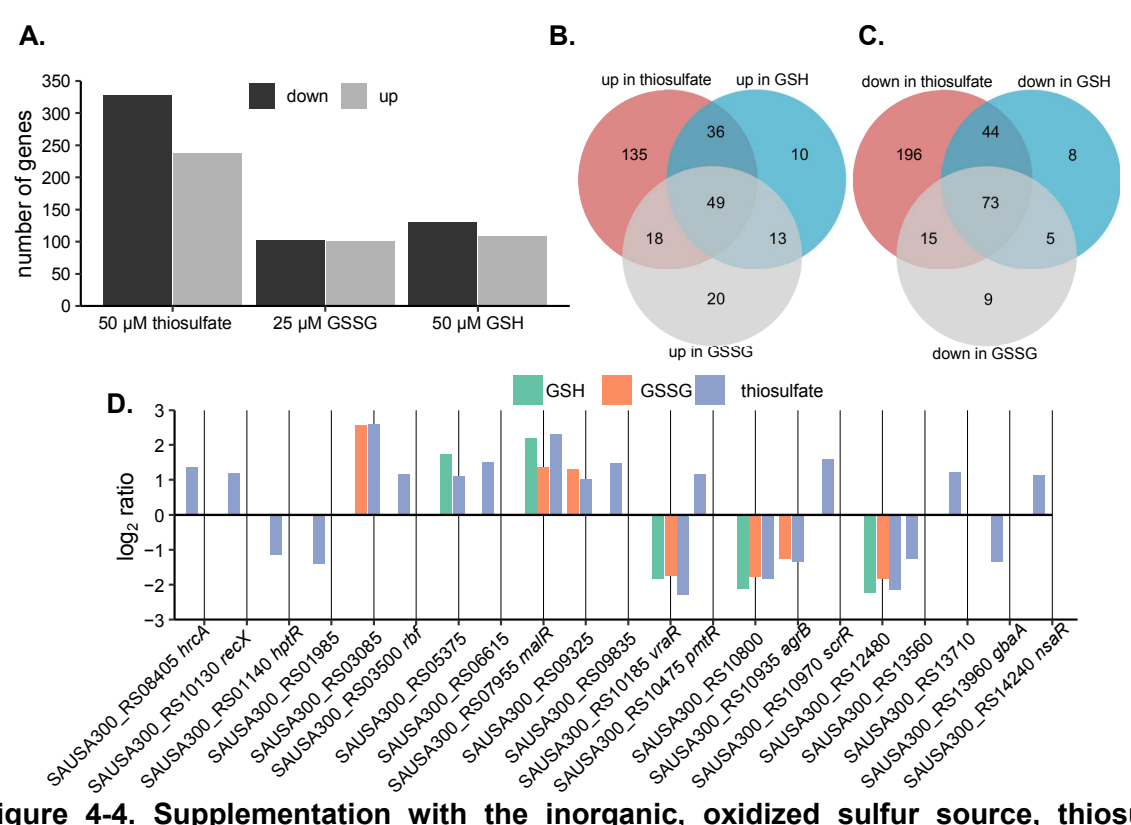


Figure 4-4. Supplementation with the inorganic, oxidized sulfur source, thiosulfate induces considerable transcriptional changes.

Differential expression in WT cells was determined by comparing supplementation with thiosulfate, Cys, GSSG, or GSH to cells grown in medium supplemented with CSSC. (A) Total number of genes that are differentially expressed in response to each source of nutrient sulfur. (B) Venn diagram comparing genes upregulated when *S. aureus* is cultured in a thiosulfate supplemented or GSH supplemented medium. *S. aureus* grown in Cys did not show any genes upregulated when compared to *S. aureus* grown in CSSC. (C) Genes that are downregulated between the three sulfur sources. Only one gene is downregulated in the Cys condition. (D) Transcriptional regulators differentially expressed when *S. aureus* is grown on GSH, GSSG or thiosulfate.

considerably change nutritional requirements. To satisfy these requirements, we hypothesize *S. aureus* alters expression of transporters. In keeping with this, 74 differentially expressed genes

out of 631 are predicted to encode a transporter (dataset S2). The list includes nickel ABC-transporters, amino acid transporters, iron transporters, and peptide transporters (dataset S2). Of the 74 differentially expressed transporters, 10 were uniquely upregulated in thiosulfate. This is in stark contrast with *S. aureus* cultured in GSH-supplemented or GSSG-supplemented media, which only have 3 or 1 predicted transporters uniquely upregulated, respectively (dataset S2).

Of the 49 shared genes upregulated in GSH, GSSG, and thiosulfate, 11 are predicted to encode proteins with transporter function. Of these 11, 4 are predicted sulfur associated transporters (Fig. 4-5 + symbols). However, based on the model of CymR regulation we expect sulfur-associated transporters to be downregulated in sulfur replete conditions. This observation led us to probe the genes upregulated in GSH, GSSG and thiosulfate and compare them to the previously reported genes upregulated in a *cymR* mutant to gain further insights into the status of CymR repression when *S. aureus* is grown on the different sulfur sources (28). The common GSH and thiosulfate upregulated genes contain *tcyP* and *tcyA*, genes encoding Cys transporters, the putative methionine importer, SAUSA300_RS02300, and two uncharacterized transporters SAUSA300_RS00915 and SAUSA300_RS01055 (Fig. 4-5). These transporter encoding genes have been shown to be under CymR control (28). We next want to expand the search to other non-transporter encoding genes in the CymR regulon. Ten genes jointly upregulated in the sulfur dataset are known to be controlled by CymR. These genes include five transporters and the non-transporter genes, *mccB*, which encodes cystathionine γ-synthase, an enzyme that produces cystathionine from Cys and homoserine, SAUSA300_RS10985, which encodes a YeeE/YedE

family protein, SAUSA300_RS00930, which encodes acyl-CoA dehydrogenase, and

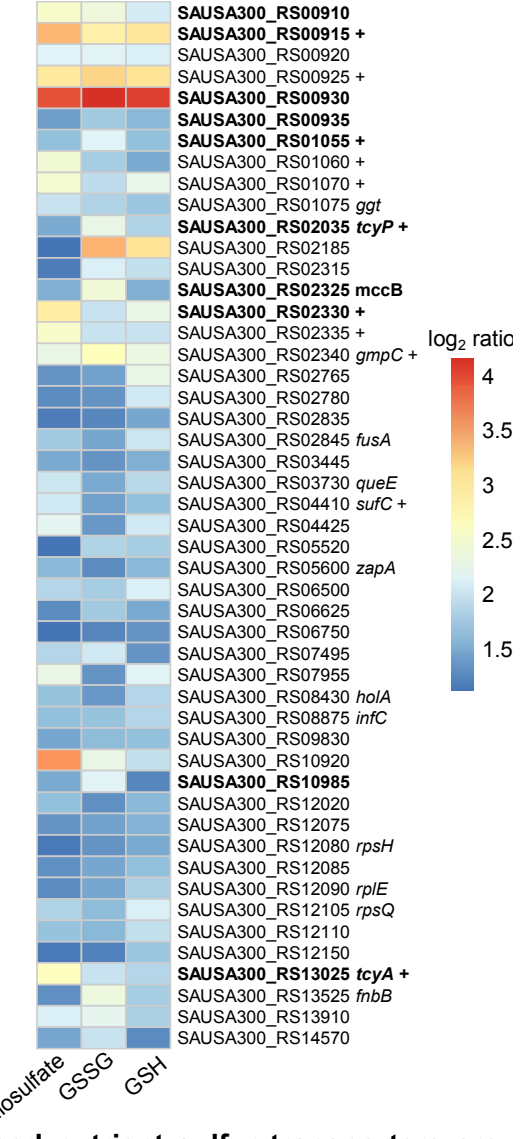


Figure 4-5. CymR repressed nutrient sulfur transporters are upregulated in response to both GSH and thiosulfate.

A heat map of genes upregulated in S. aureus cultured in medium supplemented with 50 μ M thiosulfate, 25 μ M GSSG, or 50 μ M GSH compared medium supplemented with cystine. Genes included in the heat map are at least 2-fold upregulated with an adjusted p-value <0.05. The color of the boxes indicates the log₂ expression ratio. Gene label in bold text are also upregulated in the published CymR regulon (28). A '+' indicates the gene encodes a protein with transporter-associated function.

SAUSA300_RS00935, which encodes a hypothetical protein (Fig. 4-5 bold labels) (4, 25).

The CymR-CysM complex in *S. aureus* is crucial for sulfur regulation; however, based on the model of CymR-CysM complex formation, *S. aureus* cultured in sulfur replete environments containing GSH, GSSG, and thiosulfate should contain relatively high concentrations of Cys,

which promotes CymR-CysM complex formation and repression. Thiosulfate supplementation should decrease levels of OAS because OAS is necessary for synthesis of Cys.

Decreased OAS stabilizes the CymR-CysM complex and maintains repression. Growth on GSH and GSSG should not affect OAS levels and yet CymR-regulated transporters are upregulated in these conditions. A limitation of this study is that the quantities of intracellular OAS or Cys in S. aureus grown on GSH, GSSG, or thiosulfate have not been determined. Thus, is it not known whether OAS levels exceed the threshold at which OAS can disrupts the CymR-CysM complex. Induction of sulfur transporter encoding genes and Cys metabolism genes suggests the CymR-CysM complex responds to other stimuli. An alternative mechanism of CymR repression focuses on regulation via oxidation. In this model, the Cys-25 residue in CymR acts a redox sensitive switch (204). Oxidation of CymR releases the protein from its cognate promoters (204). Maintaining thiol homeostasis is crucial for the cell to reduce the potential for generated of radical species mediated by Fenton chemistry. It is unclear whether growth of S. aureus on GSSG, GSH, or thiosulfate compared to CSSC, or Cys would lead to redox stress, but investigating intracellular thiol content of S. aureus cultured in medium containing GSSG, GSH, thiosulfate, or CSSC will determine whether growth on non-CSSC containing medium leads to increased intracellular thiols. On the other hand, monitoring the state of the CymR-CysM complex in S. aureus cultured on the different sulfur sources will reveal whether the sulfur transporters are controlled via the OAS and Cys.

Another potential explanation for induction of sulfur transporter genes upon supplementation with GSH and thiosulfate is the layer of transcriptional control afforded by changes in the expression of genes encoding regulators displaying similar expression patterns in in both GSH- and thiosulfate-supplemented *S. aureus*. In keeping with this, SAUSA300_RS07955 (*malR*) is upregulated while SAUSA300_RS10185 (*varR*), SAUSA300_RS10800, and SAUSA300_RS12480 are downregulated. Activation of these putative regulators and whether they control CymR activity or expression have not been experimentally explored. Future avenues

of study could investigate protein levels of these regulators to establish whether the change in transcript level is correlated with protein expression and subsequent studies can examine activity of these regulators.

Overall, this work describes the transcriptional response of *S. aureus* to sulfur starvation and conducts a more refined study to determine genes under CymR regulation. We observe sulfur starvation leads to upregulation of *cymR* and *fur* while genes involved in iron acquisition and oxidative stress are upregulated. This analysis demonstrates the upregulation of sulfur source transporters and catabolic enzymes when *S. aureus* is grown on medium containing GSSG, GSH and thiosulfate suggesting that the sulfur source *S. aureus* is growing on has implications for cellular physiology and control of intracellular thiol balance.

Materials and methods

Bacterial strains used in this study.

The WT *S. aureus* strain used in these studies was JE2, a derivative of the community-acquired USA300 LAC (100). The *cymR*::Tn strain was generated by transducing the transposon inactivated gene from the Network on Antimicrobial Resistance in *Staphylococcus aureus* (NARSA) into JE2 using transduction methodology (100, 118). Correct transposon location was determined using PCR.

Sulfur starvation sample collection.

WT and *cymR*::Tn *S. aureus* were cultured overnight in trypic soy broth at 37 °C, washed with PBS, and sub-cultured into 2 50 mL PN with 5 mg mL⁻¹ glucose with 25 µM CSSC in 250 mL Erlenmeyer flask at an OD₆₀₀ equal to 0.01. PN medium was prepared as previously described containing 17 amino acids but lacking Cys, asparagine, and glutamine (121). PN was supplemented with 5 mg mL⁻¹ glucose for all this work. Flasks were incubated at 37 °C and 225 rpm shaking for 4 h. The duplicate flasks were combined, centrifuged, washed with PBS, and

resuspended in 100 mL PN. The resulting culture was separated into 250 mL Erlenmeyer flasks with 50 mL. One flask of WT and *cymR*::Tn was supplemented with 25 μM CSSC. Flasks were incubated at 37 °C for 2 h.

Sulfur source growth conditions.

WT *S. aureus* was cultured overnight in TSB at 37 °C, washed with PBS, and sub-cultured into 50 mL PN and the corresponding sulfur sources in 250 mL Erlenmeyer flasks at a starting OD₆₀₀ equal to 0.01. CSSC and Cys were dissolved in 1 N HCl, and GSH, GSSG, and thiosulfate were dissolved in ddH₂O and filter sterilized. Cultures were grown for 4 h at 37 °C and 225 rpm shaking. Biological duplicate cultures were cultivated on independent days.

RNA isolation and sequencing.

50 mL cultures from the respective growth conditions were centrifuged for 10 min at 4700 rpm and at 4 °C. RNA was isolated from the resulting pellet as previously described (147). The RNA was then treated with Turbo DNase following manufacturer's instructions (ThermoFisher, Waltham, MA). rRNA depletion and paired-end RNA-sequencing was performed by Genewiz Inc. (South Plainfield, NJ) on an Illumina HiSeq using 2x 150 bp paired-end read technology.

RNA-seq data processing and visualization.

Paired-end reads were imported in Geneious and paired. Bbduk trimmed the sequences and the native Geneious mapper aligned the reads to the USA300 FRP3757 reference genome. The DESeq2 plugin in Geneious determined the differential expression with the comparisons listed in figure legends (209). Differential expression files were imported into R using RStudio and combined with gene-specific information tables for USA300_FPR3757 from Aureowiki to provide old locus tags, gene description, and protein sequence (210). Data was filtered using a log₂ ratio greater than or equal to 1 and less than or equal to -1 representing a 2-fold change and an

adjusted p-value of less than 0.05. Cluster of orthologous groups (COG) categories were determined using Eggnog mapper and genes with no COG result were categorized as unknown function (S) (211, 212). The package VennDiagram was used to generate Venn diagrams (213).

Gene Ontology term enrichment analysis using PANTHER.

Differentially expressed genes were input into PANTHER using the protein refseq accession number (214, 215). PANTHER analysis type was the PANTHER overrepresentation test, the annotation version was DOI:10.5281/zenodo.4495804 that was released 2021-02-1, and the reference list was *Staphylococcus aureus*. We employed the GO biological process complete annotation data set and used Fisher's exact test with false discovery rate (FDR) correction. We limited the results to GO terms with an FDR<0.05. Unmapped IDs were disregarded.

Acknowledgements

The *cymR* transposon mutant was provided by the Network on Antimicrobial Resistance in Staphylococcus aureus (NARSA) for distribution by BEI Resources, NIAID, NIH, and the Nebraska Transposon Mutant Library (NTML) Screening Array NR-48501. We thank Dr. Janani Ravi and the Ravi laboratory at Michigan State University for technical support. This work is funded by the National Institutes of Health R01 Al139074 and R21 Al142517.

Chapter 5 Summary and future directions

Summary

In chapter 1 we described sources of nutrient sulfur available to pathogenic bacteria in the host and review specific mechanisms of sulfur source utilization and acquisition by virulent microorganisms. Inorganic sulfur sources such as sulfate, sulfide, and thiosulfate contain sulfur in a highly oxidized state. Sulfate assimilation is an extensively described process involving a series of reductive processes that ultimately integrates the sulfur atom into the amino acid Cys (1). However, studies have reported emergence of Cys auxotrophs after host passage, suggesting Cys biosynthesis might be dispensable for chronic infection likely due to an abundance of organosulfur sources present in host tissues (64, 65). Organosulfur sources contain sulfur in a more reduced state than inorganic sulfur sources and include Cys, CSSC, Met, and GSH. Assimilation of these molecules involves direct import, in the case of Cys or CSSC, catabolism of GSH to Cys, or synthesis of Cys from Met. Cys then serves as the substrate for production of other sulfur-containing cofactors. Compared to other pathogens, S. aureus sulfur assimilation is limited by inherent genetic deficiencies. Due to the absence of critical enzymes in the sulfate assimilation pathway S. aureus does not proliferate when sulfate is supplied as the sole source of sulfur. Additionally, S. aureus cannot efficiently synthesize Cys using Met as a substrate (11, 25, 28). Prior to our work a limited number of sulfur-containing metabolites were known to promote growth of S. aureus. Work by the Foster group using qualitative agar medium growth assays discovered that S. aureus was capable of using the inorganic sulfur sources sulfide and thiosulfate, and the organosulfur sources GSH, Cys, and CSSC (11). However, the mechanisms by which S. aureus imports and assimilates these sulfur sources were not experimentally validated.

In chapter 2 we identify mechanisms of *S. aureus* nutrient sulfur acquisition by focusing on Cys utilization. A genetic approach was used to experimentally validate determinants allowing *S. aureus* to grow on Cys as a sulfur source. *S. aureus* homologues of CSSC transporters

characterized in *B. subtilis*, TcyP and TcyABC, were demonstrated to be CSSC transporters that also support proliferation on Cys and the Cys analogue NAC (42, 147). TcyABC was also shown to support growth on hCSSC as a sulfur source. A bioinformatics approach mapped TcyP conservation across bacteria and homologues are present in many pathogen-containing phyla. Genetic inactivation of *tcyA* or *tcyP* did not result in virulence defects in mono-infections in a murine model of systemic infection. However, the *tcyP* mutant was outcompeted by WT MRSA in murine hearts and livers, suggesting TcyP provides maximal fitness at these infection sites. The importance of TcyP for heart and liver colonization indicates *S. aureus* uses TcyP substrates as sulfur sources during infection; however, disruption of *tcyP* did not fully ablate colonization, signifying *S. aureus* must acquire other sulfur sources. Prior work in *S. mutans* demonstrated that TcyBC functions with GshT, a substrate binding protein capable of binding GSH, to transport GSH; however, we found neither TcyABC nor TcyP supported growth on GSH as a sulfur source (22). Based on this result, we next sought to identify the *S. aureus* GSH transporter.

Chapter 3 established that *S. aureus* acquires both GSSG as well as GSH as sulfur sources and discovered the transport system responsible for proliferation in sub-100 micromolar concentrations of these metabolites. A genetic screen revealed that genes comprising the SAUSA300_0200 to SAUSA300_0204 locus support growth on micromolar concentrations of GSH and GSSG as sulfur sources. Prior to our study, SAUSA300_0200-0204 were annotated as a nickel-peptide ABC-transporter and γ-glutamyl transpeptidase. In keeping with this annotation and the mutant proliferation phenotypes, this system was named the **g**lutathione **i**mport **s**ystem (GisABCD-Ggt). GisA was biochemically validated as an ATPase suggesting GSH and GSSG import is ATP dependent. We discovered Ggt cleaves both GSH and GSSG by quantifying glutamate released when rGgt was incubated with GSH or GSSG. Cell fractionation and immunoblot assays show Ggt is associated with the cell and the absence of a signal sequence suggests it localizes to the *S. aureus* cytoplasm. Intracellular Ggt localization is relatively rare in

bacteria and has important implications for GSH and GSSG import in *S. aureus*, including the potential for GSH to accumulate inside the cell and serve a function other than satisfying the nutrient sulfur requirement. Bioinformatic conservation studies revealed that the closely related staphylococci, *S. epidermidis* does not encode an apparent GisABCD-Ggt homologue. This finding suggested that *S. epidermidis* is not capable of utilizing GSH as a source of nutrient sulfur and that GisABCD-Ggt provides a fitness advantage to *S. aureus* over *S. epidermidis* in a GSH-and GSSG-specific manner. We observed that GSH and GSSG did not promote growth of *S. epidermidis* and that greater numbers of *S. aureus* were isolated from *S. aureus-S. epidermidis* co-cultures when GSH or GSSG were provided as sulfur sources. Outgrowth of *S. aureus* was significantly reduced when *S. epidermidis* was co-cultured with a *S. aureus* Δ*gisACBD-ggt* mutant. Finally, we investigated GisABCD-Ggt conservation across Firmicutes and found that while Ggt homologues are present across Firmicutes only select members encode homologues of a complete GisABCD system. This finding indicates that GSH and GSSG catabolism is a conserved process, but organisms have evolved different strategies for importing these nutrient sulfur sources.

In chapter 4 we sought to define the sulfur starvation regulon and determined nutrient sulfur source specific transcriptional responses. *S. aureus* encodes the global sulfur regulator CymR, that forms a complex with Cys synthase, CysM, that binds to DNA and acts as a transcriptional regressor in environments containing abundant Cys (28). The CysM-CymR complex is disrupted, and repression is relieved when OAS, a precursor required for Cys biosynthesis, accumulates in the cell. This in turn increases transcription of nutrient sulfur acquisition genes (28). An alternative mechanism of CymR-regulated gene deregulation is oxidation of an internal Cys residue in CymR that causes the repressor to undergo a conformation change releasing repression (204). Prior studies determined the CymR regulon using microarray analysis of a *cymR* mutant strain in the *S. aureus* strain SH100 cultured in a complex TSB medium. My work builds on those findings by defining both CymR dependent and sulfur starvation

dependent transcriptional changes in S. aureus strain JE2, a derivative of the current strain endemic in the United States USA300 LAC. RNA-seq was used to quantify transcriptional changes, providing greater resolution and sensitivity than microarrays (28, 216). We found that genetic inactivation of CymR leads to upregulation of 46 genes enriched for sulfur compound transport and amino acid transport. Soutourina et al. described 16 sulfur import and metabolism genes were upregulated when CymR is disrupted (28). Our data confirms upregulation of 10 of these genes including cysM (Cys synthase), tcyP and tcyABC (CSSC/Cys transporters), SAUSA300 RS20330 (putative Met transporter), and metB (cystathionine y-synthase) in a cymR mutant. Nine of the ten genes, excluding cysK, shared between our data set and the Soutourina et al. are also upregulated when WT S. aureus is grown in sulfur deplete conditions (28). Our exploration of the CymR regulon employed a more robust technology, and more relevant strains and growth conditions compared to the prior study. We also define the sulfur starvation response and show sulfur starvation leads to differential expression of 43 regulators. Furthermore, sulfur starvation leads to upregulation of genes encoding proteins in the oxidative stress response and proteins involved in iron acquisition suggesting an interplay between sulfur status and iron homeostasis.

Chapter 4 also defined sulfur source specific transcriptional responses. The type of sulfur source *S. aureus* acquires has wide implications for the physiology for the cell. For instance, utilization of inorganic sulfur sources such as thiosulfate and sulfide lead to Cys synthesis and flux of OAS as a carbon backbone from the cell. Thiosulfate assimilation also requires investment of electrons needed to reduce the oxidized sulfur atom. Conversely, proliferation on organosulfur sources does not necessitate OAS to assimilate sulfur because the sulfur is already complexed to carbon, allowing for the sulfur requirement to be fulfilled via release instead of Cys anabolism. We performed RNA-seq of *S. aureus* cultured in chemically defined medium with either CSSC, Cys, GSSG, GSH, or thiosulfate as the sulfur source and compared differential expression using *S. aureus* grown in medium with CSSC as the comparator. We found that sulfur source

transporters known to be regulated by CymR are upregulated when *S. aureus* is grown in GSH, GSSG and thiosulfate but not Cys when compared to *S. aureus* grown in CSSC. Additionally, we observe proliferation in medium supplemented with thiosulfate leads to differential expression of the greatest number of unique genes compared to the total number of unique genes expressed in response to GSH and GSSG supplementation. Chapter 4 provided evidence confirming genes known to be controlled by CymR while also providing evidence for new insights into genetic control of sulfur import and catabolism genes.

Future avenues of exploration stemming from chapters 2, 3 and 4 can be divided into 5 areas. First, defining a comprehensive set of sulfur-containing metabolites present in the host will provide a better understanding of sulfur sources available to *S. aureus* during infection. Second, elucidating which host-derived sulfur sources support growth of *S. aureus* will aid in guiding genetic analysis to detect which are catabolized during infection. Third, quantifying *S. aureus* proliferation and monitoring import of specific sulfur sources in media supplemented with more than one source of nutrient sulfur will allow us to determine whether *S. aureus* has sulfur source preferences. Fourth, identification of unknown transporters and catabolic enzymes will refine our understanding of the genetic requirements for transport of sulfur sources that satisfy the *S. aureus* sulfur requirement. Finally, future directions for chapter 4 focus on investigating the effects of growth on different sulfur sources and CymR-dependent regulation and will uncover how proliferation on different sulfur sources changes the physiology and regulation of sulfur source metabolic genes in the cell.

Future directions sulfur import and metabolism

Elucidation of the complete set of sulfur source metabolites present at the host pathogen interface.

Virulence studies carried out in Chapter 2 found that TcyP is required for maximal fitness in competition with WT in murine heart and liver; however, because of substrate promiscuity of

TcyP we do not know which nutrient sulfur sources are being acquired by the transporter (147). Moreover, GSH and Cys are abundant host metabolites, but information on the total sulfurcontaining compounds in distinct organ sites is unavailable (2, 49). S. aureus proliferates and causes disease in nearly every organ in the body, but each of these infection sites likely differ in the quantity and diversity of sulfur-containing metabolites (71). The genetically tractable nature of S. aureus allows for generation of mutations in sulfur transporters with relative ease, however, the ability to transport a substrate does not ensure that substrate is catabolized in vivo. To overcome this problem, explorations into the totality of sulfur sources present in tissues that support S. aureus proliferation can guide genetic studies. For example, host tissues can be isolated and untargeted mass spectrometry techniques can be used to quantify sulfur sources present in the tissues. Briefly, organ environments of interest would be isolated, flash frozen to halt metabolism. Organs would be homogenized and metabolites extracted. 3-benzoyl acrylate derivatizes reduced thiols blocking it from oxidation therefore allowing for accurate determination of sulfur metabolites in the infection environments. Untargeted metabolomics should be employed to investigate the totality of sulfur containing compounds in the environments. Follow-up quantitive targeted metabolomic analysis can confirm the untargeted results and determine absolution concentrations of the metabolites. Genetic studies investigating the role of transporters for which the respective substrate metabolite is present in the host can then follow.

Expanded exploration into host sulfur sources that support proliferation of S. aureus.

Work presented here focused on known metabolites as sources of nutrient sulfur for *S. aureus*. However, the host environment likely contains mixed disulfides and host polypeptides. Metabolomic analysis focused on sulfur-containing metabolites can provide insights into non-canonical sulfur sources present in the host environment. A hallmark of *S. aureus* infection is the development of tissue abscesses (217). Abscesses have been reported to contain oxidized proteins suggesting that reduced thiols present within abscesses become oxidized, potentially

complexing with other thiol-containing metabolites (218). Consistent with this, studies have shown that rat tissues contain mixed disulfides including homocysteine-Cys, GSH-Cys, and γ-glutamylcysteine-Cys during oxidative stress (219). Transport systems in other organisms have been shown to transport mixed disulfides such as homocysteine-GSH (159). A metabolomic sulfur source analysis of *S. aureus* infection sites will establish which disulfides are present at the host-pathogen interface. Growth analysis studies and genetic manipulation will determine transporters responsible for growth on the mixed disulfides observed at the site of infection. For example, if the metabolomic analysis reveals GSH-Cys is a prominent metabolite in the heart, we perform *in vitro* growth analysis combined with genetic manipulation and biochemical assays to determine the transporter responsible for growth on GSH-Cys.

An interesting aspect of the *S. aureus* infection physiology is the number of proteases it secretes into the extracellular milieu (220). Some of these secreted proteases have been shown to degrade host peptides. For example, collagen, fibrinogen, and fibronectin can be cleaved by the Cys protease staphopain B (167, 221, 222). Prior work studied whether collagen, an abundant host peptide in staphylococcal skin abscesses, could serve as a source of nutrients to *S. aureus in vitro* (167). This worked showed that collagen degradation by both host and *S. aureus* proteases liberates peptides that are imported via Opp3A and used as a source of carbon (167). Interestingly, studies have shown human polypeptides have on average a Cys prevalence of 2.3% (223). An intriguing area of study would be to study whether human-derived polypeptides enriched in Cys residues serve as sources of nutrient sulfur and determine the extracellular proteases involved in this process.

Investigation into the sulfur source preference of S. aureus.

The reactivity of thiols makes it imperative that sulfur import is tightly controlled to ensure the cell does not have excessive thiol levels within the cell. Cys or GSH, which both contain reactive thiols, can reduce ferric iron to ferrous iron which reacts with oxidants to create radical species capable of damaging DNA and proteins (110, 224). The CSSC import cycle of E. coli illustrates the necessity to maintain thiol homeostasis. E. coli imports CSSC as a sulfur source that is readily reduced to Cys once inside the cell (92). Consequently, E. coli has evolved to decreased the reactive Cys thiol by exporting excess Cys where it is oxidized back to CSSC (92). The delicate balance necessary to acquire sulfur while protecting the cell from iron-mediated oxidative damage raises an interesting question about how S. aureus regulates this balance. A subsequent question that arises is whether S. aureus has a sulfur source preference as has been demonstrated for another nutritional requirement of pathogenesis, iron. Previous work established that S. aureus prefers heme-iron over transferrin bound iron (81). One could conjecture that S. aureus strategically imports select sulfur sources or indiscriminately acquires all sulfur sources its capable of using to maximize sulfur acquisition potential. Furthermore, S. aureus could display a preference for organosulfur source over inorganic sulfur sources for optimization of cellular energetics. Genetic regulation in S. aureus shows significant regulation of CSSC/Cys transporters. In fact, TcyP is the most upregulated gene in the CymR regulon; however we do not understand whether this correlates to S. aureus seeking increased import of TcyP-dependent substrates as the priority sulfur source (28). Additionally, work examining the transcriptome of S. aureus in cystic fibrosis sputum showed the CSSC transporter, TcyABC, is the only known sulfur source transporter induced in sputum relative to exponential phase S. aureus grown in chemically defined medium (225). During infection host tissues provide multiple sulfur sources and our tcyP mutant infection data suggests that S. aureus likely acquires multiple sulfur sources to support proliferation. However, we do not know whether S. aureus is primed to import other organosulfur sources or all sulfur sources present. Future work could research S. aureus sulfur source utilization when more than one sulfur source is present. Studies can start with simple sulfur metabolite environments and move to more complex mixtures examining the sulfur sources that S. aureus imports and catabolizes. Data generated would provide insights in the strategy that S. aureus employs to assimilate sulfur in vivo. The sulfur source utilization can then be complexed

with genetic manipulation of *S. aureus* sulfur source transporters to observe how sulfur utilization changes when the ability to acquire distinct sulfur sources is disrupted. The experimental setup can utilize a radioactive sulfur containing compound and the output would radioactive decay signal. *S. aureus* could be imported with radioactive Cys to determine baseline import. Next, more sulfur sources can be supplemented in the medium along with radioactive Cys and the internal radioactive Cys level determined.

Elucidation of unknown sulfur transporters and catabolic enzymes.

While studies presented here substantially enhance our knowledge of *S. aureus* nutrient sulfur acquisition by identifying sulfur source transporters, the work also provides evidence that *S. aureus* harbors at least one additional GSH transporter. Data presented in Chapter 3 demonstrates that a $\Delta gisABCD$ -ggt mutant proliferates in medium supplemented with 750 μ M GSH, indicating that another transporter promotes growth at higher concentrations of GSH. This result also indicates an alternative, Ggt-independent mechanism of GSH catabolism. Proliferation in 750 μ M GSH is conserved in *S. epidermidis* and 375 μ M GSSG fails to enhance growth of both *S. epidermidis* and a *S. aureus* $\Delta gisABCD$ -ggt mutant, suggesting similar specificity for GSH. Comparative genomic analysis combined with transposon-sequencing using *S. aureus* $\Delta gisABCD$ -ggt cultured in chemically defined medium with 750 μ M GSH would provide insights into the identity of the other transporter and catabolic enzymes. Once the identity of the other transporter is known a more comprehensive investigation into whether GSH metabolism is important for *in vivo* proliferation of *S. aureus* can occur using a double mutant in which Gis and the other transporter are disrupted.

Exploration into mechanisms of regulation of sulfur import related genes when S. aureus is grown on GSH and thiosulfate.

CymR and CysM complex formation is essential for repression of genes encoding nutrient sulfur acquisition factors. The CymR repressor complex responds to intracellular OAS concentrations in both B. subtilis and S. aureus (28, 99). CymR-CysM forms the repressor complex in high Cys conditions and when Cys levels become depleted, OAS accumulates and disrupts the CymR-CysM repressor complex; however we observe upregulation of CymR controlled genes when S. aureus is cultured in GSSG, GSH and thiosulfate compared to CSSC (28). Cys is available in all these conditions, and the concentrations GSH and GSSG supplementation are equivalent to the Cys level available when S. aureus is cultured with CSSC. Based on the CymR repression model, CymR should be repressing expression of these genes and yet we observe expression. An area of further exploration is investigating intracellular levels of OAS when S. aureus is grown on these sulfur sources. Thiosulfate would be the only sulfur source for which utilization requires flux of OAS; though, upregulation of CymR repressed genes warrants the exploration. Recent work has suggested an additional mechanism for CymR promoter complex dissociation where an internal Cys, Cys25, can be oxidized, promoting dissociation of CymR from promoters (204). If we find that OAS concentrations are similar when S. aureus is cultured on various sulfur sources, we could investigate the state of the CymR-CysM complex when S. aureus is grown on the various sulfur sources. Alternatively, expression of sulfur source transporter genes could be controlled by another regulator that responds to GSH, GSSG, and thiosulfate. Transcription of the transcriptional regulator, SAUSA300 RS07955 (malR), increases when S. aureus is cultured in a medium supplemented with GSSG, GSH or thiosulfate as the sulfur source. We also observe joint decreased expression of genes encoding the regulators SAUSA300_RS10185 (vraR), SAUSA300_RS12480, and SAUSA300_RS10800 when S. aureus is grown on GSSG, GSH or thiosulfate as the sulfur source. Further studies examining expression of sulfur source transporters when this regulator is disrupted will decipher whether it has a role in sulfur source transporter regulation. Overall, the status of CymR when S. aureus is

grown on inorganic or organosulfur sources and investigations into activation of this transcriptional regulator are promising areas of exploration.

Concluding remarks

In summary, my dissertation determined genetic factors that support proliferation of *S. aureus* on select sulfur sources using a combination of genetic and biochemical approaches. Additionally, RNA-sequencing allowed me to characterize general and specific transcriptional responses to various sources of nutrient sulfur. The work presented here substantially advances our knowledge of the transporters that acquire nutrient sulfur sources in *S. aureus*, however, the identity of some redundant transporters and catabolic enzymes have yet to be identified. My contributions to this area set the stage for many more years of exploration and impactful studies into nutrient sulfur acquisition in the clinically important pathogen *S. aureus*.

APPENDIX

Table A-1. Bacterial strains used in chapter 2.

strain	description	reference/source		
methicillin resistant strains				
wild type	USA300 JE2	(100)		
<i>tcyA</i> ::Tn	<i>tcyA::</i> erm	(100)		
<i>tcyP</i> ::Tn	<i>tcyP</i> ::erm	(100)		
<i>tcyP</i> ::Tn	tcyP::tet	this study		
<i>tcyAP</i> ::Tn	tcyA::erm tcyP::tet	this study		
methicillin sensitive strains				
wild type	Newman	(101)		
tcyA::Tn	<i>tcyA</i> ::erm	this study		
<i>tcyP</i> ::Tn	tcyP::erm	this study		
tcyP::Tn	tcyP::tet	this study		
<i>tcyAP</i> ::Tn	tcyA::erm tcyP::tet	this study		

Table A-2. Primers used in chapter 2.

primers	description	sequence
tcyP ORF F	sequencing tcyP ORF	AAGTTCAACATATTGACTTATCCGGC
<i>tcyP</i> ORF R	sequencing tcyP ORF	TAGGAATTGAATATTTGACCAAACC
$P_{tcyP}F$	sequencing tcyP promoter	GCGAGCCATCATGTGCAATATTACG
P_{tcyP} R	sequencing tcyP promoter	CGAATCGCACAAGTGCACACTC
pKK22 F	amplification for pKK22 for Gibson assembly	GCGGCCGCTAGCCTAGGAGC
pKK22 R	amplification for pKK22 for Gibson assembly	ATCGCCTGTCACTTTGCTTGATATATGA
P <i>tcyP</i>	amplification of PtcyP tcyP for	AGCAAAGTGACAGGCGATGCGGCCGCA
<i>tcyP</i> F	cloning into pKK22	GAATTTTTACAACGTGTTTG
PtcyP tcyP R	amplification of PtcyP tcyP for cloning into pKK22	GAGCTCCTAGGCTAGCGGCCTTAGTGTG AAGTTAATGCAG
P _{tcyABC} tcyABC	amplification of P _{tcyABC} tcyABC for cloning into pKK22	AGCAAAGTGACAGGCGATGCTGTTGGCA ACAGTTTATG
P _{tcyABC}	amplification of P_{tcyABC} tcyABC for	TACCGAGCTCCTAGGCTAGCTTATTCTTC
tcyABC	cloning into pKK22	ATTTATAACATTTAAGAAAC
rho F	qRT-PCR	AAACGTCCGCATTTCCAAGC
rho R	qRT-PCR	TGGCGCCACTATTAAACCAC
<i>tcyA</i> F	qRT-PCR	TATTGGCTGCATGCGGAAAC
tcyA R	qRT-PCR	AATGGTGCATAAGTCCCCTCAG
<i>tcyP</i> F	qRT-PCR	TGCTGCGATTGTTGGTGTTG
<i>tcyP</i> R	qRT-PCR	ATTTCGCTTCCACGTGCTTG

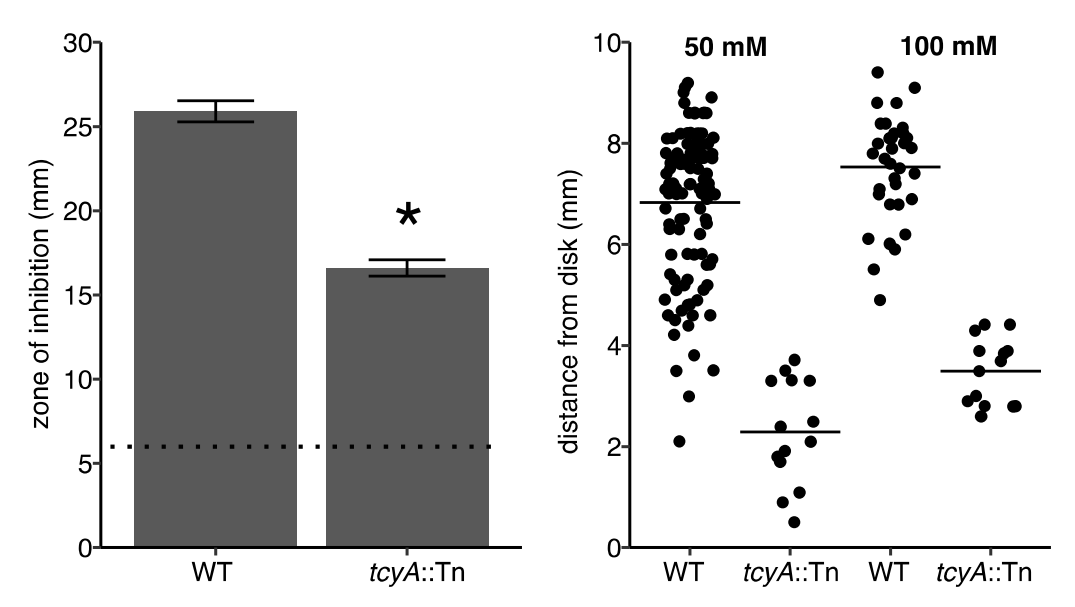


Figure A-1. Strain Newman tcyA mutants demonstrate enhanced selenocystine resistance. (A) WT and tcyA::Tn were plated as a lawn on TSA and a disk supplemented with 100 mM selenocystine was added to the plate. The dotted line represents the disk diameter (6 mm). The mean zone of inhibition of at least three independent trials is presented. Error bars represent \pm 1 standard error of the mean. (B) WT Newman or tcyA::Tn selenocystine resistant mutant colonies grew the indicated distance from a sterile Whatman paper disk containing 50 mM or 100 mM selenocystine. The bar represents the mean distance from the disk. * Indicates P<0.05 determined from student's t-test.

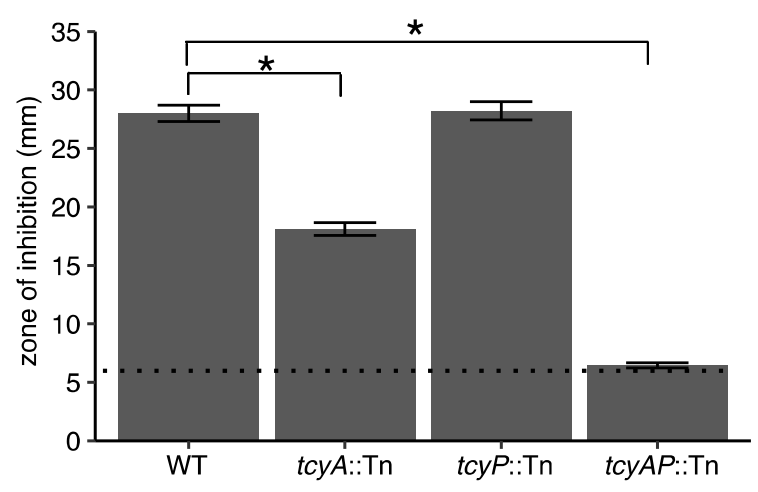


Figure A-2. Newman TcyABC and TcyP are required for selenocystine sensitivity. The zone of inhibition in the presence of 100 mM selenocystine was measured for WT, tcyA::Tn, tcyP::Tn, and tcyAP::Tn. The mean zone of inhibition of at least three independent trials is presented. The dotted line represents the disk diameter (6 mm). The error bars represent \pm 1 standard error of the mean. * Indicates P<0.05 determined from student's t-test.

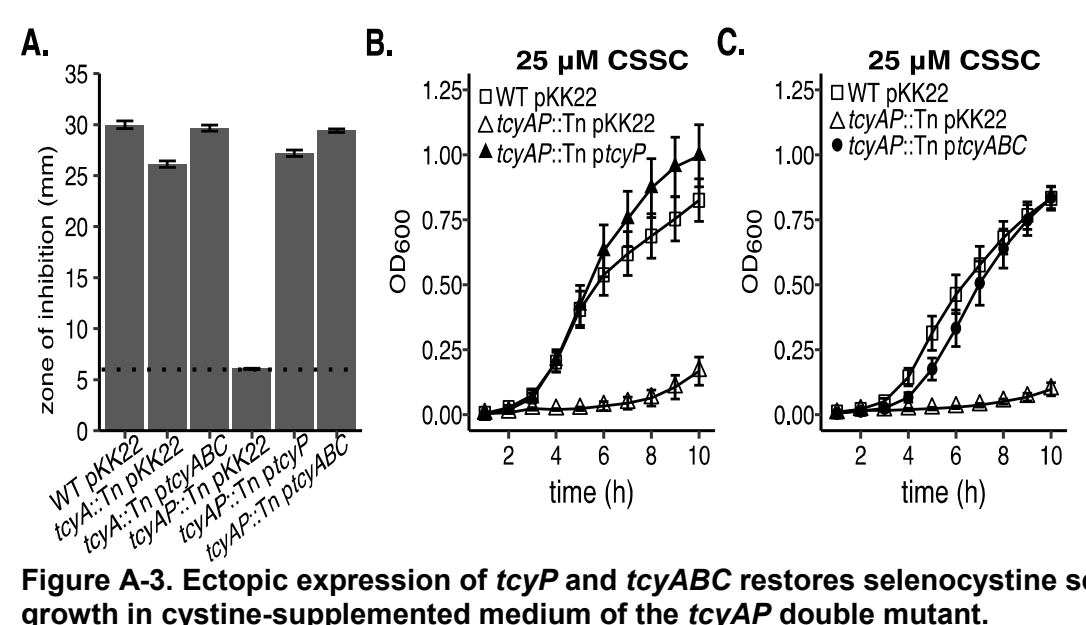


Figure A-3. Ectopic expression of tcvP and tcvABC restores selenocystine sensitivity and growth in cystine-supplemented medium of the tcyAP double mutant.

(A) Selenocystine resistance of WT harboring a pKK22 empty vector (WT pKK22), the tcyA::Tn mutant strain harboring a pKK22 empty vector (tcvA::Tn pKK22), the tcvA::Tn mutant harboring pKK22 vector containing tcyABC under the control of its native promoter (tcyA::Tn ptcyABC), the tcyA::Tn tcyP::Tn double mutant harboring a pKK22 empty vector (tcyAP::Tn pKK22), the tcyA::Tn tcyP::Tn mutant strain harboring a pKK22 vector containing tcyP under the control of its native promoter (tcyAP::Tn ptcyP), or the tcyA::Tn tcyP::Tn mutant harboring pKK22 vector containing tcyABC under the control of its native promoter (tcyAP::Tn ptcyABC) was determined in the presence of 100 mM selenocystine. The dotted line represents the disk diameter (6 mm). (B-C) Growth of the indicated strains was monitored in medium supplemented with 25 µM cystine. The mean of at least three independent trials is presented, error bars represent ± 1 standard error of the mean.

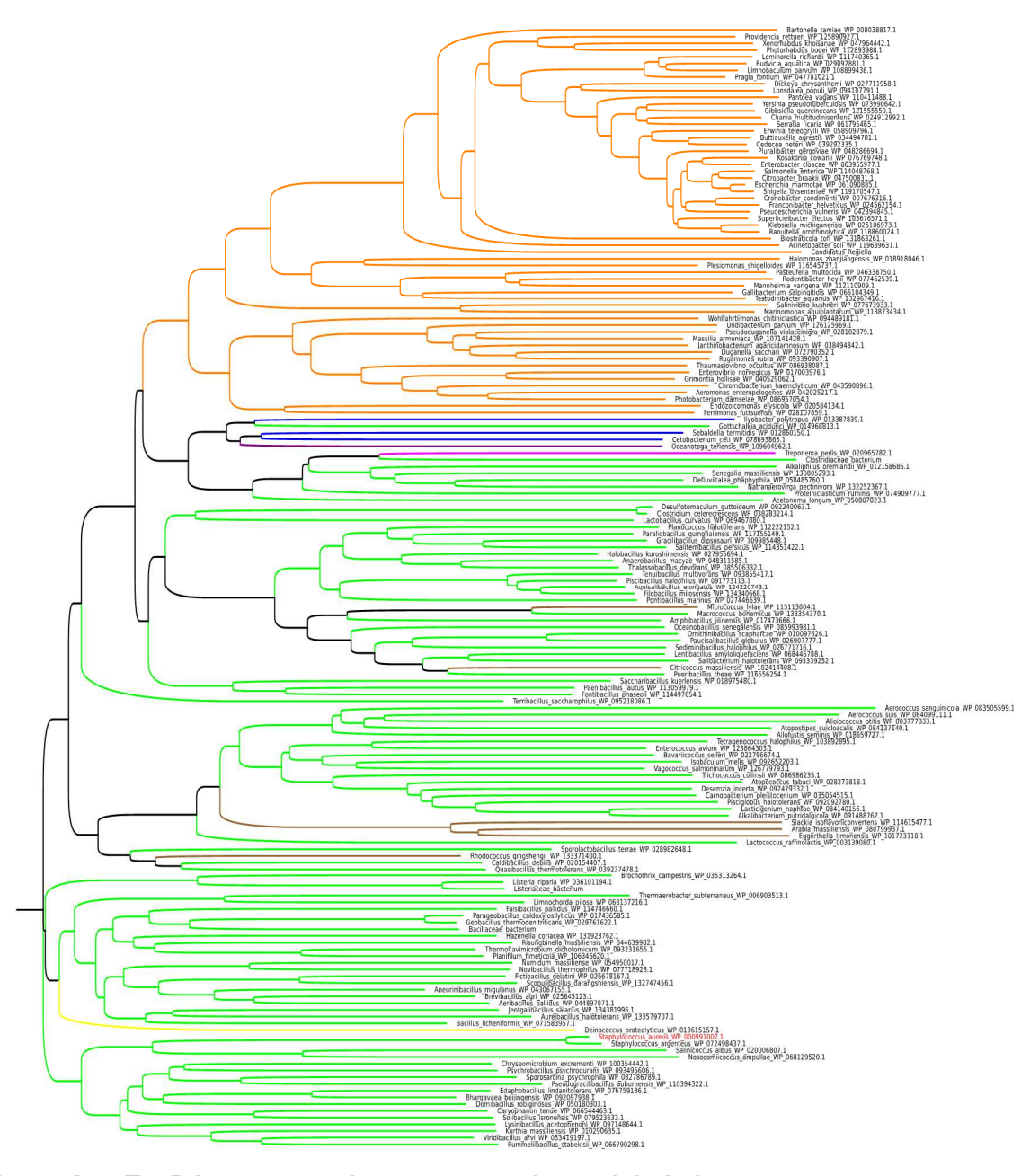


Figure A-4. TcyP is conserved across many bacterial phyla.

Homologues of TcyP are present in Proteobacteria (orange), Firmicutes (green), Fusobacteria (blue), Thermotogae (purple), Spirochaetes (magenta), Actinobacteria (brown), and Deinococcus (yellow). The query, TcyP protein from *S. aureus*, is highlighted in red.

Table B-1. Bacterial strains used in chapter 3.

strain	description	reference
methicillin-resistant S. aureus		
JE2	wildtype	(100)
SAUSA300_0200::Tn (<i>gisA)</i>	Tn insertion in <i>gisA</i>	this study
NE392		
SAUSA300_0201::Tn <i>(gisB)</i>	Tn insertion in <i>gisB</i>	this study
NE541		
SAUSA300_0202::Tn (<i>gisC</i>)	Tn insertion in <i>gisC</i>	this study
NE457		
SAUSA300_0203::Tn (<i>gisD</i>)	Tn insertion in <i>gisD</i>	this study
NE215	To be entire to see	Alete etcelo
ggt::Tn NE254	Tn insertion in ggt	this study
∆gisABCD-ggt	deletion of gisABCD-ggt	this study
<i>gisB</i> ::Tn <i>tcyP</i> ::Tn	Tn insertion in <i>gisB</i> with erythromycin	this study
	resistance, Tn insertion in <i>tcy</i> P with	
<i>ggt</i> ::Tn pOS1 P _{lat}	tetracycline resistance Tn insertion in pOS1 P _{lgt} empty vector	this study
ggt::Tn pOS1 P _{lgt} ::ggt	Th insertion in ggt with pOS1 Plgt::ggt	this study
ggt::Tn pOS1 Plgt::ggt-His	Th insertion in ggt with pOS1 Pigt.:ggt The insertion in ggt with pOS1 Pigt::ggt	this study
gg m poor r igggi iis	with His-tag	tilis study
NEB 3016 pET28b::ggt	NEB 3016 <i>slyD</i> mutant with pET28b:: <i>ggt</i>	this study
NEB 3015 pET28b::gisA	NEB 3016 slyD mutant with pET28b::gisA	this study
JE2 pOS1 P _{lgt}	JE2 pOS1 pOS1 P _{lat} empty vector	this study
clinical isolates	p : p : - : : : : : : : : :	
1055	MRSA abscess hand cellulitis	this study
1056	MRSA abscess left arm	this study
1057	MRSA left wrist/ index finger	this study
1058	MSSA left foot diagnosis is osteomyelitis	this study
1059	MSSA bone from the coccyx/chronic	this study
	osteomyelitis	
Staphylococcus epidermidis	Strain RP62a	(77)
Staphylococcus epidermidis	clinical isolate	this study

Table B-2. Primers used in chapter 3.

Table B-2. Primers	• • • • • • • • • • • • • • • • • • •	
name	sequence 5'-3'	description
pET28b:: <i>ggt</i> F	AAGAAGGAGATATACCATGGTCATTA ACTTAAATGACAAAC	amplify <i>ggt</i> ORF without stop codon to clone into pET28b
pET28b:: <i>ggt</i> R	GATGATGGCTGCTGCCCATGTCT TGTGATACTATCTCGAT	amplify <i>ggt</i> ORF without stop codon to clone into pET28b
pKOR1-mcs ∆ <i>gis</i> upstream F	CTGCTAGCTAGCTAGAGATATCAAAC GATAAAAAATATACAAATAAAAATCTA ATTGTAG	amplify 1kB upstream of SAUSA300_0201 to clone into pKOR1-mcs
pKOR1 ∆ <i>gis</i> upstream R	AGCGTATAAAAAGTCATGCGTTGTGC AAC	amplify 1 kB upstream of SAUSA300_0201 to clone into pKOR1-mcs
pKOR1-mcs ∆gis downstream F	CGCATGACTTTTTATACGCTTGATATG AAGTTTG	amplify 1 kB downstream of SASUA300_0204 to clone into pKOR1-mcs
pKOR1-mcs ∆gis downstream R	CGG AAC CGG TAC CAA TGG ATA TCT ATG TTT TTG GCA ATG AAG TG	amplify 1kB downstream of SAUSA300_0204 to clone into pKOR1-mcs
pET28b:: <i>gisA</i> F	ACTTTAAGAAGGAGATATACATGTCA AATTTATTAGAAGTCAAC	amplify <i>gisA</i> ORF without stop codon to clone into pET28b
pET28b:: <i>gisA</i> R	AGTGGTGGTGGTGGTGCGATTT AGCAATAACTGCTAC	amplify <i>gisA</i> ORF without stop codon to clone into pET28b
pOS1 P _{lgt} ∷ <i>ggt</i> F	ACAATTGAGGTGAACATATGGTCATT AACTTAAATGACAAAC	amplify <i>ggt</i> ORF to clone into pOS1 P _{lgt}
pOS1 P _{lgt} ∷ <i>ggt</i> R	CTACCCCTTGTTTGGATCCCTATCTT GTGATACTATCTC	amplify <i>ggt</i> ORF to clone into pOS1 P _{lgt} reverse primer
pOS1 P _{lgt} ∷ <i>ggt</i> -His F	AAATACAATTGAGGTGAACATATGGT CATTAACTTAAATGACAAACAG	amplify <i>ggt</i> with His-tag from pET28B:: <i>ggt</i> to clone into pOS1 P _{lgt}
pOS1 P _{lgt} ∷ <i>ggt</i> -His R	AGCTTGGCTGCAGGTCGACGGATCC TCAGTGGTGGTGGTG	amplify <i>ggt</i> with His-tag from pET28B:: <i>ggt</i> to clone into pOS1 P _{lgt}

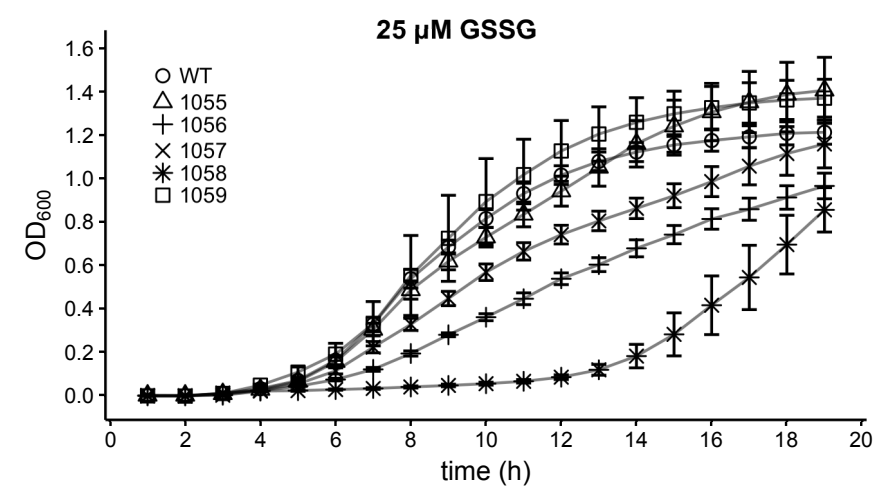


Figure B-1. Supplementation with GSSG as the sole source of nutrient sulfur stimulates growth of clinical isolates.

WT and clinical isolates were grown in medium containing 25 µM GSSG. The mean OD600 of at least 3 independent trials is depicted and error bars represent ± 1 standard error of the mean.

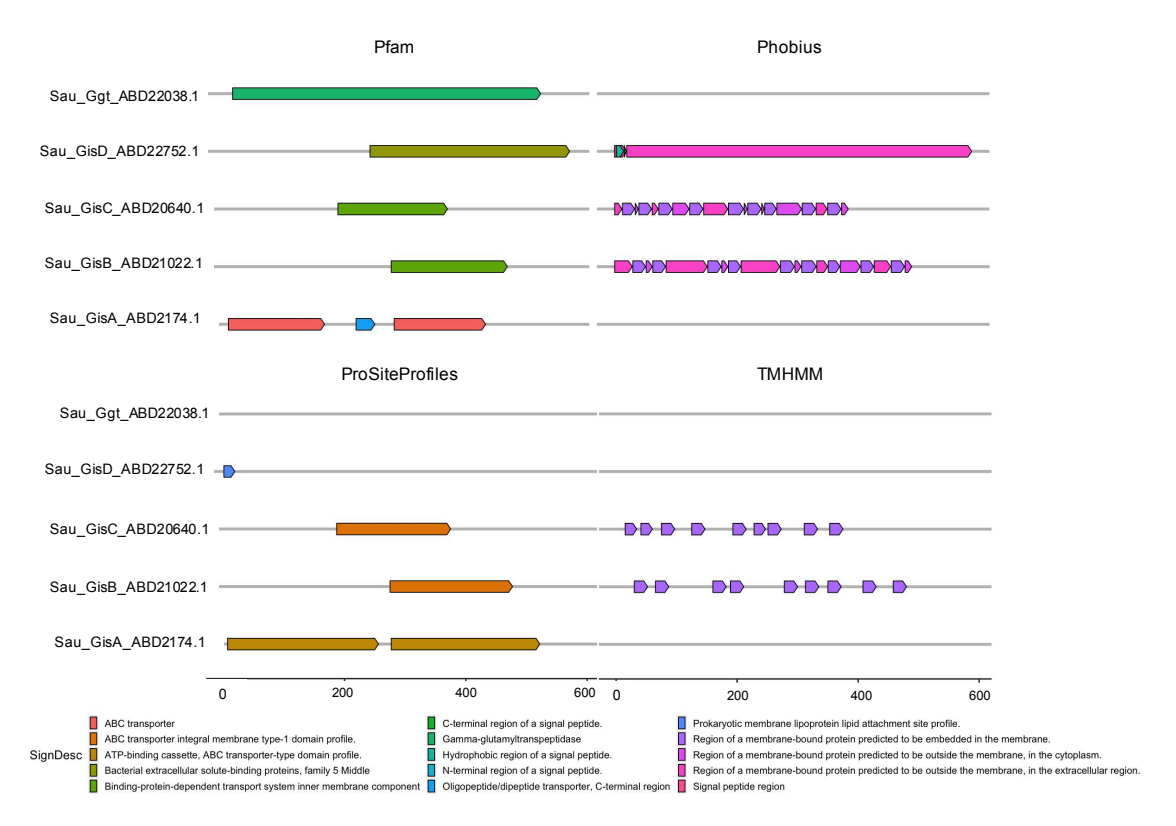


Figure B-2. Domain architectures and secondary structure predictions for the *S. aureus* GisABCD-Ggt system.

Domains were predicted using InterProScan (3,4); see Methods. Results from four main analyses are shown here for the query proteins: Pfam, Phobius, ProSiteProfiles, TMHMM.

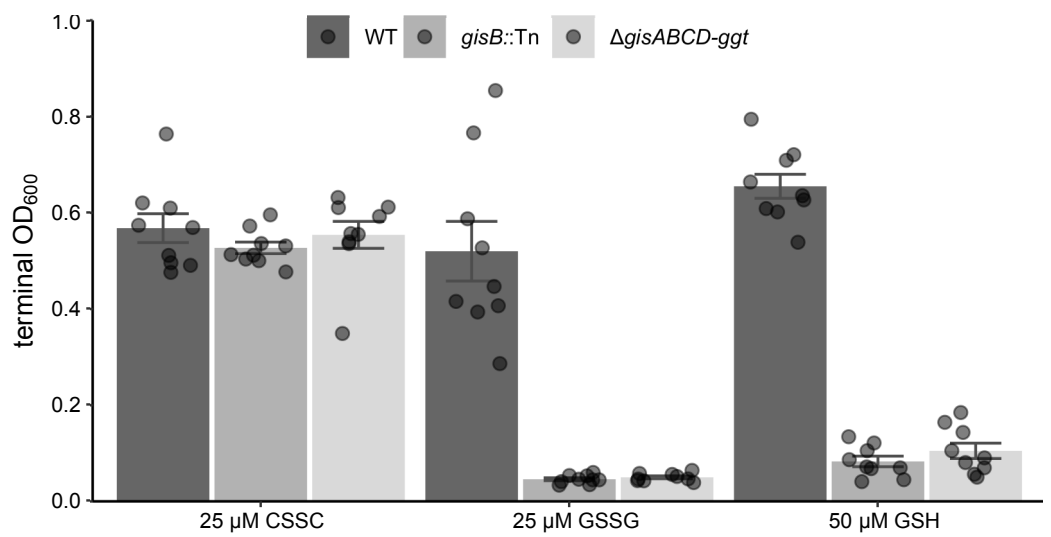


Figure B-3. GisABCD-Ggt promotes anaerobic growth in media supplemented with GSSG or GSH.

WT, gisB::Tn, and $\Delta gisABCD$ -ggt were grown in chemically defined medium in the presence of the listed sulfur sources. Chemicals were prepared anaerobically to maintain them in their respective states. Each point represents one terminal OD_{600} and each bar represents the mean of at least three independent trials and error bars represent \pm 1 standard error of the mean.

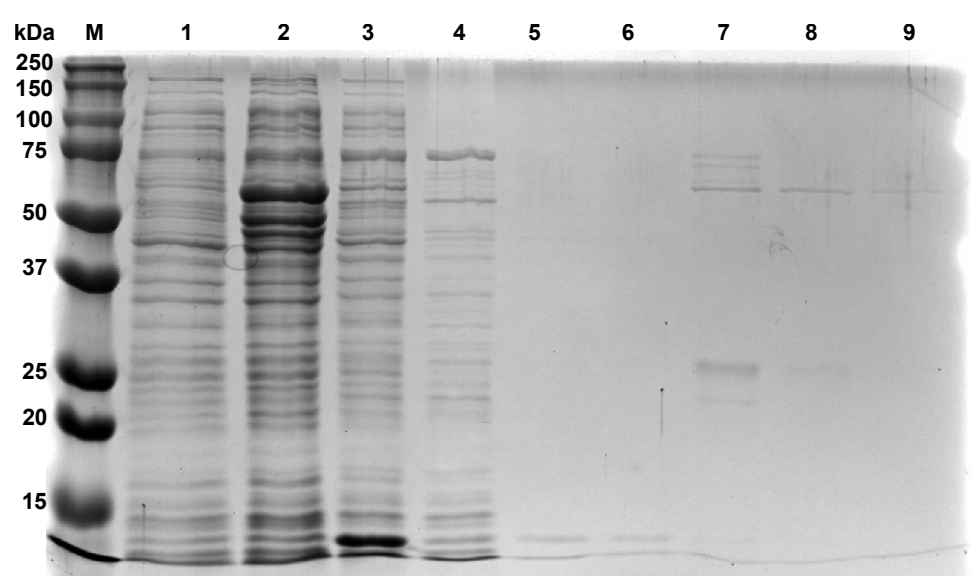
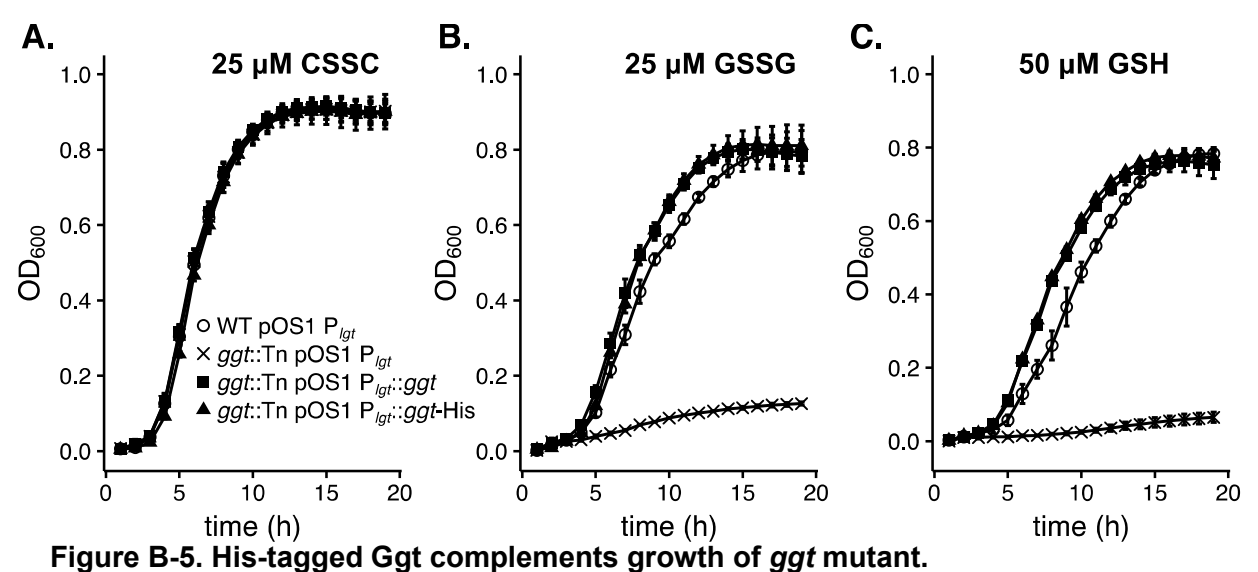


Figure B-4. Coomassie blue stained SDS-PAGE gel demonstrating purification of histidine tagged GisA expressed in *E. coli*.

Lanes: M, molecular weight ladder; 1, prior to induction with IPTG; 2, 4 hours after IPTG induction; 3, lysate; 4, initial flowthrough of the Ni-NTA column; 5 and 6, fractions from 20 mM imidazole elution; 7, fraction from 100 mM imidazole elution; 8 and 9, fractions from 400 mM imidazole elution.



(A) Strains grown in medium supplemented with 25 μM cystine, (B) 25 μM GSSG, or (C) 50 μM GSH. Presented is the mean of at least three independent trials and error bars represent ± 1 standard error of the mean.

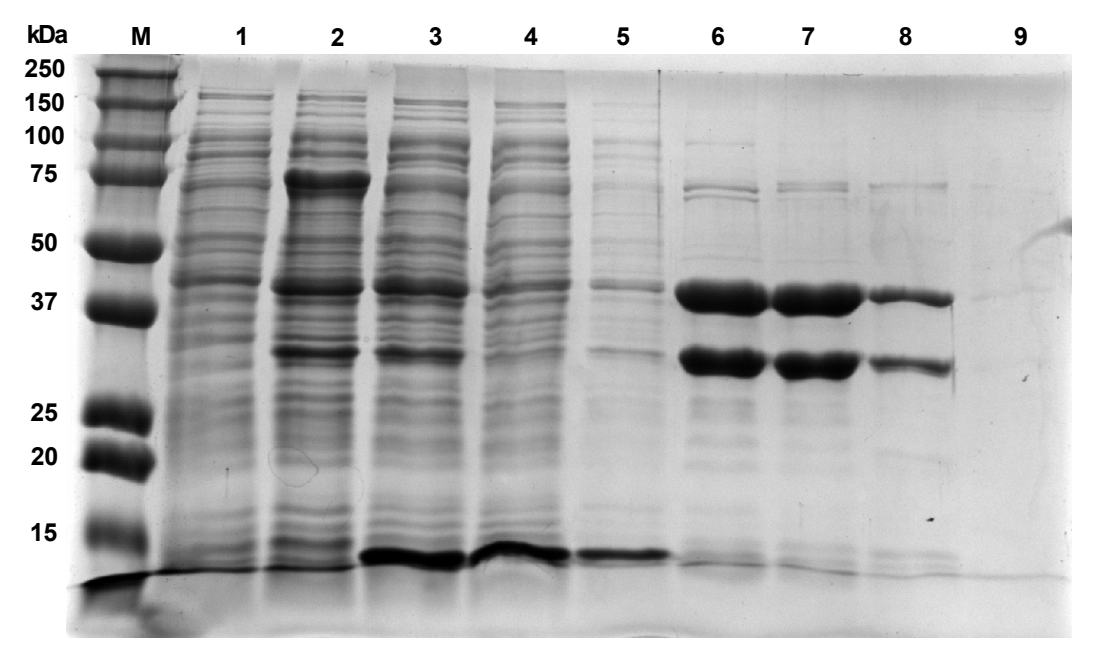


Figure B-6. Heterologous expression and purification of *S. aureus* Ggt from *E. coli*.

Lanes: M, molecular weight ladder; 1, prior to induction with IPTG; 2, 4 hours after IPTG induction; 3, sate; 4, initial flowthrough of the Ni-NTA column; 5, fraction from 20 mM imidazole wash; 6, fraction from 50 mM imidazole wash; 7, fraction from 100 mM imidazole elution; 8 and 9, fractions from 400 mM imidazole elution.

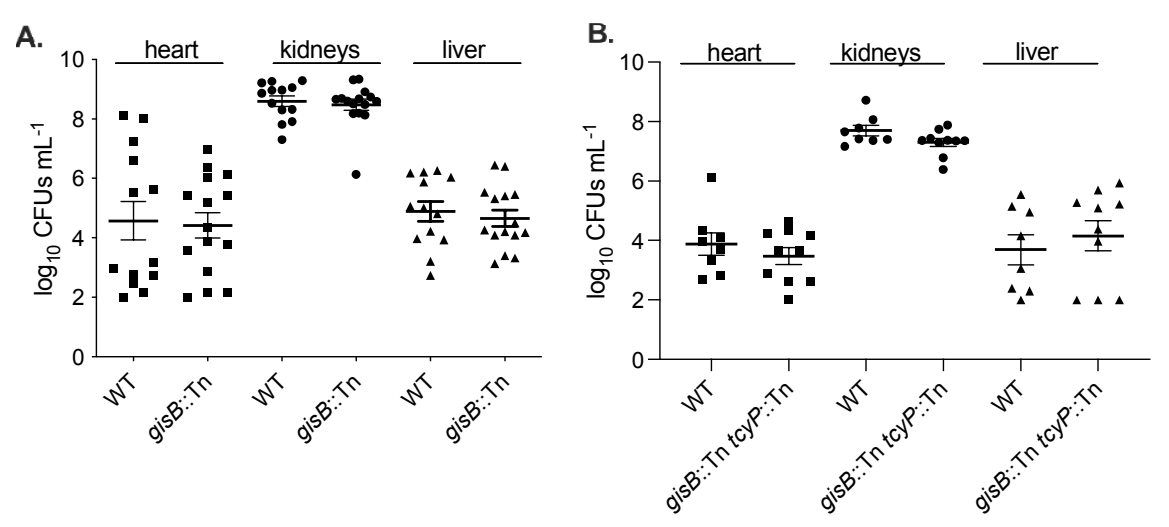


Figure B-7. Inactivation of *gisB* or *gisB* and *tcyP* does not affect virulence in a murine systemic model of infection.

(A) C57BL/6 mice were systemically infected with WT or gisB::Tn and infection proceeded for 96 hours. (B) Balb/c mice were systemically infected with WT or $gisB\ tcyP$ and infection proceeded for 96 hours. Bacterial burdens are presented as $log_{10}\ CFUs\ mL^{-1}$ for liver, combined left and right kidneys, and heart. The line represents the mean and error bars represent \pm 1 standard error of the mean.

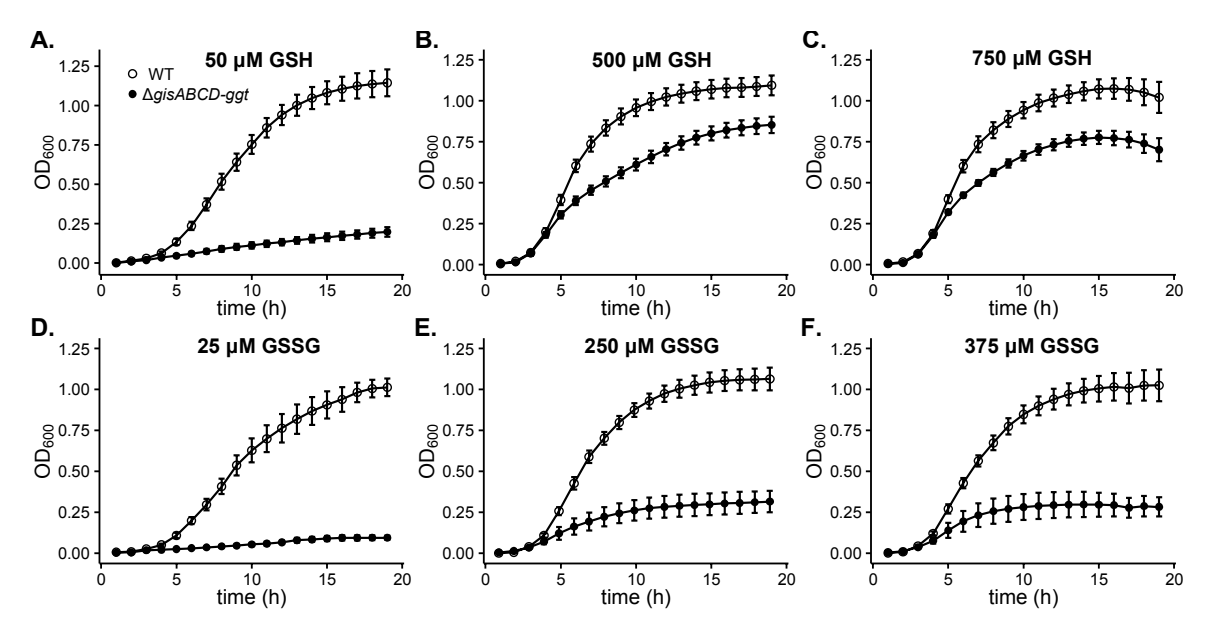


Figure B-8. Gis mutant can grow in physiologically relevant concentrations of GSH. WT and $\Delta gisABCD$ -ggt cultured in medium containing the indicated sulfur sources. Mean OD_{600} of at least 3 independent trails is presented and error bars depict \pm 1 standard error of the mean.

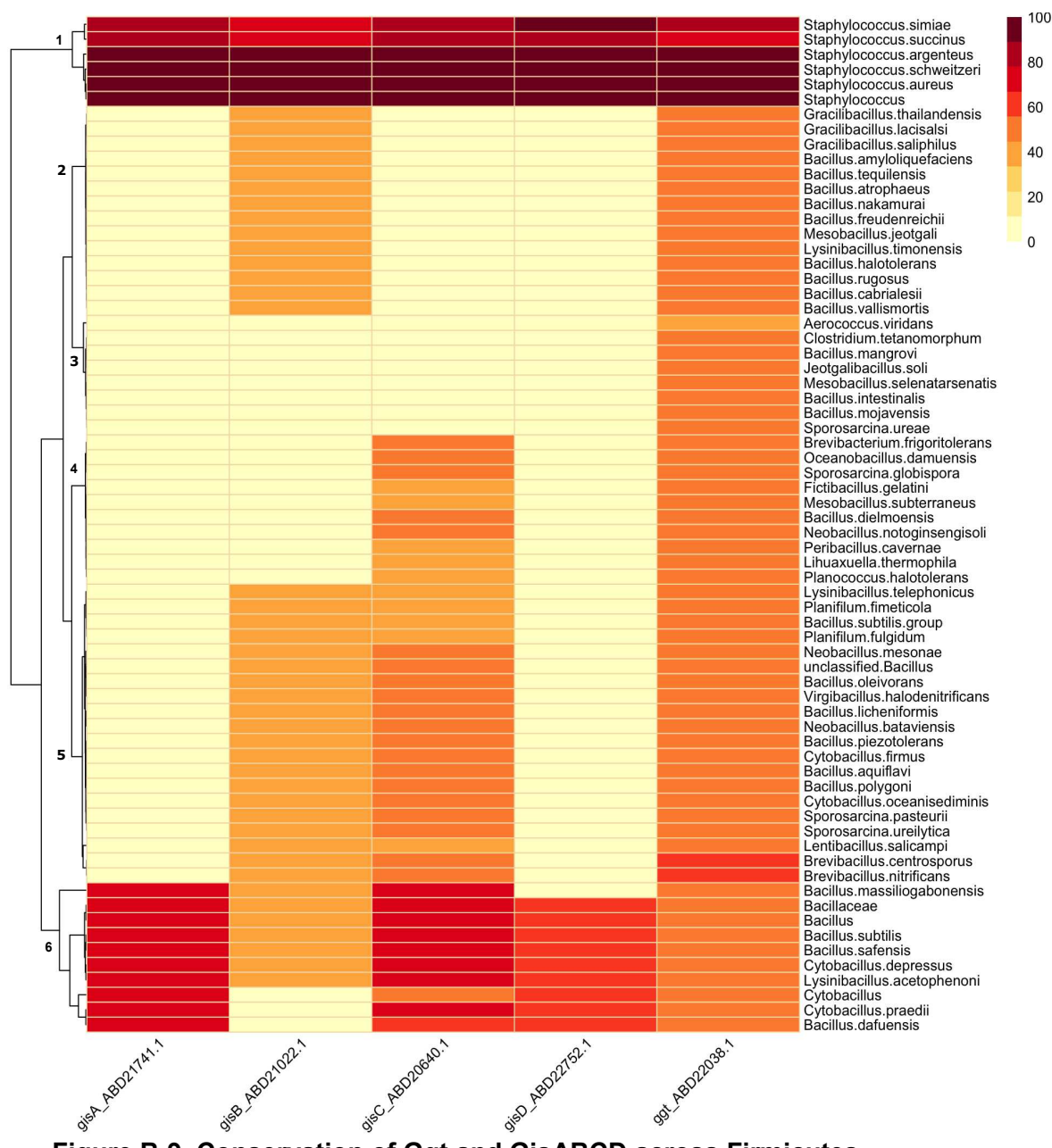


Figure B-9. Conservation of Ggt and GisABCD across Firmicutes.Percent similarity of *S. aureus* Ggt was queried, and results were limited to Firmicutes encoding a glutamyl transpeptidase domain. *S. aureus* GisABCD was subsequently queried using this dataset.

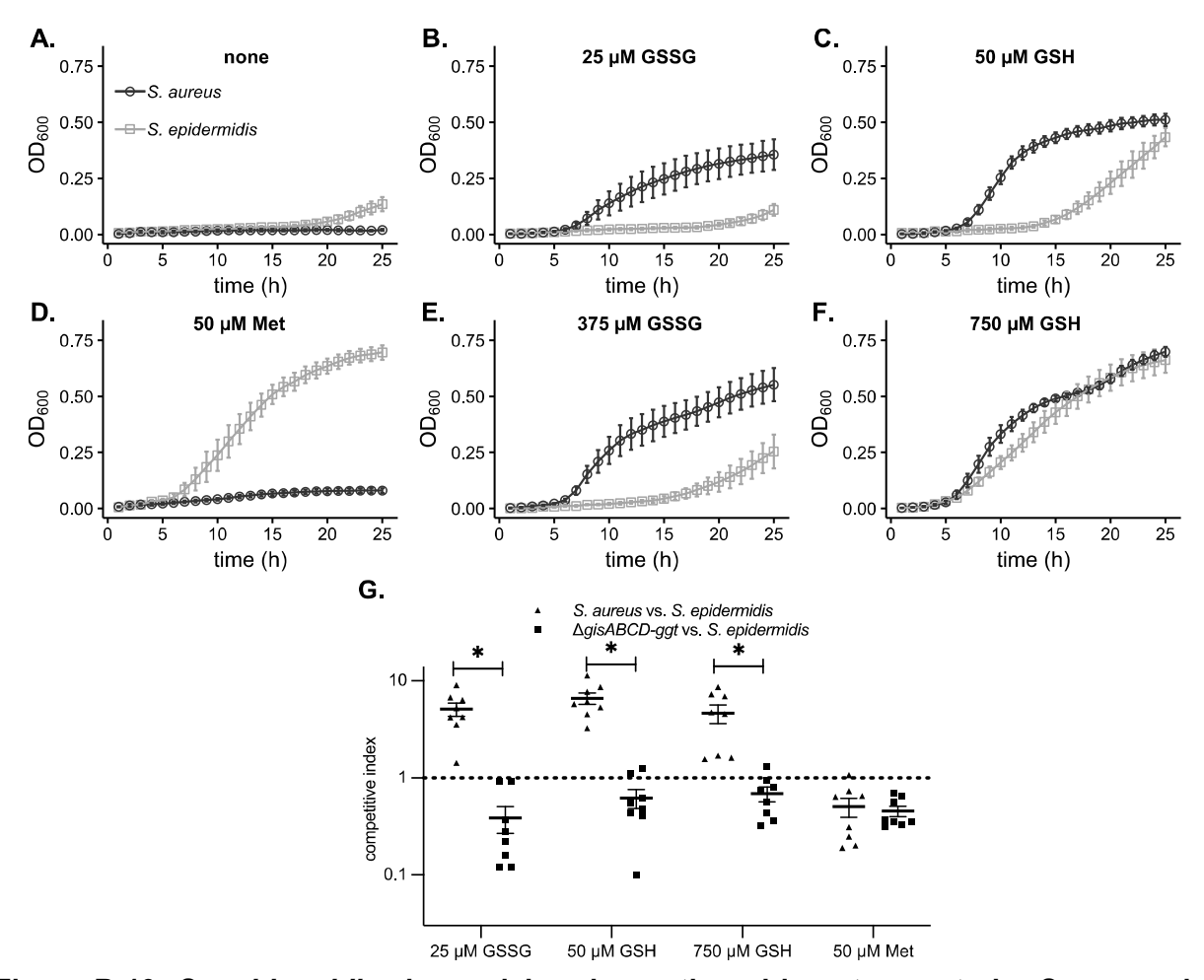


Figure B-10. *S. epidermidis* shows delayed growth and is outcompete by *S. aureus* in GSH containing media.

(A-F) S. aureus and a clinical isolate of S. epidermidis were grown in PN_{mod} containing the listed sulfur source. Presented is the mean OD_{600} of at least three independent trials and the error bars depict \pm 1 standard error of the mean. (G) In vitro competition of the clinical isolate of S. epidermidis and S. aureus in PN_{mod} containing the listed sulfur sources. The individual trial competitive index is presented. The line represents the mean, and the error depict \pm 1 standard error of the mean.

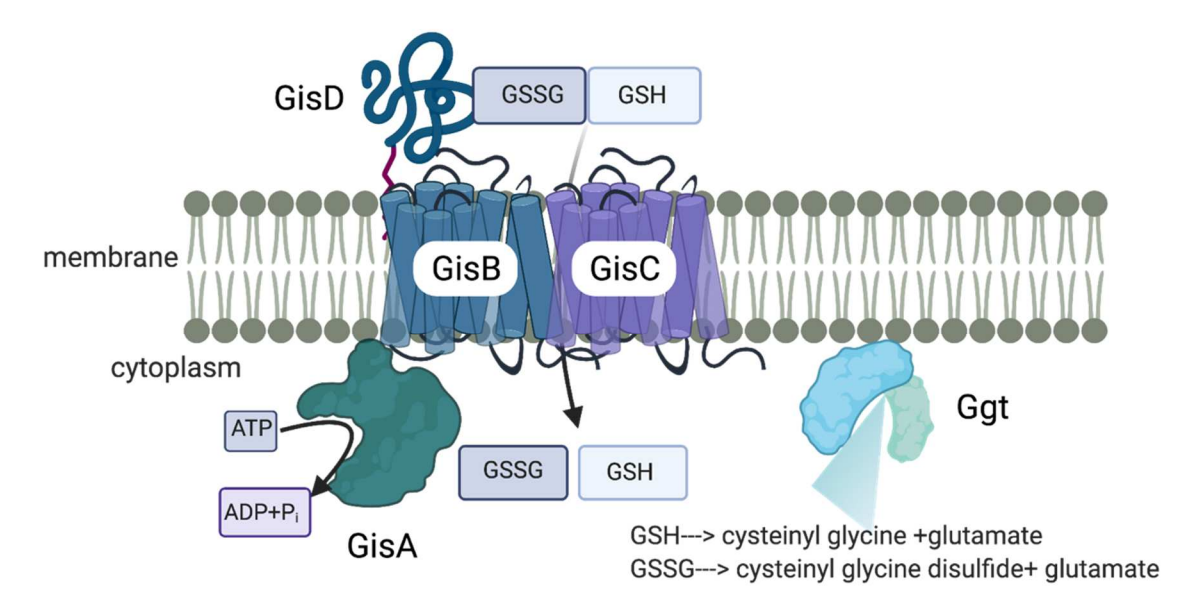


Figure B-11. A proposed model of GisABCD-Ggt acquisition of GSH and GSSG.

Bioinformatic predictions and experimental evidence allow us to synthesis a model for how *S. aureus* imports and catabolizes GSH and GSSG. GisD, a predicted substate binding protein, binds GSH and GSSG in the extracellular milieu, which are then translocated through the transmembrane permeases GisBC aided by the hydrolysis of ATP by GisA. Finally, GSH and GSSG are cleaved inside of the cell by Ggt generating cysteinyl glycine and cysteinyl glycine disulfide and glutamate based upon this model. Model was created using BioRender.

Table C-1. Genes that are shared between our data and the published *cymR* mutant data.

locus gene name	gene name	published dataset ^a
up in all three data sets		
SAUSA300_RS00910		sulfur
SAUSA300_RS00915		sulfur
SAUSA300_RS00930		sulfur
SAUSA300_RS01055		sulfur
SAUSA300_RS02035	tcyP	sulfur
SAUSA300_RS02325	тссВ	sulfur
SAUSA300_RS02330		sulfur
SAUSA300_RS10985		sulfur
SAUSA300_RS13025	tcyA	sulfur
SAUSA300_RS01875		envelope
SAUSA300_RS15260		envelope
up in WT sulfur deplete and published	cymR mutant	
SAUSA300_RS00935		sulfur
SAUSA300_RS00940b	fdh	sulfur
SAUSA300_RS02320b	mccA	sulfur
SAUSA300_RS12345b	ydbM	sulfur
SAUSA300_RS13015 ^b	tcyC	sulfur
SAUSA300_RS13020 ^b	tcyB	sulfur
SAUSA300_RS02345		envelope
SAUSA300_RS04145		envelope
SAUSA300_RS12435		envelope

^a The *cymR* mutant dataset is broken into sulfur associated genes and cell envelope associated genes (28). ^bgenes are upregulated in *cymR*::Tn CSSC but are below adjusted p-value cutoff of <0.05 (data not shown).

REFERENCES

REFERENCES

- Beinert H. 2000. A tribute to sulfur. Eur. J. Biochem. 267:5657–5664.
- 2. **Meister A, Anderson ME**. 1983. Glutathione. Annu. Rev. Biochem. **52**:711–760.
- 3. **Hoppe B**, **Kemper MJ**, **Hvizd MG**, **Sailer DE**, **Langman CB**. 1998. Simultaneous determination of oxalate, citrate and sulfate in children's plasma with ion chromatography. Kidney Int. **53**:1348–1352.
- 4. **Kredich NM**. 1996. Biosynthesis of Cysteine, p. 514–527. *In* Neidhardt (ed.), *Escherichia coli* and *Salmonella*, cellular and molecular biology.
- 5. **Lill R**, **Mühlenhoff U**. 2006. Iron-sulfur protein biogenesis in eukaryotes: components and mechanisms. Annu. Rev. Cell Dev. Biol. **22**:457–486.
- 6. **Gebhardt MJ**, **Gallagher LA**, **Jacobson RK**, **Usacheva EA**, **Peterson LR**, **Zurawski DV**, **Shuman HA**. 2015. Joint Transcriptional Control of Virulence and Resistance to Antibiotic and Environmental Stress in *Acinetobacter baumannii*. MBio **6**:e01660-15.
- 7. **Fontán P, Aris V, Ghanny S, Soteropoulos P, Smith I**. 2008. Global transcriptional profile of *Mycobacterium tuberculosis* during THP-1 human macrophage infection. Infect. Immun. **76**:717–725.
- 8. **Sassetti CM**, **Boyd DH**, **Rubin EJ**. 2001. Comprehensive identification of conditionally essential genes in mycobacteria. Proc. Natl. Acad. Sci. USA **98**:12712–12717.
- 9. **Nakamura T**, **Iwahashi H**, **Eguchi Y**. 1984. Enzymatic proof for the identity of the S-sulfocysteine synthase and cysteine synthase B of *Salmonella* typhimurium. J. Bacteriol. **158**:1122–1127.
- 10. **Nakamura T, Kon Y, Iwahashi H, Eguchi Y**. 1983. Evidence that thiosulfate assimilation by *Salmonella* typhimurium is catalyzed by cysteine synthase B. J. Bacteriol. **156**:656–662.
- 11. **Lithgow JK**, **Hayhurst EJ**, **Cohen G**, **Aharonowitz Y**, **Foster SJ**. 2004. Role of a cysteine synthase in *Staphylococcus aureus*. J. Bacteriol. **186**:1579–1590.
- 12. **Dubois T, Dancer-Thibonnier M, Monot M, Hamiot A, Bouillaut L, Soutourina O, Martin-Verstraete I, Dupuy B**. 2016. Control of *Clostridium difficile* Physiopathology in Response to Cysteine Availability. Infect. Immun. **84**:2389–2405.
- 13. **Robinson CV**, **Elkins MR**, **Bialkowski KM**, **Thornton DJ**, **Kertesz MA**. 2012. Desulfurization of mucin by *Pseudomonas aeruginosa*: influence of sulfate in the lungs of cystic fibrosis patients. J. Med. Microbiol. **61**:1644–1653.
- 14. **Seiflein TA**, **Lawrence JG**. 2001. Methionine-to-cysteine recycling in *Klebsiella*

- aerogenes. J. Bacteriol. 183:336-346.
- 15. Vorwerk H, Mohr J, Huber C, Wensel O, Schmidt-Hohagen K, Gripp E, Josenhans C, Schomburg D, Eisenreich W, Hofreuter D. 2014. Utilization of host-derived cysteine-containing peptides overcomes the restricted sulphur metabolism of *Campylobacter jejuni*. Mol. Microbiol. **93**:1224–1245.
- 16. **Alkhuder K**, **Meibom KL**, **Dubail I**, **Dupuis M**, **Charbit A**. 2009. Glutathione provides a source of cysteine essential for intracellular multiplication of *Francisella tularensis*. PLoS Pathog. **5**:e1000284.
- 17. **Stenson TH**, **Patton AK**, **Weiss AA**. 2003. Reduced glutathione is required for pertussis toxin secretion by *Bordetella pertussis*. Infect. Immun. **71**:1316–1320.
- 18. **Takahashi H, Hirose K, Watanabe H**. 2004. Necessity of meningococcal gamma-glutamyl aminopeptidase for *Neisseria meningitidis* growth in rat cerebrospinal fluid (CSF) and CSF-like medium. J. Bacteriol. **186**:244–247.
- 19. **Suzuki H, Koyanagi T, Izuka S, Onishi A, Kumagai H**. 2005. The yliA, -B, -C, and -D genes of *Escherichia coli* K-12 encode a novel glutathione importer with an ATP-binding cassette. J. Bacteriol. **187**:5861–5867.
- 20. **Wang Z**, **Zhang M**, **Shi X**, **Xiang Q**. 2017. Purification and Characterization of an ATPase GsiA from *Salmonella enterica*. Biomed Res. Int. **2017**:3076091.
- 21. **Vergauwen B, Elegheert J, Dansercoer A, Devreese B, Savvides SN**. 2010. Glutathione import in *Haemophilus influenzae* Rd is primed by the periplasmic hemebinding protein HbpA. Proc. Natl. Acad. Sci. USA **107**:13270–13275.
- 22. Vergauwen B, Verstraete K, Senadheera DB, Dansercoer A, Cvitkovitch DG, Guédon E, Savvides SN. 2013. Molecular and structural basis of glutathione import in Gram-positive bacteria via GshT and the cystine ABC importer TcyBC of *Streptococcus mutans*. Mol. Microbiol. 89:288–303.
- 23. **Potter AJ**, **Trappetti C**, **Paton JC**. 2012. *Streptococcus pneumoniae* uses glutathione to defend against oxidative stress and metal ion toxicity. J. Bacteriol. **194**:6248–6254.
- 24. **Xayarath B**, **Marquis H**, **Port GC**, **Freitag NE**. 2009. *Listeria monocytogenes* CtaP is a multifunctional cysteine transport-associated protein required for bacterial pathogenesis. Mol. Microbiol. **74**:956–973.
- 25. **Guédon E**, **Martin-Verstraete I**. 2007. Cysteine metabolism and its regulation in bacteria, p. 195–218. *In* Wendisch, VF (ed.), Amino acid biosynthesis ~ pathways, regulation and metabolic engineering. Springer Berlin Heidelberg, Berlin, Heidelberg.
- 26. **Kim J**, **Senadheera DB**, **Lévesque CM**, **Cvitkovitch DG**. 2012. TcyR regulates L-cystine uptake via the TcyABC transporter in *Streptococcus mutans*. FEMS Microbiol. Lett. **328**:114–121.
- 27. **Cowie DB**, **Bolton ET**, **Sands MK**. 1951. Sulfur metabolism in *Escherichia coli*. II. Competitive utilization of labeled and nonlabeled sulfur compounds. J. Bacteriol. **62**:63–

- 28. **Soutourina O, Poupel O, Coppée J-Y, Danchin A, Msadek T, Martin-Verstraete I.** 2009. CymR, the master regulator of cysteine metabolism in *Staphylococcus aureus*, controls host sulphur source utilization and plays a role in biofilm formation. Mol. Microbiol. **73**:194–211.
- 29. **Ivankovich AD**, **Braverman B**, **Stephens TS**, **Shulman M**, **Heyman HJ**. 1983. Sodium Thiosulfate Disposition in Humans Relation to Sodium Nitroprusside Toxicity. Anesthesiology: The Journal of the American Society of Anesthesiologists **58**:11–17.
- 30. Psychogios N, Hau DD, Peng J, Guo AC, Mandal R, Bouatra S, Sinelnikov I, Krishnamurthy R, Eisner R, Gautam B, Young N, Xia J, Knox C, Dong E, Huang P, Hollander Z, Pedersen TL, Smith SR, Bamforth F, Greiner R, McManus B, Newman JW, Goodfriend T, Wishart DS. 2011. The human serum metabolome. PLoS One 6:e16957.
- 31. **Cynober LA**. 2002. Plasma amino acid levels with a note on membrane transport: characteristics, regulation, and metabolic significance. Nutrition **18**:761–766.
- 32. Tavazzi B, Lazzarino G, Leone P, Amorini AM, Bellia F, Janson CG, Di Pietro V, Ceccarelli L, Donzelli S, Francis JS, Giardina B. 2005. Simultaneous high performance liquid chromatographic separation of purines, pyrimidines, N-acetylated amino acids, and dicarboxylic acids for the chemical diagnosis of inborn errors of metabolism. Clin. Biochem. 38:997–1008.
- 33. Wishart DS, Tzur D, Knox C, Eisner R, Guo AC, Young N, Cheng D, Jewell K, Arndt D, Sawhney S, Fung C, Nikolai L, Lewis M, Coutouly M-A, Forsythe I, Tang P, Shrivastava S, Jeroncic K, Stothard P, Amegbey G, Block D, Hau DD, Wagner J, Miniaci J, Clements M, Gebremedhin M, Guo N, Zhang Y, Duggan GE, Macinnis GD, Weljie AM, Dowlatabadi R, Bamforth F, Clive D, Greiner R, Li L, Marrie T, Sykes BD, Vogel HJ, Querengesser L. 2007. HMDB: the human metabolome database. Nucleic Acids Res. 35:D521-6.
- 34. **Smiley DW**, **Wilkinson BJ**. 1983. Survey of taurine uptake and metabolism in *Staphylococcus aureus*. J. Gen. Microbiol. **129**:2421–2428.
- 35. **Kredich N**. 1971. Regulation of L-Cysteine Biosynthesis in *Salmonella* typhimurium. Effects of Growth on varying sulfur sources and O-Acetyl-L-Serine on Gene Expression. J. Biol. Chem. **246**:3474–3484.
- 36. **Ostrowski J**, **Kredich NM**. 1990. In vitro interactions of CysB protein with the cysJIH promoter of *Salmonella* typhimurium: inhibitory effects of sulfide. J. Bacteriol. **172**:779–785.
- 37. André G, Haudecoeur E, Monot M, Ohtani K, Shimizu T, Dupuy B, Martin-Verstraete I. 2010. Global regulation of gene expression in response to cysteine availability in *Clostridium perfringens*. BMC Microbiol. **10**:234.
- 38. **Ewann F**, **Hoffman PS**. 2006. Cysteine metabolism in *Legionella pneumophila*: characterization of an L-cystine-utilizing mutant. Appl. Environ. Microbiol. **72**:3993–4000.

- 39. **Stainer DW**, **SCHOLTE MJ**. 1971. A Simple Chemically Defined Medium for the Production of Phase I *Bordetella pertussis*. J. Gen. Microbiol. **63**:211–220.
- 40. **Catlin BW**. 1977. Nutritional requirements and auxotyping, p. . *In* Roberts, RB (ed.), *The Gonococcus*.
- 41. Schär J, Stoll R, Schauer K, Loeffler DIM, Eylert E, Joseph B, Eisenreich W, Fuchs TM, Goebel W. 2010. Pyruvate carboxylase plays a crucial role in carbon metabolism of extra- and intracellularly replicating *Listeria monocytogenes*. J. Bacteriol. **192**:1774–1784.
- 42. **Burguière P, Auger S, Hullo M-F, Danchin A, Martin-Verstraete I**. 2004. Three different systems participate in L-cystine uptake in *Bacillus subtilis*. J. Bacteriol. **186**:4875–4884.
- 43. **Tsai H-N**, **Hodgson DA**. 2003. Development of a synthetic minimal medium for *Listeria monocytogenes*. Appl. Environ. Microbiol. **69**:6943–6945.
- 44. **Schauer K**, **Geginat G**, **Liang C**, **Goebel W**, **Dandekar T**, **Fuchs TM**. 2010. Deciphering the intracellular metabolism of *Listeria monocytogenes* by mutant screening and modelling. BMC Genomics **11**:573.
- 45. **Figge RM**. 2007. Methionine Biosynthesis in *Escherichia coli* and *Corynebacterium glutamicum*, p. 163–193. *In* Wendisch, VF (ed.), Amino acid biosynthesis ~ pathways, regulation and metabolic engineering. Springer Berlin Heidelberg, Berlin, Heidelberg.
- 46. Wheeler PR, Coldham NG, Keating L, Gordon SV, Wooff EE, Parish T, Hewinson RG. 2005. Functional demonstration of reverse transsulfuration in the *Mycobacterium tuberculosis* complex reveals that methionine is the preferred sulfur source for pathogenic *Mycobacteria*. J. Biol. Chem. 280:8069–8078.
- 47. Zhang Z, Feige JN, Chang AB, Anderson IJ, Brodianski VM, Vitreschak AG, Gelfand MS, Saier MH. 2003. A transporter of *Escherichia coli* specific for L- and D-methionine is the prototype for a new family within the ABC superfamily. Arch. Microbiol. 180:88–100.
- 48. **Fahey RC**, **Brown WC**, **Adams WB**, **Worsham MB**. 1978. Occurrence of glutathione in bacteria. J. Bacteriol. **133**:1126–1129.
- 49. **Masip L**, **Veeravalli K**, **Gerogiou G**. 2006. The Many Faces of Glutathione in Bacteria. Antioxid. Redox Signal. **8**:753–762.
- 50. **Suzuki H**, **Kamatani S**, **Kim ES**, **Kumagai H**. 2001. Aminopeptidases A, B, and N and dipeptidase D are the four cysteinylglycinases of *Escherichia coli* K-12. J. Bacteriol. **183**:1489–1490.
- 51. **Sjovall J**. 1959. Dietary glycine and taurine on bile acid conjugation in man. bile acids and steroids 75. Exp. Biol. Med. **100**:676–678.
- 52. Schwartz NB, Lyle S, Ozeran JD, Li H, Deyrup A, Ng K, Westley J. 1998. Sulfate

- activation and transport in mammals: system components and mechanisms. Chem. Biol. Interact. **109**:143–151.
- 53. Spyrakis F, Singh R, Cozzini P, Campanini B, Salsi E, Felici P, Raboni S, Benedetti P, Cruciani G, Kellogg GE, Cook PF, Mozzarelli A. 2013. Isozyme-specific ligands for O-acetylserine sulfhydrylase, a novel antibiotic target. PLoS One 8:e77558.
- 54. **Mazumder M**, **Gourinath S**. 2016. Structure-Based Design of Inhibitors of the Crucial Cysteine Biosynthetic Pathway Enzyme O-Acetyl Serine Sulfhydrylase. Curr. Top. Med. Chem. **16**:948–959.
- 55. Benoni R, Pertinhez TA, Spyrakis F, Davalli S, Pellegrino S, Paredi G, Pezzotti A, Bettati S, Campanini B, Mozzarelli A. 2016. Structural insight into the interaction of O-acetylserine sulfhydrylase with competitive, peptidic inhibitors by saturation transfer difference-NMR. FEBS Lett. **590**:943–953.
- 56. Salsi E, Bayden AS, Spyrakis F, Amadasi A, Campanini B, Bettati S, Dodatko T, Cozzini P, Kellogg GE, Cook PF, Roderick SL, Mozzarelli A. 2010. Design of O-acetylserine sulfhydrylase inhibitors by mimicking nature. J. Med. Chem. **53**:345–356.
- 57. Campanini B, Pieroni M, Raboni S, Bettati S, Benoni R, Pecchini C, Costantino G, Mozzarelli A. 2015. Inhibitors of the sulfur assimilation pathway in bacterial pathogens as enhancers of antibiotic therapy. Curr. Med. Chem. **22**:187–213.
- 58. **Schnell R, Sriram D, Schneider G**. 2015. Pyridoxal-phosphate dependent mycobacterial cysteine synthases: Structure, mechanism and potential as drug targets. Biochim. Biophys. Acta **1854**:1175–1183.
- 59. Amori L, Katkevica S, Bruno A, Campanini B, Felici P, Mozzarelli A, Costantino G. 2012. Design and synthesis of trans-2-substituted-cyclopropane-1-carboxylic acids as the first non-natural small molecule inhibitors of O-acetylserine sulfhydrylase. Medchemcomm 3:1111.
- 60. **Brunner K**, **Steiner EM**, **Reshma RS**, **Sriram D**, **Schnell R**, **Schneider G**. 2017. Profiling of in vitro activities of urea-based inhibitors against cysteine synthases from *Mycobacterium tuberculosis*. Bioorg. Med. Chem. Lett. **27**:4582–4587.
- 61. Brunner K, Maric S, Reshma RS, Almqvist H, Seashore-Ludlow B, Gustavsson A-L, Poyraz Ö, Yogeeswari P, Lundbäck T, Vallin M, Sriram D, Schnell R, Schneider G. 2016. Inhibitors of the Cysteine Synthase CysM with Antibacterial Potency against Dormant *Mycobacterium tuberculosis*. J. Med. Chem. **59**:6848–6859.
- 62. Palde PB, Bhaskar A, Pedró Rosa LE, Madoux F, Chase P, Gupta V, Spicer T, Scampavia L, Singh A, Carroll KS. 2016. First-in-Class Inhibitors of Sulfur Metabolism with Bactericidal Activity against Non-Replicating *M. tuberculosis*. ACS Chem. Biol. 11:172–184.
- 63. **Barth AL**, **Pitt TL**. 1995. Auxotrophy of *Burkholderia (Pseudomonas) cepacia* from cystic fibrosis patients. J. Clin. Microbiol. **33**:2192–2194.
- 64. Farrior JW, Kloos WE. 1976. Sulfur amino acid auxotrophy in *Micrococcus* species

- isolated from human skin. Can. J. Microbiol. 22:1680–1690.
- 65. **McIver CJ**, **Tapsall JW**. 1988. Characteristics of cysteine-requiring strains of *Klebsiella* isolated from urinary tract infections. J. Med. Microbiol. **26**:211–215.
- 66. **Gibreel TM**, **Sifaw Ghenghesh K**. 2002. Cysteine-dependent Uropathogens: Isolation, Identification and Susceptibility to Antimicrobial Agents . Jamahiriya Med J **2**:52–54.
- 67. Bouatra S, Aziat F, Mandal R, Guo AC, Wilson MR, Knox C, Bjorndahl TC, Krishnamurthy R, Saleem F, Liu P, Dame ZT, Poelzer J, Huynh J, Yallou FS, Psychogios N, Dong E, Bogumil R, Roehring C, Wishart DS. 2013. The human urine metabolome. PLoS One 8:e73076.
- 68. Klevens RM, Morrison MA, Nadle J, Petit S, Gershman K, Ray S, Harrison LH, Lynfield R, Dumyati G, Townes JM, Craig AS, Zell ER, Fosheim GE, McDougal LK, Carey RB, Fridkin SK, Active Bacterial Core surveillance (ABCs) MRSA Investigators. 2007. Invasive methicillin-resistant *Staphylococcus aureus* infections in the United States. JAMA 298:1763–1771.
- 69. Cabell CH, Jollis JG, Peterson GE, Corey GR, Anderson DJ, Sexton DJ, Woods CW, Reller LB, Ryan T, Fowler VG. 2002. Changing patient characteristics and the effect on mortality in endocarditis. Arch. Intern. Med. **162**:90–94.
- 70. Kallen AJ, Mu Y, Bulens S, Reingold A, Petit S, Gershman K, Ray SM, Harrison LH, Lynfield R, Dumyati G, Townes JM, Schaffner W, Patel PR, Fridkin SK, Active Bacterial Core surveillance (ABCs) MRSA Investigators of the Emerging Infections Program. 2010. Health care-associated invasive MRSA infections, 2005-2008. JAMA 304:641–648.
- 71. **Salgado-Pabón W**, **Schlievert PM**. 2014. Models matter: the search for an effective *Staphylococcus aureus* vaccine. Nat. Rev. Microbiol. **12**:585–591.
- 72. **Gordon RJ**, **Lowy FD**. 2008. Pathogenesis of methicillin-resistant *Staphylococcus aureus* infection. Clin. Infect. Dis. **46 Suppl 5**:S350-9.
- 73. **Kluytmans J**, **van Belkum A**, **Verbrugh H**. 1997. Nasal carriage of *Staphylococcus aureus*: epidemiology, underlying mechanisms, and associated risks. Clin. Microbiol. Rev. **10**:505–520.
- 74. **Miles AA**. 1941. Some problems of wound infection. Lancet **238**:507–510.
- 75. Lowy FD. 1998. Staphylococcus aureus infections. N. Engl. J. Med. 339:520–532.
- 76. **Gould JC**, **McKILLOP EJ**. 1954. The carriage of *Staphylococcus pyogenes var. aureus* in the human nose. J. Hyg. (Lond.) **52**:304–310.
- 77. **Vitko NP**, **Grosser MR**, **Khatri D**, **Lance TR**, **Richardson AR**. 2016. Expanded Glucose Import Capability Affords *Staphylococcus aureus* Optimized Glycolytic Flux during Infection. MBio **7**.
- 78. Halsey CR, Lei S, Wax JK, Lehman MK, Nuxoll AS, Steinke L, Sadykov M, Powers

- **R**, **Fey PD**. 2017. Amino Acid Catabolism in *Staphylococcus aureus* and the Function of Carbon Catabolite Repression. MBio **8**.
- 79. **Richardson AR**, **Libby SJ**, **Fang FC**. 2008. A nitric oxide-inducible lactate dehydrogenase enables *Staphylococcus aureus* to resist innate immunity. Science **319**:1672–1676.
- 80. Li C, Sun F, Cho H, Yelavarthi V, Sohn C, He C, Schneewind O, Bae T. 2010. CcpA mediates proline auxotrophy and is required for *Staphylococcus aureus* pathogenesis. J. Bacteriol. **192**:3883–3892.
- 81. **Skaar EP**, **Humayun M**, **Bae T**, **DeBord KL**, **Schneewind O**. 2004. Iron-source preference of *Staphylococcus aureus* infections. Science **305**:1626–1628.
- 82. Mazmanian SK, Skaar EP, Gaspar AH, Humayun M, Gornicki P, Jelenska J, Joachmiak A, Missiakas DM, Schneewind O. 2003. Passage of heme-iron across the envelope of *Staphylococcus aureus*. Science **299**:906–909.
- 83. **Kehl-Fie TE**, **Zhang Y**, **Moore JL**, **Farrand AJ**, **Hood MI**, **Rathi S**, **Chazin WJ**, **Caprioli RM**, **Skaar EP**. 2013. MntABC and MntH contribute to systemic *Staphylococcus aureus* infection by competing with calprotectin for nutrient manganese. Infect. Immun. **81**:3395–3405.
- 84. **Dale SE**, **Doherty-Kirby A**, **Lajoie G**, **Heinrichs DE**. 2004. Role of siderophore biosynthesis in virulence of *Staphylococcus aureus*: identification and characterization of genes involved in production of a siderophore. Infect. Immun. **72**:29–37.
- 85. Thurlow LR, Joshi GS, Clark JR, Spontak JS, Neely CJ, Maile R, Richardson AR. 2013. Functional modularity of the arginine catabolic mobile element contributes to the success of USA300 methicillin-resistant *Staphylococcus aureus*. Cell Host Microbe 13:100–107.
- 86. Lan L, Cheng A, Dunman PM, Missiakas D, He C. 2010. Golden pigment production and virulence gene expression are affected by metabolisms in *Staphylococcus aureus*. J. Bacteriol. **192**:3068–3077.
- 87. Hammer ND, Reniere ML, Cassat JE, Zhang Y, Hirsch AO, Indriati Hood M, Skaar EP. 2013. Two heme-dependent terminal oxidases power *Staphylococcus aureus* organ-specific colonization of the vertebrate host. MBio **4**.
- 88. **Hammer ND**, **Schurig-Briccio LA**, **Gerdes SY**, **Gennis RB**, **Skaar EP**. 2016. CtaM Is Required for Menaquinol Oxidase aa3 Function in *Staphylococcus aureus*. MBio **7**.
- 89. **Dastgheyb SS**, **Otto M**. 2015. Staphylococcal adaptation to diverse physiologic niches: an overview of transcriptomic and phenotypic changes in different biological environments. Future Microbiol **10**:1981–1995.
- 90. Krismer B, Liebeke M, Janek D, Nega M, Rautenberg M, Hornig G, Unger C, Weidenmaier C, Lalk M, Peschel A. 2014. Nutrient limitation governs *Staphylococcus aureus* metabolism and niche adaptation in the human nose. PLoS Pathog. 10:e1003862.

- 91. **Weidenmaier C**, **Goerke C**, **Wolz C**. 2012. *Staphylococcus aureus* determinants for nasal colonization. Trends Microbiol. **20**:243–250.
- 92. **Chonoles Imlay KR**, **Korshunov S**, **Imlay JA**. 2015. Physiological Roles and Adverse Effects of the Two Cystine Importers of *Escherichia coli*. J. Bacteriol. **197**:3629–3644.
- 93. **Lensmire JM**, **Hammer ND**. 2018. Nutrient sulfur acquisition strategies employed by bacterial pathogens. Curr. Opin. Microbiol. **47**:52–58.
- 94. Cheng AG, Kim HK, Burts ML, Krausz T, Schneewind O, Missiakas DM. 2009. Genetic requirements for *Staphylococcus aureus* abscess formation and persistence in host tissues. FASEB J. **23**:3393–3404.
- 95. **Ubbink JB**, **Hayward Vermaak WJ**, **Bissbort S**. 1991. Rapid high-performance liquid chromatographic assay for total homocysteine levels in human serum. J. Chromatogr. **565**:441–446.
- 96. **Baptist EW**, **Kredich NM**. 1977. Regulation of L-cystine transport in *Salmonella* typhimurium. J. Bacteriol. **131**:111–118.
- 97. **Soutourina O**, **Dubrac S**, **Poupel O**, **Msadek T**, **Martin-Verstraete I**. 2010. The pleiotropic CymR regulator of *Staphylococcus aureus* plays an important role in virulence and stress response. PLoS Pathog. **6**:e1000894.
- 98. **Hullo M-F**, **Martin-Verstraete I**, **Soutourina O**. 2010. Complex phenotypes of a mutant inactivated for CymR, the global regulator of cysteine metabolism in *Bacillus subtilis*. FEMS Microbiol. Lett. **309**:201–207.
- 99. Even S, Burguière P, Auger S, Soutourina O, Danchin A, Martin-Verstraete I. 2006. Global control of cysteine metabolism by CymR in *Bacillus subtilis*. J. Bacteriol. **188**:2184–2197.
- 100. **Fey PD**, **Endres JL**, **Yajjala VK**, **Widhelm TJ**, **Boissy RJ**, **Bose JL**, **Bayles KW**. 2013. A genetic resource for rapid and comprehensive phenotype screening of nonessential *Staphylococcus aureus* genes. MBio **4**:e00537-12.
- 101. **Duthie ES**. 1952. Variation in the antigenic composition of staphylococcal coagulase. J. Gen. Microbiol. **7**:320–326.
- 102. **Longo A**, **Di Toro M**, **Galimberti C**, **Carenzi A**. 1991. Determination of N-acetylcysteine in human plasma by gas chromatography-mass spectrometry. J. Chromatogr. **562**:639–645.
- 103. **Kim HK**, **Missiakas D**, **Schneewind O**. 2014. Mouse models for infectious diseases caused by *Staphylococcus aureus*. J. Immunol. Methods **410**:88–99.
- 104. **Sekowska A**, **Kung HF**, **Danchin A**. 2000. Sulfur metabolism in *Escherichia coli* and related bacteria: facts and fiction. J Mol Microbiol Biotechnol **2**:145–177.
- 105. Kredich NM. 2008. Biosynthesis of Cysteine. Ecosal Plus 3.

- 106. **ter Beek J**, **Guskov A**, **Slotboom DJ**. 2014. Structural diversity of ABC transporters. J. Gen. Physiol. **143**:419–435.
- 107. **Lewinson O**, **Livnat-Levanon N**. 2017. Mechanism of action of ABC importers: conservation, divergence, and physiological adaptations. J. Mol. Biol. **429**:606–619.
- 108. **Rice AJ**, **Park A**, **Pinkett HW**. 2014. Diversity in ABC transporters: type I, II and III importers. Crit Rev Biochem Mol Biol **49**:426–437.
- 109. Kumar P, Kesari P, Kokane S, Ghosh DK, Kumar P, Sharma AK. 2019. Crystal structures of a putative periplasmic cystine-binding protein from *Candidatus Liberibacter asiaticus*: insights into an adapted mechanism of ligand binding. FEBS J.
- 110. **Park S**, **Imlay JA**. 2003. High levels of intracellular cysteine promote oxidative DNA damage by driving the fenton reaction. J. Bacteriol. **185**:1942–1950.
- 111. **Bulut H**, **Moniot S**, **Licht A**, **Scheffel F**, **Gathmann S**, **Saenger W**, **Schneider E**. 2012. Crystal structures of two solute receptors for L-cystine and L-cysteine, respectively, of the human pathogen *Neisseria gonorrhoeae*. J. Mol. Biol. **415**:560–572.
- 112. Müller A, Thomas GH, Horler R, Brannigan JA, Blagova E, Levdikov VM, Fogg MJ, Wilson KS, Wilkinson AJ. 2005. An ATP-binding cassette-type cysteine transporter in *Campylobacter jejuni* inferred from the structure of an extracytoplasmic solute receptor protein. Mol. Microbiol. **57**:143–155.
- 113. Cassat JE, Hammer ND, Campbell JP, Benson MA, Perrien DS, Mrak LN, Smeltzer MS, Torres VJ, Skaar EP. 2013. A secreted bacterial protease tailors the *Staphylococcus aureus* virulence repertoire to modulate bone remodeling during osteomyelitis. Cell Host Microbe **13**:759–772.
- 114. Burlak C, Hammer CH, Robinson M-A, Whitney AR, McGavin MJ, Kreiswirth BN, Deleo FR. 2007. Global analysis of community-associated methicillin-resistant *Staphylococcus aureus* exoproteins reveals molecules produced in vitro and during infection. Cell Microbiol. 9:1172–1190.
- 115. Kolar SL, Ibarra JA, Rivera FE, Mootz JM, Davenport JE, Stevens SM, Horswill AR, Shaw LN. 2013. Extracellular proteases are key mediators of *Staphylococcus aureus* virulence via the global modulation of virulence-determinant stability. Microbiologyopen 2:18–34.
- 116. **Wymann MP**, **von Tscharner V**, **Deranleau DA**, **Baggiolini M**. 1987. The onset of the respiratory burst in human neutrophils. Real-time studies of H2O2 formation reveal a rapid agonist-induced transduction process. J. Biol. Chem. **262**:12048–12053.
- 117. Diep BA, Stone GG, Basuino L, Graber CJ, Miller A, des Etages S-A, Jones A, Palazzolo-Ballance AM, Perdreau-Remington F, Sensabaugh GF, DeLeo FR, Chambers HF. 2008. The arginine catabolic mobile element and staphylococcal chromosomal cassette mec linkage: convergence of virulence and resistance in the USA300 clone of methicillin-resistant *Staphylococcus aureus*. J. Infect. Dis. 197:1523–1530.

- 118. **Schneewind O**, **Missiakas D**. 2014. Genetic manipulation of *Staphylococcus aureus*. Curr Protoc Microbiol **32**:Unit 9C.3.
- 119. **Bose JL**, **Fey PD**, **Bayles KW**. 2013. Genetic tools to enhance the study of gene function and regulation in *Staphylococcus aureus*. Appl. Environ. Microbiol. **79**:2218–2224.
- 120. Krute CN, Krausz KL, Markiewicz MA, Joyner JA, Pokhrel S, Hall PR, Bose JL. 2016. Generation of a stable plasmid for in vitro and in vivo studies of staphylococcus species. Appl. Environ. Microbiol. 82:6859–6869.
- 121. **Pattee PA**, **Neveln DS**. 1975. Transformation analysis of three linkage groups in Staphylococcus aureus. J. Bacteriol. **124**:201–211.
- 122. **Theis T**, **Skurray RA**, **Brown MH**. 2007. Identification of suitable internal controls to study expression of a *Staphylococcus aureus* multidrug resistance system by quantitative real-time PCR. J. Microbiol. Methods **70**:355–362.
- 123. Opperman TJ, Williams JD, Houseweart C, Panchal RG, Bavari S, Peet NP, Moir DT, Bowlin TL. 2010. Efflux-mediated bis-indole resistance in *Staphylococcus aureus* reveals differential substrate specificities for MepA and MepR. Bioorg. Med. Chem. 18:2123–2130.
- 124. **Sihto H-M**, **Tasara T**, **Stephan R**, **Johler S**. 2014. Validation of reference genes for normalization of qPCR mRNA expression levels in *Staphylococcus aureus* exposed to osmotic and lactic acid stress conditions encountered during food production and preservation. FEMS Microbiol. Lett. **356**:134–140.
- 125. **Sievers F**, **Higgins DG**. 2018. Clustal Omega for making accurate alignments of many protein sequences. Protein Sci. **27**:135–145.
- 126. Sievers F, Wilm A, Dineen D, Gibson TJ, Karplus K, Li W, Lopez R, McWilliam H, Remmert M, Söding J, Thompson JD, Higgins DG. 2011. Fast, scalable generation of high-quality protein multiple sequence alignments using Clustal Omega. Mol. Syst. Biol. 7:539.
- 127. **Rambaut A**. 2009. FigTree. Computer software, Distributed by the author.
- 128. Marchler-Bauer A, Bo Y, Han L, He J, Lanczycki CJ, Lu S, Chitsaz F, Derbyshire MK, Geer RC, Gonzales NR, Gwadz M, Hurwitz DI, Lu F, Marchler GH, Song JS, Thanki N, Wang Z, Yamashita RA, Zhang D, Zheng C, Geer LY, Bryant SH. 2017. CDD/SPARCLE: functional classification of proteins via subfamily domain architectures. Nucleic Acids Res. 45:D200–D203.
- 129. **Quevillon E, Silventoinen V, Pillai S, Harte N, Mulder N, Apweiler R, Lopez R**. 2005. InterProScan: protein domains identifier. Nucleic Acids Res. **33**:W116-20.
- 130. **Käll L**, **Krogh A**, **Sonnhammer ELL**. 2004. A combined transmembrane topology and signal peptide prediction method. J. Mol. Biol. **338**:1027–1036.

- 131. **Ayala-Castro C**, **Saini A**, **Outten FW**. 2008. Fe-S cluster assembly pathways in bacteria. Microbiol. Mol. Biol. Rev. **72**:110–25.
- 132. Ramsey KM, Ledvina HE, Tresko TM, Wandzilak JM, Tower CA, Tallo T, Schramm CE, Peterson SB, Skerrett SJ, Mougous JD, Dove SL. 2020. Tn-Seq reveals hidden complexity in the utilization of host-derived glutathione in *Francisella tularensis*. PLoS Pathog. **16**:e1008566.
- 133. **Vergauwen B, Pauwels F, Vaneechoutte M, Van Beeumen JJ**. 2003. Exogenous glutathione completes the defense against oxidative stress in *Haemophilus influenzae*. J. Bacteriol. **185**:1572–1581.
- **Tate SS**, **Meister A**. 1981. γ-Glutamyl transpeptidase: catalytic, structural and functional aspects. Mol. Cell. Biochem. **39**:357–368.
- 135. **Cooper AJ**. 1983. Biochemistry of sulfur-containing amino acids. Annu. Rev. Biochem. **52**:187–222.
- 136. **Frackenpohl J, Arvidsson PI, Schreiber JV, Seebach D**. 2001. The Outstanding Biological Stability of β- and γ-Peptides toward Proteolytic Enzymes: An In Vitro Investigation with Fifteen Peptidases. Chembiochem **2**:445–455.
- 137. **Suzuki H**, **Kumagai H**, **Tochikura T**. 1986. gamma-Glutamyltranspeptidase from *Escherichia coli* K-12: formation and localization. J. Bacteriol. **168**:1332–1335.
- 138. **Xu K**, **Strauch MA**. 1996. Identification, sequence, and expression of the gene encoding gamma-glutamyltranspeptidase in *Bacillus subtilis*. J. Bacteriol. **178**:4319–4322.
- 139. **Takahashi H, Watanabe H**. 2004. Post-translational processing of *Neisseria meningitidis* gamma-glutamyl aminopeptidase and its association with inner membrane facing to the cytoplasmic space. FEMS Microbiol. Lett. **234**:27–35.
- 140. Wüstner S, Anderl F, Wanisch A, Sachs C, Steiger K, Nerlich A, Vieth M, Mejías-Luque R, Gerhard M. 2017. *Helicobacter pylori* γ-glutamyl transferase contributes to colonization and differential recruitment of T cells during persistence. Sci. Rep. **7**:13636.
- 141. Elhosseiny NM, Elhezawy NB, Sayed RM, Khattab MS, El Far MY, Attia AS. 2020. γ-Glutamyltransferase as a Novel Virulence Factor of *Acinetobacter baumannii* Inducing Alveolar Wall Destruction and Renal Damage in Systemic Disease. J. Infect. Dis. 222:871–879.
- 142. **Ricci V**, **Giannouli M**, **Romano M**, **Zarrilli R**. 2014. *Helicobacter pylori* gamma-glutamyl transpeptidase and its pathogenic role. World J. Gastroenterol. **20**:630–638.
- 143. **McGovern KJ**, **Blanchard TG**, **Gutierrez JA**, **Czinn SJ**, **Krakowka S**, **Youngman P**. 2001. gamma-Glutamyltransferase is a *Helicobacter pylori* virulence factor but is not essential for colonization. Infect. Immun. **69**:4168–4173.
- 144. Kluytmans JA, Mouton JW, Ijzerman EP, Vandenbroucke-Grauls CM, Maat AW, Wagenvoort JH, Verbrugh HA. 1995. Nasal carriage of *Staphylococcus aureus* as a major risk factor for wound infections after cardiac surgery. J. Infect. Dis. **171**:216–219.

- 145. Pöther D-C, Gierok P, Harms M, Mostertz J, Hochgräfe F, Antelmann H, Hamilton CJ, Borovok I, Lalk M, Aharonowitz Y, Hecker M. 2013. Distribution and infection-related functions of bacillithiol in *Staphylococcus aureus*. Int. J. Med. Microbiol. **303**:114–123.
- 146. Newton GL, Arnold K, Price MS, Sherrill C, Delcardayre SB, Aharonowitz Y, Cohen G, Davies J, Fahey RC, Davis C. 1996. Distribution of thiols in microorganisms: mycothiol is a major thiol in most actinomycetes. J. Bacteriol. 178:1990–1995.
- 147. Lensmire JM, Dodson JP, Hsueh BY, Wischer MR, Delekta PC, Shook JC, Ottosen EN, Kies PJ, Ravi J, Hammer ND. 2020. The *Staphylococcus aureus* Cystine Transporters TcyABC and TcyP Facilitate Nutrient Sulfur Acquisition during Infection. Infect. Immun. 88.
- 148. **Oinonen C**, **Rouvinen J**. 2000. Structural comparison of Ntn-hydrolases. Protein Sci. **9**:2329–2337.
- 149. **Suzuki H**, **Kumagai H**. 2002. Autocatalytic processing of gamma-glutamyltranspeptidase. J. Biol. Chem. **277**:43536–43543.
- 150. West MB, Wickham S, Quinalty LM, Pavlovicz RE, Li C, Hanigan MH. 2011. Autocatalytic cleavage of human gamma-glutamyl transpeptidase is highly dependent on N-glycosylation at asparagine 95. J. Biol. Chem. 286:28876–28888.
- 151. **Okada T, Suzuki H, Wada K, Kumagai H, Fukuyama K**. 2006. Crystal structures of gamma-glutamyltranspeptidase from *Escherichia coli*, a key enzyme in glutathione metabolism, and its reaction intermediate. Proc. Natl. Acad. Sci. USA **103**:6471–6476.
- 152. **Suzuki H**, **Kumagai H**, **Tochikura T**. 1986. gamma-Glutamyltranspeptidase from *Escherichia coli* K-12: purification and properties. J. Bacteriol. **168**:1325–1331.
- 153. **Bendtsen JD**, **Nielsen H**, **Widdick D**, **Palmer T**, **Brunak S**. 2005. Prediction of twinarginine signal peptides. BMC Bioinformatics **6**:167.
- 154. Armenteros JJA, Tsirigos KD, Sønderby CK, Petersen TN, Winther O, Brunak S, von Heijne G, Nielsen H. 2019. SignalP 5.0 improves signal peptide predictions using deep neural networks. Nat. Biotechnol. 37:420–423.
- 155. **Navarre WW**, **Ton-That H**, **Faull KF**, **Schneewind O**. 1998. Anchor structure of staphylococcal surface proteins. J. Bio. Chem. **273**:29135–29142.
- 156. **Schneewind O**, **Mihaylova-Petkov D**, **Model P**. 1993. Cell wall sorting signals in surface proteins of gram-positive bacteria. EMBO J. **12**:4803–4811.
- 157. Tong SYC, Schaumburg F, Ellington MJ, Corander J, Pichon B, Leendertz F, Bentley SD, Parkhill J, Holt DC, Peters G, Giffard PM. 2015. Novel staphylococcal species that form part of a *Staphylococcus aureus*-related complex: the non-pigmented *Staphylococcus argenteus* sp. nov. and the non-human primate-associated *Staphylococcus schweitzeri* sp. nov. Int. J. Syst. Evol. Microbiol. **65**:15–22.

- 158. **Thurlow LR**, **Stephens AC**, **Hurley KE**, **Richardson AR**. 2020. Lack of nutritional immunity in diabetic skin infections promotes *Staphylococcus aureus* virulence. Sci. Adv. 6
- 159. **Sherrill C**, **Fahey RC**. 1998. Import and metabolism of glutathione by *Streptococcus mutans*. J. Bacteriol. **180**:1454–1459.
- 160. Newton GL, Rawat M, La Clair JJ, Jothivasan VK, Budiarto T, Hamilton CJ, Claiborne A, Helmann JD, Fahey RC. 2009. Bacillithiol is an antioxidant thiol produced in Bacilli. Nat. Chem. Biol. 5:625–627.
- 161. **Suzuki H**, **Hashimoto W**, **Kumagai H**. 1999. Glutathione metabolism in *Escherichia coli*. Journal of Molecular Catalysis B: Enzymatic **6**:175–184.
- 162. Stewart LJ, Ong C-LY, Zhang MM, Brouwer S, McIntyre L, Davies MR, Walker MJ, McEwan AG, Waldron KJ, Djoko KY. 2020. Role of Glutathione in Buffering Excess Intracellular Copper in *Streptococcus pyogenes*. MBio 11.
- 163. **Desai PR**, **Thakur A**, **Ganguli D**, **Paul S**, **Morschhäuser J**, **Bachhawat AK**. 2011. Glutathione utilization by *Candida albicans* requires a functional glutathione degradation (DUG) pathway and OPT7, an unusual member of the oligopeptide transporter family. J. Biol. Chem. **286**:41183–41194.
- 164. **Kaur H**, **Ganguli D**, **Bachhawat AK**. 2012. Glutathione degradation by the alternative pathway (DUG pathway) in *Saccharomyces cerevisiae* is initiated by (Dug2p-Dug3p)2 complex, a novel glutamine amidotransferase (GATase) enzyme acting on glutathione. J. Biol. Chem. **287**:8920–8931.
- 165. **Kumar A, Tikoo S, Maity S, Sengupta S, Sengupta S, Kaur A, Bachhawat AK**. 2012. Mammalian proapoptotic factor ChaC1 and its homologues function as γ-glutamyl cyclotransferases acting specifically on glutathione. EMBO Rep. **13**:1095–1101.
- 166. Hiron A, Borezée-Durant E, Piard J-C, Juillard V. 2007. Only one of four oligopeptide transport systems mediates nitrogen nutrition in *Staphylococcus aureus*. J. Bacteriol. 189:5119–5129.
- 167. **Lehman MK**, **Nuxoll AS**, **Yamada KJ**, **Kielian T**, **Carson SD**, **Fey PD**. 2019. Protease-Mediated Growth of *Staphylococcus aureus* on Host Proteins Is opp3 Dependent. MBio **10**.
- 168. **Borezée-Durant E**, **Hiron A**, **Piard J-C**, **Juillard V**. 2009. Dual role of the oligopeptide permease Opp3 during growth of *Staphylococcus aureus* in milk. Appl. Environ. Microbiol. **75**:3355–3357.
- 169. **Nakayama R**, **Kumagai H**, **Tochikura T**. 1984. Purification and properties of gamma-glutamyltranspeptidase from *Proteus mirabilis*. J. Bacteriol. **160**:341–346.
- 170. Song J-Y, Choi Y-J, Kim J-M, Kim Y-R, Jo J-S, Park J-S, Park H-J, Song Y-G, Lee K-H, Kang H-L, Baik S-C, Youn H-S, Cho M-J, Rhee K-H, Lee W-K. 2011. Purification and Characterization of *Helicobacter pylori* γ-Glutamyltranspeptidase. J. Bacteriol. Virol. 41:255.

- 171. **Donald Allison R**. 1985. [51] γ-Glutamyl transpeptidase: Kinetics and mechanism, p. 419–437. *In* Glutamate, glutamine, glutathione, and related compounds. Elsevier.
- 172. Schaumburg F, Pauly M, Anoh E, Mossoun A, Wiersma L, Schubert G, Flammen A, Alabi AS, Muyembe-Tamfum J-J, Grobusch MP, Karhemere S, Akoua-Koffi C, Couacy-Hymann E, Kremsner PG, Mellmann A, Becker K, Leendertz FH, Peters G. 2015. Staphylococcus aureus complex from animals and humans in three remote African regions. Clin. Microbiol. Infect. 21:345.e1-8.
- 173. Okuda KV, Toepfner N, Alabi AS, Arnold B, Bélard S, Falke U, Menschner L, Monecke S, Ruppelt-Lorz A, Berner R. 2016. Molecular epidemiology of *Staphylococcus aureus* from Lambaréné, Gabon. Eur. J. Clin. Microbiol. Infect. Dis. 35:1963–1973.
- 174. Ateba Ngoa U, Schaumburg F, Adegnika AA, Kösters K, Möller T, Fernandes JF, Alabi A, Issifou S, Becker K, Grobusch MP, Kremsner PG, Lell B. 2012. Epidemiology and population structure of *Staphylococcus aureus* in various population groups from a rural and semi urban area in Gabon, Central Africa. Acta Trop. **124**:42–47.
- 175. Schaumburg F, Alabi AS, Köck R, Mellmann A, Kremsner PG, Boesch C, Becker K, Leendertz FH, Peters G. 2012. Highly divergent *Staphylococcus aureus* isolates from African non-human primates. Environ. Microbiol. Rep. **4**:141–146.
- 176. Olatimehin A, Shittu AO, Onwugamba FC, Mellmann A, Becker K, Schaumburg F. 2018. *Staphylococcus aureus* Complex in the Straw-Colored Fruit Bat (Eidolon helvum) in Nigeria. Front. Microbiol. **9**:162.
- 177. Holt DC, Holden MTG, Tong SYC, Castillo-Ramirez S, Clarke L, Quail MA, Currie BJ, Parkhill J, Bentley SD, Feil EJ, Giffard PM. 2011. A very early-branching *Staphylococcus aureus* lineage lacking the carotenoid pigment staphyloxanthin. Genome Biol. Evol. **3**:881–895.
- 178. **Ng JWS**, **Holt DC**, **Lilliebridge RA**, **Stephens AJ**, **Huygens F**, **Tong SYC**, **Currie BJ**, **Giffard PM**. 2009. Phylogenetically distinct *Staphylococcus aureus* lineage prevalent among indigenous communities in northern Australia. J. Clin. Microbiol. **47**:2295–2300.
- 179. **Dupieux C, Blondé R, Bouchiat C, Meugnier H, Bes M, Laurent S, Vandenesch F, Laurent F, Tristan A**. 2015. Community-acquired infections due to *Staphylococcus argenteus* lineage isolates harbouring the Panton-Valentine leucocidin, France, 2014. Euro Surveill. **20**.
- 180. **Frank DN**, **Feazel LM**, **Bessesen MT**, **Price CS**, **Janoff EN**, **Pace NR**. 2010. The human nasal microbiota and *Staphylococcus aureus* carriage. PLoS One **5**:e10598.
- 181. **Kimura K**, **Tran L-SP**, **Uchida I**, **Itoh Y**. 2004. Characterization of *Bacillus subtilis* gamma-glutamyltransferase and its involvement in the degradation of capsule polygamma-glutamate. Microbiology (Reading, Engl.) **150**:4115–4123.
- 182. **Wu R**, **Richter S**, **Zhang R**, **Anderson VJ**, **Missiakas D**, **Joachimiak A**. 2009. Crystal structure of *Bacillus anthracis* transpeptidase enzyme CapD. J. Biol. Chem. **284**:24406–

24414.

- 183. **Wickham S**, **West MB**, **Cook PF**, **Hanigan MH**. 2011. Gamma-glutamyl compounds: substrate specificity of gamma-glutamyl transpeptidase enzymes. Anal. Biochem. **414**:208–214.
- 184. **Bae T**, **Schneewind O**. 2006. Allelic replacement in *Staphylococcus aureus* with inducible counter-selection. Plasmid **55**:58–63.
- 185. **Krogh A**, **Larsson B**, **von Heijne G**, **Sonnhammer ELL**. 2001. Predicting transmembrane protein topology with a hidden Markov model: application to complete genomes. J. Mol. Biol. **305**:567–580.
- 186. **Käll L**, **Krogh A**, **Sonnhammer ELL**. 2007. Advantages of combined transmembrane topology and signal peptide prediction--the Phobius web server. Nucleic Acids Res. **35**:W429-32.
- 187. Mistry J, Chuguransky S, Williams L, Qureshi M, Salazar GA, Sonnhammer ELL, Tosatto SCE, Paladin L, Raj S, Richardson LJ, Finn RD, Bateman A. 2021. Pfam: The protein families database in 2021. Nucleic Acids Res. 49:D412–D419.
- 188. Blum M, Chang H-Y, Chuguransky S, Grego T, Kandasaamy S, Mitchell A, Nuka G, Paysan-Lafosse T, Qureshi M, Raj S, Richardson L, Salazar GA, Williams L, Bork P, Bridge A, Gough J, Haft DH, Letunic I, Marchler-Bauer A, Mi H, Natale DA, Necci M, Orengo CA, Pandurangan AP, Rivoire C, Sigrist CJA, Sillitoe I, Thanki N, Thomas PD, Tosatto SCE, Wu CH, Bateman A, Finn RD. 2021. The InterPro protein families and domains database: 20 years on. Nucleic Acids Res. 49:D344–D354.
- 189. Sigrist CJA, Cerutti L, de Castro E, Langendijk-Genevaux PS, Bulliard V, Bairoch A, Hulo N. 2010. PROSITE, a protein domain database for functional characterization and annotation. Nucleic Acids Res. 38:D161-6.
- 190. Wilkins D. 2020. gggenes: Draw Gene Arrow Maps in "ggplot2". Computer software.
- 191. **Rule CS**, **Patrick M**, **Sandkvist M**. 2016. Measuring in vitro atpase activity for enzymatic characterization. J. Vis. Exp.
- 192. **Ogrodzinski MP**, **Teoh ST**, **Yu L**, **Broadwater D**, **Ensink E**, **Lunt SY**. 2019. Measuring the nutrient metabolism of adherent cells in culture. Methods Mol. Biol. **1862**:37–52.
- 193. National Research Council (US) Committee for the Update of the Guide for the Care and Use of Laboratory Animals. 2011. Guide for the care and use of laboratory animals, 8th ed. National Academies Press (US), Washington (DC).
- 194. **Altschul SF**, **Gish W**, **Miller W**, **Myers EW**, **Lipman DJ**. 1990. Basic local alignment search tool. J. Mol. Biol. **215**:403–410.
- 195. Boratyn GM, Schäffer AA, Agarwala R, Altschul SF, Lipman DJ, Madden TL. 2012. Domain enhanced lookup time accelerated BLAST. Biol. Direct 7:12.
- 196. O'Leary NA, Wright MW, Brister JR, Ciufo S, Haddad D, McVeigh R, Rajput B,

- Robbertse B, Smith-White B, Ako-Adjei D, Astashyn A, Badretdin A, Bao Y, Blinkova O, Brover V, Chetvernin V, Choi J, Cox E, Ermolaeva O, Farrell CM, Goldfarb T, Gupta T, Haft D, Hatcher E, Hlavina W, Joardar VS, Kodali VK, Li W, Maglott D, Masterson P, McGarvey KM, Murphy MR, O'Neill K, Pujar S, Rangwala SH, Rausch D, Riddick LD, Schoch C, Shkeda A, Storz SS, Sun H, Thibaud-Nissen F, Tolstoy I, Tully RE, Vatsan AR, Wallin C, Webb D, Wu W, Landrum MJ, Kimchi A, Tatusova T, DiCuccio M, Kitts P, Murphy TD, Pruitt KD. 2016. Reference sequence (RefSeq) database at NCBI: current status, taxonomic expansion, and functional annotation. Nucleic Acids Res. 44:D733-45.
- 197. **Kanehisa M, Furumichi M, Sato Y, Ishiguro-Watanabe M, Tanabe M**. 2021. KEGG: integrating viruses and cellular organisms. Nucleic Acids Res. **49**:D545–D551.
- 198. **Kanehisa M**. 2019. Toward understanding the origin and evolution of cellular organisms. Protein Sci. **28**:1947–1951.
- 199. **Kanehisa M**, **Goto S**. 2000. KEGG: Kyoto encyclopedia of genes and genomes. Nucleic Acids Res. **28**:27–30.
- 200. **Human Microbiome Project Consortium**. 2012. Structure, function and diversity of the healthy human microbiome. Nature **486**:207–214.
- 201. Mashruwala AA, Pang YY, Rosario-Cruz Z, Chahal HK, Benson MA, Mike LA, Skaar EP, Torres VJ, Nauseef WM, Boyd JM. 2015. Nfu facilitates the maturation of iron-sulfur proteins and participates in virulence in *Staphylococcus aureus*. Mol. Microbiol. 95:383–409.
- 202. Roche B, Aussel L, Ezraty B, Mandin P, Py B, Barras F. 2013. Iron/sulfur proteins biogenesis in prokaryotes: formation, regulation and diversity. Biochim. Biophys. Acta 1827:455–469.
- 203. **Hindson VJ**. 2003. Serine acetyltransferase of *Escherichia coli*: substrate specificity and feedback control by cysteine. Biochem. J. **375**:745–752.
- 204. **Ji Q, Zhang L**, **Sun F**, **Deng X**, **Liang H**, **Bae T**, **He C**. 2012. *Staphylococcus aureus* CymR is a new thiol-based oxidation-sensing regulator of stress resistance and oxidative response. J. Biol. Chem. **287**:21102–21109.
- 205. **Shepard EM**, **Boyd ES**, **Broderick JB**, **Peters JW**. 2011. Biosynthesis of complex iron-sulfur enzymes. Curr. Opin. Chem. Biol. **15**:319–327.
- 206. Roche B, Aussel L, Ezraty B, Mandin P, Py B, Barras F. 2013. Iron/sulfur proteins biogenesis in prokaryotes: formation, regulation and diversity. Biochim. Biophys. Acta 1827:923–937.
- 207. **Horsburgh MJ**, **Clements MO**, **Crossley H**, **Ingham E**, **Foster SJ**. 2001. PerR controls oxidative stress resistance and iron storage proteins and is required for virulence in *Staphylococcus aureus*. Infect. Immun. **69**:3744–3754.
- 208. **Imperi F**, **Tiburzi F**, **Fimia GM**, **Visca P**. 2010. Transcriptional control of the pvdS iron starvation sigma factor gene by the master regulator of sulfur metabolism CysB in

- Pseudomonas aeruginosa. Environ. Microbiol. 12:1630–1642.
- 209. **Love MI**, **Huber W**, **Anders S**. 2014. Moderated estimation of fold change and dispersion for RNA-seq data with DESeq2. Genome Biol. **15**:550.
- 210. Fuchs S, Mehlan H, Bernhardt J, Hennig A, Michalik S, Surmann K, Pané-Farré J, Giese A, Weiss S, Backert L, Herbig A, Nieselt K, Hecker M, Völker U, Mäder U. 2018. AureoWiki-The repository of the *Staphylococcus aureus* research and annotation community. Int. J. Med. Microbiol. 308:558–568.
- 211. Huerta-Cepas J, Forslund K, Coelho LP, Szklarczyk D, Jensen LJ, von Mering C, Bork P. 2017. Fast Genome-Wide Functional Annotation through Orthology Assignment by eggNOG-Mapper. Mol. Biol. Evol. **34**:2115–2122.
- 212. Huerta-Cepas J, Szklarczyk D, Heller D, Hernández-Plaza A, Forslund SK, Cook H, Mende DR, Letunic I, Rattei T, Jensen LJ, von Mering C, Bork P. 2019. eggNOG 5.0: a hierarchical, functionally and phylogenetically annotated orthology resource based on 5090 organisms and 2502 viruses. Nucleic Acids Res. 47:D309–D314.
- 213. **Chen H**, **Boutros PC**. 2011. VennDiagram: a package for the generation of highly-customizable Venn and Euler diagrams in R. BMC Bioinformatics **12**:35.
- 214. **Mi H, Muruganujan A, Huang X, Ebert D, Mills C, Guo X, Thomas PD**. 2019. Protocol Update for large-scale genome and gene function analysis with the PANTHER classification system (v.14.0). Nat. Protoc. **14**:703–721.
- 215. **Mi H, Ebert D, Muruganujan A**, **Mills C**, **Albou L-P**, **Mushayamaha T**, **Thomas PD**. 2021. PANTHER version 16: a revised family classification, tree-based classification tool, enhancer regions and extensive API. Nucleic Acids Res. **49**:D394–D403.
- 216. **Wilhelm BT**, **Landry J-R**. 2009. RNA-Seq-quantitative measurement of expression through massively parallel RNA-sequencing. Methods **48**:249–257.
- 217. **Cheng AG**, **DeDent AC**, **Schneewind O**, **Missiakas D**. 2011. A play in four acts: *Staphylococcus aureus* abscess formation. Trends Microbiol. **19**:225–232.
- 218. Spraggins JM, Rizzo DG, Moore JL, Rose KL, Hammer ND, Skaar EP, Caprioli RM. 2015. MALDI FTICR IMS of Intact Proteins: Using Mass Accuracy to Link Protein Images with Proteomics Data. J Am Soc Mass Spectrom 26:974–985.
- 219. **Giustarini D**, **Dalle-Donne I**, **Milzani A**, **Rossi R**. 2011. Low molecular mass thiols, disulfides and protein mixed disulfides in rat tissues: influence of sample manipulation, oxidative stress and ageing. Mech. Ageing Dev. **132**:141–148.
- 220. **Shaw L**, **Golonka E**, **Potempa J**, **Foster SJ**. 2004. The role and regulation of the extracellular proteases of *Staphylococcus aureus*. Microbiology (Reading, Engl.) **150**:217–228.
- 221. **Ohbayashi T, Irie A, Murakami Y, Nowak M, Potempa J, Nishimura Y, Shinohara M, Imamura T**. 2011. Degradation of fibrinogen and collagen by staphopains, cysteine proteases released from *Staphylococcus aureus*. Microbiology (Reading, Engl.)

157:786–792.

- 222. Massimi I, Park E, Rice K, Muller-Esterl W, Sauder D, McGavin MJ. 2002. Identification of a novel maturation mechanism and restricted substrate specificity for the SspB cysteine protease of *Staphylococcus aureus*. J. Biol. Chem. **277**:41770–41777.
- 223. **Miseta A**, **Csutora P**. 2000. Relationship between the occurrence of cysteine in proteins and the complexity of organisms. Mol. Biol. Evol. **17**:1232–1239.
- 224. **Imlay JA**, **Chin SM**, **Linn S**. 1988. Toxic DNA damage by hydrogen peroxide through the Fenton reaction in vivo and in vitro. Science **240**:640–642.
- 225. **Ibberson CB**, **Whiteley M**. 2019. The *Staphylococcus aureus* Transcriptome during Cystic Fibrosis Lung Infection. MBio **10**.